

REPUBLIQUE DU CAMEROUN

Paix-Travail-Patrie



DEPARTEMENT DE GENIE CIVIL
DEPARTMENT OF CIVIL ENGINEERING

REPUBLIC OF CAMEROON

Peace-Work-Fatherland



UNIVERSITÀ
DEGLI STUDI
DI PADOVA

DEPARTMENT OF CIVIL, ARCHITECTURAL
AND ENVIRONMENTAL ENGINEERING

**INFLUENCE OF MASONRY INFILLS ON THE BEHAVIOR OF
REINFORCED CONCRETE FRAMED STRUCTURES:
CONCEIVED CASE STUDY OF AN R+2 RESIDENTIAL
BUILDING IN YAOUNDE**

*A thesis submitted in partial fulfilment of the requirements for the degree of Master of Engineering
(MEng) in Civil Engineering*

Curriculum: Structural Engineering

Presented by

TSAKEM DONGMO Aaron Gaius

Student number: 16TP21114

Supervised by:

Prof. Carmelo MAJORANA

Co-Supervised by:

Eng. Giuseppe CARDILLO

Dr. Eng. Guillaume Hervé POH'SIE

ACADEMIC YEAR: 2020/2021

REPUBLIQUE DU CAMEROUN

Paix-Travail-Patrie



DEPARTEMENT DE GENIE CIVIL
DEPARTMENT OF CIVIL ENGINEERING

REPUBLIC OF CAMEROON

Peace-Work-Fatherland



UNIVERSITÀ
DEGLI STUDI
DI PADOVA

DEPARTMENT OF CIVIL, ARCHITECTURAL
AND ENVIRONMENTAL ENGINEERING

**INFLUENCE OF MASONRY INFILLS ON THE BEHAVIOR OF
REINFORCED CONCRETE FRAMED STRUCTURES:
CONCEIVED CASE STUDY OF AN R+2 RESIDENTIAL
BUILDING IN YAOUNDE**

*A thesis submitted in partial fulfilment of the requirements for the degree of Master of Engineering
(MEng) in Civil Engineering*

Curriculum: Structural Engineering

Presented by

TSAKEM DONGMO Aaron Gaius

Student number: 16TP21114

Supervised by:

Prof. Carmelo MAJORANA

Co-Supervised by:

Eng. Giuseppe CARDILLO

Dr. Eng. Guillaume Hervé POH'SIE

ACADEMIC YEAR: 2020/2021

DEDICATION

To

M. DONGMO BERNARD

In gratitude for all the love with which you cover me and the support that you bring for the success of my studies and my accomplishment.

ACKNOWLEDGEMENTS

This work would not have been completed without the combined efforts of individuals who contributed directly and/or indirectly to its realization. Acknowledging this fact, I wish to express my sincere thanks and gratitude to:

- The **President of the jury** for accepting to preside the jury;
- The **Examiner of the jury** for his observations aimed at ameliorating this work;
- **Professors George NKENG** and **Carmelo MAJORANA** for all their academic and administrative support during these five years spent at National Advanced School of Public Works (NASPW) in Master's in Engineering (MEng) program in partnership with University of Padua;
- **Prof. MBESSA Michel**, the head of the Civil Engineering department, for his tutoring and valuable words of advice;
- **Prof. Carmelo MAJORANA**, Dr. Eng. **POH'SIE Guillaume Hervé** and Eng. **Giuseppe CARDILLO** for their guidance and availability towards me throughout the realization of this work;
- All the teaching staff of The National Advanced School of Public Works and University of Padua for their good quality teaching and their motivation that kept us studying;
- All my classmates and my friends of the 7th batch of MEng program of NASPW who were a source of motivation, tenacity and encouragement throughout these years spent together.
- My special thanks goes to my mother **Mrs DONGMO JEANNETTE** for the great support, care, advices and the experiences they provided to me throughout this research work.
- My brothers, sisters and loved ones, from Cameroon and abroad for their warm-hearted encouragements and love.
- I am equally thankful to the entire staff of **JUNCTIONER CONSTRUCTION ENGINEERING** who opened their doors for me to carry out my research work.
- Finally, I thank all those who contributed directly or indirectly to this work.

LIST OF ABBREVIATIONS AND SYMBOLS

LIST OF ABBREVIATIONS

CAE	Computer Aided Engineering
EC	Eurocode
FEMA	Federal Emergency Management Agency
MI	Masonry Infill
RC	Reinforced Concrete
SAP	Structural Analysis Program
SLS	Serviceability Limit State
SSI	Soil-Structure-Interaction
ULS	Ultimate Limit State

LIST OF SYMBOLS

A	Area of the cross section
a	Infill wall strut representation width
A_c	Area of the concrete cross section
A_{min}	Minimum section area
A_{net}	Net area of the cross section
A_s	Area of the steel reinforcement section
A_{sw}	Cross sectional area of the shear reinforcement
C_{min}	Minimum concrete cover
I_{xx}	Moment of inertia of the section along x-axis
I_{yy}	Moment of inertia of the section along y-axis
M_{Ed}	Bending moment at support

M_{Rd}	Resisting moment
M_{Sd}	Soliciting bending moment
T	Period of the structure with fixed base
V_s	Shear velocity
W	Weight of the structure
a_i	Shifting distance
b	Width of the element
b_t	Mean width of the tension zone
b_w	Smallest width of the cross section in the tensile area
c	Concrete cover
d	Effective height of the section
f_{cd}	Design resisting strength of the concrete
f_{ctm}	Tensile strength of the concrete
f_y	Design yielding strength of the steel
f_{yd}	Design yielding strength of the steel
f_{yk}	Characteristic yield strength
f_{ywd}	Design yield strength of the shear reinforcement
G_k	Permanent load applied on the building
h	Height of the level i
h_{wi}	Height of the wall i;
i	Gyration radius of the uncracked concrete section
j	Index denoting the mode of vibration
K	Stiffness of the structure
l	Span length of the beam
l_o	Effective length of the element
l_{wi}	Length of the section of the wall i

s_l	Maximum longitudinal spacing
s_t	Maximum transversal spacing
ΔC_{dur}	Add /reduction of minimum cover for use of additional protection
\emptyset_l	Minimum diameter of the longitudinal bars
σ	Contact pressure
γ	Specific weight
γ_c	Partial factor for concrete
γ_s	Partial safety factor for steel
Ψ_E	Combination coefficient for variable action
λ	Slenderness
λ_1	Strut width coefficient
λ_{lim}	Limit value of slenderness
ν	Poisson's ratio
ρ_w	Shear reinforcement ratio
ρ_w'	Minimum shear reinforcement ratio
σ_c	Stress in the concrete
σ_s	Stress in the reinforcement

ABSTRACT

The main objective of this work was to study the influence of infill walls (masonry) on the behavior of Reinforced Concrete buildings. Infill walls are non-load-bearing panels, used to separate rooms and they are more often assimilated as distributed loads during the design of Reinforced Concrete buildings. Different steps have been followed with the intention to enlighten the contribution of infill wall in the structural design of RC buildings. A literature review was first carried out to highlight the types and properties of materials used for infill walls, a brief review of experiments conducted on masonry infill influence on buildings, the failure mechanisms, and the different numerical modelling technics used until date. Secondly, our conceived case study, which was a three-storey reinforced concrete residential building, was modelled and from it, we carried a modal analysis using the software SAP2000. Then four models of a reinforced concrete framed structure was modelled using the simplified micro-modelling method. A Finite element analysis was performed on these four models under dynamic explicit loading steps with fixed base in order to study the stresses, strain and the lateral and vertical deformability of the structure. The different dynamic analysis have been achieved using the finite element software ABAQUS CAE. A comparative study have been perform between frame without infill wall, the frame with infill wall and the frame with infill wall including openings (door or window). The results showed that the presence of infill wall increases the global stiffness, the rigidity and reduces the horizontal and vertical deformability of the building. It also affects the deflection of the horizontal elements. In addition, some defects like cracks have been observed on the structure after analysis. This bring another interesting problem on which further studies can be focused on. This work only limited to the structural aspect, and did not take into account the economical and constructional aspects.

Key words: masonry infill wall, reinforced concrete, stiffness, rigidity, deformability.

RESUME

L'objectif principal de ce travail était d'étudier l'influence des murs de remplissage (maçonnerie) sur le comportement des bâtiments en béton armé. Les murs de remplissage sont des panneaux non porteurs, utilisés pour séparer les pièces et ils sont le plus souvent assimilés à des charges réparties lors de la conception des bâtiments en béton armé. Différentes étapes ont été suivies dans le but d'éclairer la contribution du mur de remplissage dans la conception structurelle des bâtiments. Une revue de la littérature a d'abord été réalisée pour mettre en évidence les types et les propriétés des matériaux utilisés pour les murs de remplissage, une brève revue des expériences menées sur l'influence du remplissage en maçonnerie sur les bâtiments, les mécanismes de rupture et les différentes techniques de modélisation numérique utilisées jusqu'à présent. Deuxièmement, notre cas d'étude conçu était un bâtiment résidentiel en béton armé de trois étages à partir duquel nous avons effectué une analyse modale à l'aide du logiciel SAP2000. Puis quatre modèles d'une ossature en béton armé ont été modélisés en utilisant la méthode de micro-modélisation simplifiée. Une analyse par éléments finis a été effectuée sur ces quatre modèles sous des étapes dynamiques de chargement explicite à base fixe afin d'étudier les contraintes, les déformations et la déformabilité latérale et verticale de la structure. Les différentes analyses dynamiques ont été réalisées à l'aide du logiciel ABAQUS CAE. Une étude comparative a été réalisée entre l'ossature sans mur de remplissage, l'ossature avec mur de remplissage et l'ossature avec mur de remplissage incluant des ouvertures (porte ou fenêtre). Les résultats ont montré que la présence de mur de remplissage augmente la raideur globale, la rigidité et réduit la déformabilité horizontale et verticale du bâtiment. Cela affecte également la déflexion des éléments horizontaux. De plus, certains défauts comme des fissures ont été observés sur la structure après analyse. Ceci amène un autre problème intéressant sur lequel des études ultérieures peuvent être focalisées. Ce travail s'est limité à l'aspect structurel, et n'a pas pris en compte les aspects économiques et constructifs.

Mots clés : mur de remplissage en maçonnerie, béton armé, raideur, rigidité, flèche

LIST OF FIGURES

Figure 1-1. Solid Clay block unit	5
Figure 1-2: Hollow Clay brick units	6
Figure 1-3: Solid Concrete Block Unit	8
Figure 1-4. Hollow Concrete block units	9
Figure 1-5: Mortar used in brick joints in masonry walls.	10
Figure 1-6: Effect of brick strength at different mortar strength (on the left) and the Effect of thickness on brickwork strength (on the right).....	12
Figure 1-7: Graph of shear stress against precompression of a masonry.	13
Figure 1-8: Direct tensile strength graph	14
Figure 1-9: Typical stress-strain curve of brick masonry	15
Figure 1-10: Diagonal Strut modelling.....	18
Figure 1-11: Strut Models.....	19
Figure 1-12: Horizontal cracks on masonry wall	21
Figure 1-13: Step cracking along mortar joint on masonry wall.	21
Figure 1-14: Diagonal cracks due to compressional forces on wall	22
Figure 1-15: Corner-crushing occurring on masonry wall.	23
Figure 1-16: Usual crack pattern for a wall under bi-axial bending.....	24
Figure 1-17: Possible out of plane cracks on a masonry wall.	24
Figure 1-18: Flexural collapse on a column with the development of a plastic hinge.	25
Figure 1-19: Column failure due to axial load.....	26
Figure 1-20: Shear failure on column	26
Figure 1-21: Failure at the beam-column joint due to large shear forces and bending moment in the loaded corner	27
Figure 1-22: Soft-storey mechanisms due to absence at the first floor of the building	28
Figure 1-23: Failure of masonry wall and reinforced concrete frame	30
Figure 1-24: Finite element models for infill panels adapted respectively (Crisafulli, al.2000, Amato and al.2008)	31
Figure 1-25: Behaviour of the filled frame under horizontal loading.	34
Figure 2-1 Illustration of the concrete cover	37
Figure 2-2: Moment reduction at supports (Djeukoua 2019)	39

Figure 2-3: Shifting of the moment curve representation (Djeukoua 2019)	40
Figure 2-4: Example of a beam with reinforcements.	41
Figure 2-5: Neutral axis position in the beam section	41
Figure 2-6: Longitudinal spacing and transversal spacing of a beam.	43
Figure 2-7: Geometric characteristics of a transversal beam section	44
Figure 2-8: M-N diagram computation of a rectangular column section in both loading directions	47
Figure 2-9: Example of M-N diagram (D'Antino et al., 2016).....	49
Figure 2-10: Geometrical elements in Abaqus CAE	51
Figure 2-11: Numerical models of masonry wall; (a) prototype masonry wall, (b) detailed micro modelling, (c) semi-micro modelling and (d) macro modelling	52
Figure 2-12: Representing the schematic of the compressive stress-strain curve for structural analysis.	54
Figure 2-13: Stress-strain curve of concrete in compression.....	54
Figure 2-14: The idealized stress-strain curve for reinforcing rebars.....	55
Figure 2-15: Empty frame model	56
Figure 2-16: Infilled frame model	56
Figure 2-17: Infilled frame with opening (door)	57
Figure 2-18: Infilled frame with opening (window).....	57
Figure 3-1: Structural plan of case study	61
Figure 3-2: 3D model of the building (SAP2000).....	62
Figure 3-3: Topographic view of Mbankomo town	62
Figure 3-4: Most solicited beam to design (load distribution)	65
Figure 3-5: Simple support model	66
Figure 3-6: Applied Load Combinations.....	67
Figure 3-7: Bending moment Diagram for the load combinations.....	67
Figure 3-8: Shear diagram for the loads combinations.....	68
Figure 3-9: Envelop of moment diagram.....	68
Figure 3-10: Envelop of the shear diagram	69
Figure 3-11: Bending moment envelop curve at SLS	70
Figure 3-12: Most solicited column.....	71
Figure 3-13: Axial force on most solicited column.....	72
Figure 3-14: M-N interaction diagram	73
Figure 3-15: Natural Frequencies of Empty and Infilled RC framed structure.....	75

Figure 3-16: Models for the local dynamic analysis on Abaqus a) Empty RC frame b) Infilled RC frame
c) Infilled RC frame with window and d) Infilled frame with door 78

Figure 3-17: Von Mises stress- time graph for the vertical and horizontal loading 82

Figure 3-18: Equivalent Plastic strain - time graph of vertical and horizontal loading 85

Figure 3-19: Strain-time graph of vertical and horizontal loading 88

LIST OF TABLE

Table 1.1: Clay bricks compressive strength and water absorption properties.....	5
Table 1.2: Strength and absorption requirements for concrete brick.....	8
Table 1.3: Compressive Strength factors of masonry wall.....	11
Table 1.4: Summary of national codes on reinforced concrete frame with masonry infill.	16
Table 1.5: Summary of expressions proposed to compute w/d	32
Table 2.1: Properties of concrete, rebars and masonry units (Al-Chaar and al (2002))	53
Table 2.2: Concrete implemented material parameters	55
Table 2.3: Joint stiffness for the brick-mortar interaction	59
Table 3.1: Applied loads on structure	63
Table 3.2: Concrete Properties.....	64
Table 3.3: Reinforcement rebars.....	64
Table 3.4: Longitudinal steel reinforcement of the beam.....	69
Table 3.5: Stress verification of beam	70
Table 3.6: Beam deflection verification.....	71
Table 3.7: Steel reinforcement section area.....	72
Table 3.8: Slenderness Verification of column.....	73
Table 3.9: Infill material Properties	74
Table 3.10: Natural frequencies and mode of vibration of the structure at different construction configuration.....	74
Table 3.11: Deformed shape at different modes of vibration	75
Table 3.12: Von Mises Stress states for vertical and horizontal loading on different model configurations (illustrations scaling is of 150 on ABAQUS CEA).....	79
Table 3.13: Equivalent plastic strain.....	83
Table 3.14: Displacement of structure under vertical and horizontal loading.....	86

TABLE OF CONTENT

DEDICATION	i
ACKNOWLEDGEMENTS	ii
LIST OF ABBREVIATIONS AND SYMBOLS	iii
ABSTRACT	vi
RESUME	vii
LIST OF FIGURES	viii
LIST OF TABLE	xi
TABLE OF CONTENT	xii
GENERAL INTRODUCTION	1
CHAPTER 1 LITERATURE REVIEW	3
Introduction	3
1.1. Masonry infill	3
1.1.1. Definition	3
1.1.2. Constituents materials of masonry infills (masonry units)	4
1.1.3. Properties of masonry infills	11
1.2. Guidelines in national codes due to effect of masonry infill panels.....	15
1.2.1 Eurocode 8 (EC 8).....	17
1.2.2 Fema 273, Fema 306.....	18
1.3. Failure modes of the masonry infills	19
1.3.1. Failure parallel to the plane of the infill wall (In-plane).....	20
1.3.2. Failure in the plane perpendicular to the wall (out of plane)	23
1.4. Failure modes of the reinforced frame structure.....	25
1.4.1. Flexural Collapse	25
1.4.2. Failure due to axial load.....	25
1.4.3. Shear failure of the column	26
1.4.4. Beam-column joint failure	27

1.5. Failure of the frame-infill composite.....	27
1.6. Brief notes from experimental test on infill influence on the structural response of frames 28	
1.7. Design and calculation of reinforced concrete structures with masonry infill	30
1.7.1. Methods based on the finite element theory (micro modelling technic).....	31
Conclusion	34
CHAPTER 2: METHODOLOGY	35
Introduction.....	35
2.1. Site recognition.....	35
2.2. Site visit	35
2.3. Data collection	35
2.3.1. Topographic/relief data	35
2.3.2. Structural data	35
2.4. Design of Structural Elements	37
2.4.1. Durability and concrete cover	37
2.4.2. The Beams.....	38
2.4.3. The Column design	45
2.5. Numerical Analysis	50
2.5.1. Geometrical Modelling (part module)	50
2.5.2. Material property Modelling.....	53
2.5.3. Assembly modelling	55
2.5.4. Step modelling	58
2.5.5. Interaction Modelling.....	58
2.5.6. Load Modelling.....	59
2.5.7. Meshing modelling	59
2.5.8. Job module (Numerical analysis of the structure)	59
2.5.9. Visualization module	60
Conclusion	60
CHAPTER 3: RESULTS AND INTERPRETATIONS OF THE ANALYSIS	61

Introduction.....	61
3.1. General presentation of the site	61
3.2. Topographic/Relief data	62
3.3. Geographic and Climatic data	63
3.4. Structural Element Design.....	63
3.4.1. Imposed Load	63
3.4.2. Load Combinations	63
3.4.3. Material properties	64
3.4.4. Durability and Concrete Cover Determination	65
3.4.5. Beam Design Results.....	65
3.4.6. Column design results	71
3.5. Analysis results and interpretation.....	74
3.5.1. Modal analysis results	74
3.5.2. Local Dynamic Analysis of infill walls	77
Conclusion	89
GENERAL CONCLUSION	90
BIBLIOGRAPHY	i
ANNEXES.....	iv

GENERAL INTRODUCTION

Reinforced concrete (RC) has widely been used for the construction of the structural frames of multi-storey buildings since World War II. When structures were designed against external actions, they were considered to resist inertia loads associated with a ground acceleration equal to the maximum acceleration value recorded up to that time. As monitoring networks have improved and become more efficient around the world in recent decades, it has been demonstrated that external actions imposed on structures during their life span are actually greater than the design value initially considered. Because the majority of these structures have not collapsed, the additional external (wind or seismic) energy appears to have been absorbed by "non-structural" members such as the infill walls. As a result, non-structural elements are expected to sustain damage, the severity of which is determined by how much energy they dissipate when subjected to forces.

In spite of their significant contribution to the overall load-carrying capacity, masonry infilled walls are usually ignored during the structural analysis and design of the RC frame. This mainly because of the absence of analytical tools capable of accurately simulating the behaviour of the infill walls in the mathematical models representing the whole structure, also due to the incomplete knowledge of the behaviour of quasi-brittle materials and to the absence of conclusive experimental and analytical results to actualise a reliable design procedure for this type of structures. Furthermore, the available experimental data describing the behaviour of masonry infill walls is described as dispersed due to the large number of parameters associated with the properties of the materials involved (concrete and masonry). In addition, the boundary conditions between the infill frame and the structural elements of the RC frame, the lateral stiffness of the frame and the infill wall, and the type of loading applied.

Assuring the highest level of safety is significant from an economic and strategic view. This applies to both historical and new reinforced structures against dynamic loading, for example, earthquakes and wind. This can be accomplished if the dynamic characteristics of the buildings such as natural frequencies, mode shapes and the various internal solicitations are firmly determined. These parameters are key to the determination of the finite element model updating, structural control, damage detection, and long-term structural health monitoring. Kubalski et al. [25] adopted numerical models in order to describe the inelastic behavior of the system, as demonstrated by the acquired results of the overall structural response as well as the damage propagation within the infill wall.

Our work aims to:

- Study the influence of masonry infills on the behaviour of reinforced concrete framed structures
- Contribute to the acknowledgement of the different failure modes of masonry infill due to their interaction with the RC frame(in-plane failures and out-of-plane failures)
- Present and propose a simple and efficient method of designing masonry infills in reinforced concrete framed structures
- Evaluate the dynamic characteristics of such structures with regard to the presence or absence of infills.

To attend this objective, this work is divided in three chapters. The first chapter will be a review of the literature and will allow us to master basic concepts about the infill walls, the type of RC buildings and failure mechanism. The second chapter will present a methodology, which will be a guideline that will lead us to obtain our results. Finally, at the third and last chapter, the results of the analysis on different frames with and without infill walls

CHAPTER 1 LITERATURE REVIEW

Introduction

Many numerical investigations have been carried out till date, based mainly on the finite elements analysis method, concerned with the investigation of the effect of various parameters associated with the previously mentioned uncertainties (such as thickness, material properties and openings) on the overall structural response of infilled frames. In addition, experimental studies have been carried out on the same subject. Moghadam and Dowling have reported an extensive review of research on in plane testing and modelling of masonry infilled frames up to 1987. Madan et al. have presented a comprehensive review of the relevant literature published between 1987 and 1997. More updated state-of-the-art reports can be found in Crisafulli et al. and, recently, Asteris et al. However, even with this data these uncertainties have not been significantly reduced.

In order to apprehend the importance of masonry infill on the behavior of RC framed structures, this chapter is intended to provide us with an important and sufficient knowledge on the concept of masonry infills, the codes regulating masonry constructions in reinforced concrete structures, brief notes from experimental test on infill influence on the structural response of frames, the failures occurring in such structures and the design methods used till date to.

1.1. Masonry infill

1.1.1. Definition

Masonry is one of the oldest forms of construction known to humans. The term masonry refers generally to brick, tile, stone, concrete-block etc. However, many different definitions of masonry are in vogue. The International Building Code (IBC 2009) defines masonry as “a built-up construction or combination of building units or materials of clay, shale, concrete, glass, gypsum, stone or other approved units bonded together with or without mortar or grout or other accepted methods of joining.” ASTM E631 defines masonry as “construction usually in mortar, of natural building stone or manufactured units such as brick, concrete block, adobe, glass, block tile, manufacture stone, or gypsum block.” The McGraw-Hill Dictionary of Scientific and Technical Terms defines masonry as “construction of stone or similar materials such as concrete or brick.” A commonality in these various definitions is that masonry essentially is an assemblage of individual units which may be of the same or different kind, and which are bonded together in some way to perform an intended function.

1.1.2. Constituents materials of masonry infills (masonry units)

Masonry construction is accomplished by laying masonry units by hand. As such, they can be laid in a variety of arrangements. Units of different sizes can be used in the same construction. For example, various-sized rectangular units having sawed, dressed, or squared surfaces, properly bonded and laid in mortar, can be used for wall construction, an arrangement of units referred to as ashlar masonry. Masonry units can be solid or hollow. Solid masonry consists of masonry units that are solid (i.e., without any voids) and laid contiguously with the joints between the units filled with mortar.

Materials from which masonry units can be made include clay or shale, concrete, calcium silicate (or sand lime), stone, and glass. The two major types of masonry units used in general masonry construction are clay building brick and concrete building brick and blocks. Both types of units can be either solid or hollow. Examples of the other forms of masonry units are stone, cut stone, prefabricated stone, ashlar, marble, glass, autoclave aerated concrete (AAC), and thin masonry.

In construction, masonry units are assembled together with mortar joints in between them. Mortar is applied to the top and bottom horizontal surfaces of units, which are referred to as bedding areas. The horizontal layer of mortar on which a masonry unit is laid is called the bed joint. Most masonry units are rectangular, and defined by their three dimensions: width, height, and length, in that order.

1.1.2.1. Clay building brick

Second only to stone, bricks and tiles are the oldest masonry units used in construction. Clay masonry units (bricks) are formed from clay through moulding, pressing, or extrusion process. Their physical properties depend on raw materials, method of forming, and firing temperature. The latter is important because it must cause incipient fusion, a melting and joining of clay particles that is necessary for developing strength and durability of clay masonry units. They are available in a wide variety of shapes, sizes, colours, and strengths. Bricks may be solid or hollow. It is best to contact the manufacturers for their availability with regard to size, shape, and colour.

i. Solid clay units

It is a unit whose net cross-sectional area, in every plane parallel to the bearing surface, is 75% or more of its gross cross-sectional area measured in the same plane. A solid brick may have a maximum coring of 25%.

Bricks are graded according to their weathering resistance. The effect of weathering on a brick is related to the weathering index, which, for any locality, is the product of the average annual number of freezing cycle days and the average annual winter rainfall in mm. Grade requirements for face exposures are listed in figure below

- GRADE SW (Severe Weathering) bricks are intended for use where a high and uniform degree of resistance to frost action and disintegration by weathering is desired and the exposure is such that the brick may freeze when permeated with water.
- GRADE MW (Moderate Weathering) bricks are used where they will be exposed to temperatures below freezing, but unlikely to be permeated with water, and where a moderate and non-uniform degree of resistance to frost action is permissible.
- GRADE NW (Negligible Weathering) applies to building brick only and is intended for use in backup or interior masonry



Figure 1-1. Solid Clay block unit

Table 1.1: Clay bricks compressive strength and water absorption properties

Clay Brick Type	Compressive Strength (KN/m ²)*	Water Absorption (% weight/weight)
Low absorption, solid	79,299	5.7
Medium absorption, solid	45,004	12
High absorption, frog	31,800	21.8

Source: Fried and Law 1995.

* Tested in nonstandard manner of a full single brick capped with mortar on top and bottom

Types of facing bricks

- TYPE FBS (Face Brick Standard) brick is for general use in exposed masonry construction. Most bricks are manufactured to meet the requirement of Type FBS.
- TYPE FBX (Face Brick Extra) brick is for general use in exposed masonry construction where a higher degree of precision and a lower permissible variation in size than that permitted for Type FBS brick is required.
- TYPE FBA (Face Brick Architectural) brick is manufactured and selected to produce characteristic architectural effects resulting from non-uniformity in size and texture of the individual units

ii. Hollow clay units

It is a unit whose net cross-sectional area in any plane parallel to the bearing surface is less than 75% of its gross cross-sectional area measured in the same plane. Hollow clay units are classified by Grade and Type as outlined below.

Two grades of hollow brick are covered: Grade SW and Grade MW. These grades are similar to the grades for solid brick.



Figure 1-2: Hollow Clay brick units

Types of hollow brick

- TYPE HBS (Hollow Brick Standard) is for general use in exposed exterior and interior masonry walls and partitions where a wider colour range and a greater variation in size than is permitted for Type HBX hollow brick.

- TYPE HBX (Hollow Brick Extra) is for general use in exposed exterior and interior masonry walls and partitions where a high degree of mechanical perfection, a narrow colour range, and a minimal variation in size is required.

- TYPE HBA (Hollow Brick Architectural) is manufactured and selected to produce characteristic architectural effects resulting from non-uniformity in size, colour and texture of the individual units.

- TYPE HBB (Hollow Brick Basic) is for general use in masonry walls and partitions where colour and texture are not a consideration, and where a greater variation in size is permitted than is required by Type HBX hollow brick.

Dry bricks and bricks with high suction rates tend to absorb large quantities of water from mortar, which often results in poor bond adhesion hence becoming a weak spot in the structure in which it is found. Therefore, wetting the dry bricks a few hours prior to laying is advisable so the cores are moist while the surface is dry. Bricks in this condition, with a dry surface and wet core, are preferred since they tend to bond well with the mortar. Note that very wet or saturated bricks should be avoided since they may not bond well to the mortar. Saturated bricks move easily and do not stay in position (float), thus making bricklaying extremely difficult and slow. To check the internal moisture condition of a brick, the bricklayer or inspector should occasionally break a brick and observe the interior dampness condition.

Brick properties often vary significantly depending on the clay type and the manufacturer. Consultation with the local brick manufacturer is advisable for specific information on the intended brick for a project.

1.1.2.2. Concrete masonry

Load bearing concrete masonry units can be either concrete bricks or hollow load bearing concrete masonry units. Concrete bricks and hollow units are made primarily of Portland cement, water, and appropriate aggregates, with or without the addition of other materials. Concrete bricks and hollow units can be made from lightweight, normal weight, or both types of aggregates.

i. Concrete brick

Concrete bricks are usually solid units that are used for specific purposes. Some applications include the top or bearing course of load bearing masonry walls, the exterior walls of masonry fireplaces, and the construction of catch basins or manholes. Concrete brick must also be able to withstand higher compression capacity.

Unlike masonry units specified under ASTM C90, concrete brick maintain the Grade N and Grade S designation requirements.

- Grade N: For general use in walls above and below grade which may or may not be exposed to moisture or weather.
- Grade S: For use in above-grade exterior walls with weather-resistant protective coatings, or walls not exposed to weather.



Figure 1-3: Solid Concrete Block Unit

Table 1.2: Strength and absorption requirements for concrete brick

Compressive Strength, Min, For Concrete Brick Tested Flatwise (Psi)			Water Absorption Max, (Avg. Of 3 Brick) With Oven Dry Weight Of Concrete (Ib/Ft ³)		
Average Gross Area			Weight Classification		
Grade	Avg. Of 3 Concrete Brick	Individual Concrete Brick	Light Weight Less Than 105	Medium Weight Less Than 125 To 105	Normal Weight 125 Or More
N	3500	3000	15	13	10
S	2500	2000	18	15	13

ii. Hollow loadbearing concrete masonry unit

There are two categories of hollow concrete masonry units:

- Standard Units require that no overall dimension (width, height and length) differ by more than 1/8 in. from the specified standard dimensions.
- Particular Feature Units have dimensions specified in accordance with the following (local suppliers should be consulted to determine achievable dimensional tolerances):

1. For moulded face units, no overall dimension (width, height and length) may vary by more than 1/8 in. from the specified standard dimension. Dimensions of moulded features (ribs, scores, hex-shapes, pattern, etc.) must be within 1/16 in. of the specified standard dimensions and must be within 1/16 in. of the specified placement on the unit.

2. For split-faced units, all non-split overall dimensions may differ by no more than 1/8 in. from the specified standard dimensions. On split faces, overall dimensions will vary.

3. For slumped units, no overall height dimension may differ by more than 1/8 in. from the specified standard dimension. On slumped faces, overall dimensions will vary.

Concrete blocks have customarily been manufactured in modular nominal dimensions that are multiples of 8 in. (i.e., standard block are nominally 8 in. high by 16 in. long), as shown by the examples in the figure below:

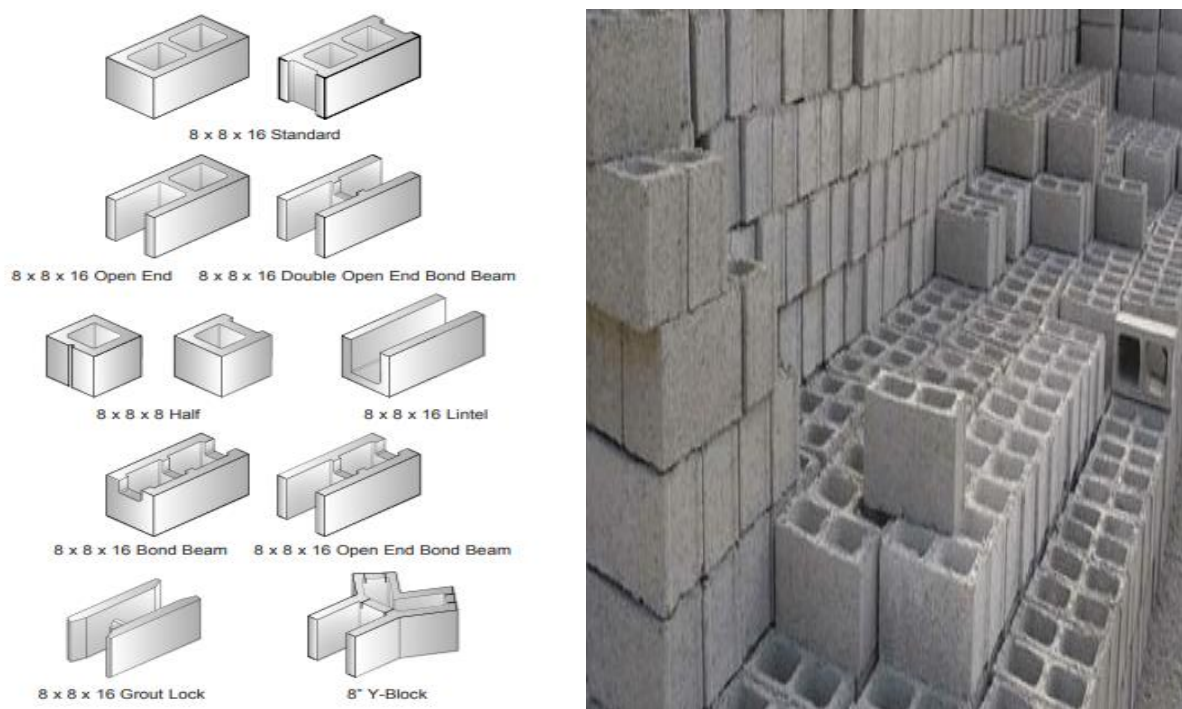


Figure 1-4. Hollow Concrete block units

Concrete block, if stored for a period of time, can achieve climatic balance and perform satisfactorily with a minimum of shrinkage. Thus, concrete block units should be protected from the weather even during storage at the jobsite. Units not covered and exposed to rain or snow at the jobsite may not meet moisture requirements until they dry. Concrete masonry units should be aged a sufficient period of time to achieve a climatic moisture balance condition. This period of time is

dependent on the materials, the moisture content, the density or permeability of the block and the humidity of the area. Construction methods have a significant influence on the performance of concrete masonry units. As the wall is constructed, the mortar head joint and the adjacent units restrain the units.

1.1.2.3. Mortar

The second component in brickwork is mortar, which for loadbearing brickwork should be a cement: lime: sand mix in a defined proportion. For low-strength bricks a weaker mortar, 1:2:9 mix by volume may be appropriate.

In deciding the type of mortar, the properties needing to be considered are:

- Development of early strength.
- Workability, i.e. ability to spread easily.
- Water retentivity, i.e. the ability of mortar to retain water against the suction of brick. (If water is not retained and is extracted quickly by a high-absorptive brick, there will be insufficient water left in the mortar joint for hydration of the cement, resulting in poor bond between brick and mortar.)
- Proper development of bond with the brick.
- Resistance to cracking and rain penetration.
- Resistance to frost and chemical attack, e.g. by soluble sulphate.
- Immediate and long-term appearance

There were originally five types of mortar which were designated as M, S, N, O, and K



Figure 1-5: Mortar used in brick joints in masonry walls.

1.1.3. Properties of masonry infills

Structural design in masonry requires a clear understanding of the behaviour of the composite unit-mortar material under various stress conditions. Masonry walls are primarily vertical loadbearing elements with compressive stress resistance as the primary design factor. However, because walls are frequently required to withstand horizontal shear forces or lateral wind pressure, the strength of masonry in shear and tension must also be considered. Current empirical values for masonry design strength have been derived from tests on piers, walls, and small specimens. While this has resulted in safe designs, it gives very little insight into the behaviour of the material under stress so that more detailed discussion on masonry strength is required.

1.1.3.1. Compressive strength

The factors set out in the table below are of importance in determining the compressive strength of masonry.

Table 1.3: Compressive Strength factors of masonry wall

<i>Unit characteristics</i>	<i>Mortar characteristics</i>	<i>Masonry</i>
Strength	Strength:	Bond
Type and geometry:	mix	Direction of stressing
solid	water/cement ratio	Local stress raisers
perforated	water retentivity	
hollow	Deformation characteristics	
height/thickness ratio	relative to unit	
absorption characteristics		

A number of important points have been derived from masonry compression tests and associated standard material tests. First, masonry loaded in uniform compression will fail either by the formation of tension cracks parallel to the axis of loading or by a type of shear failure along specific lines of weakness, the mode of failure depending on whether the mortar is weak or strong relative to the units. Secondly, it is observed that the strength of masonry in compression is smaller than the nominal compressive strength of the units as given by a standard compressive test. On the other hand, the masonry strength may greatly exceed the cube crushing strength of the mortar used in it. Finally, it has been shown that the compressive strength of masonry varies roughly as the square root of the nominal unit crushing strength and as the third or fourth root of the mortar cube strength. It is possible to conclude from these observations that:

1. The secondary tensile stresses, which cause the splitting type of failure, result from the restrained deformation of the mortar in the bed joints of the masonry.
2. The apparent crushing strength of the unit in a standard test is not a direct measure of the strength of the unit in the masonry, since the mode of failure is different in the two situations.
3. Mortar withstands higher compressive stresses in a brickwork bed joint, because of the lateral restraint on its deformation from the unit.

In masonry, the units have to resist the tensile forces resulting from restraint of the lateral strains in the mortar. Thus for given materials and joint thickness, the greater the height of the unit the greater the resistance to these forces and the greater the compressive strength of the masonry. In other words, for a given unit height, there will be a decrease in the strength of the masonry if we increase the thickness of the mortar joint. This effect is significant for brickwork, as shown in the figure below, but unimportant in blockwork where the ratio of joint thickness to unit height is small.

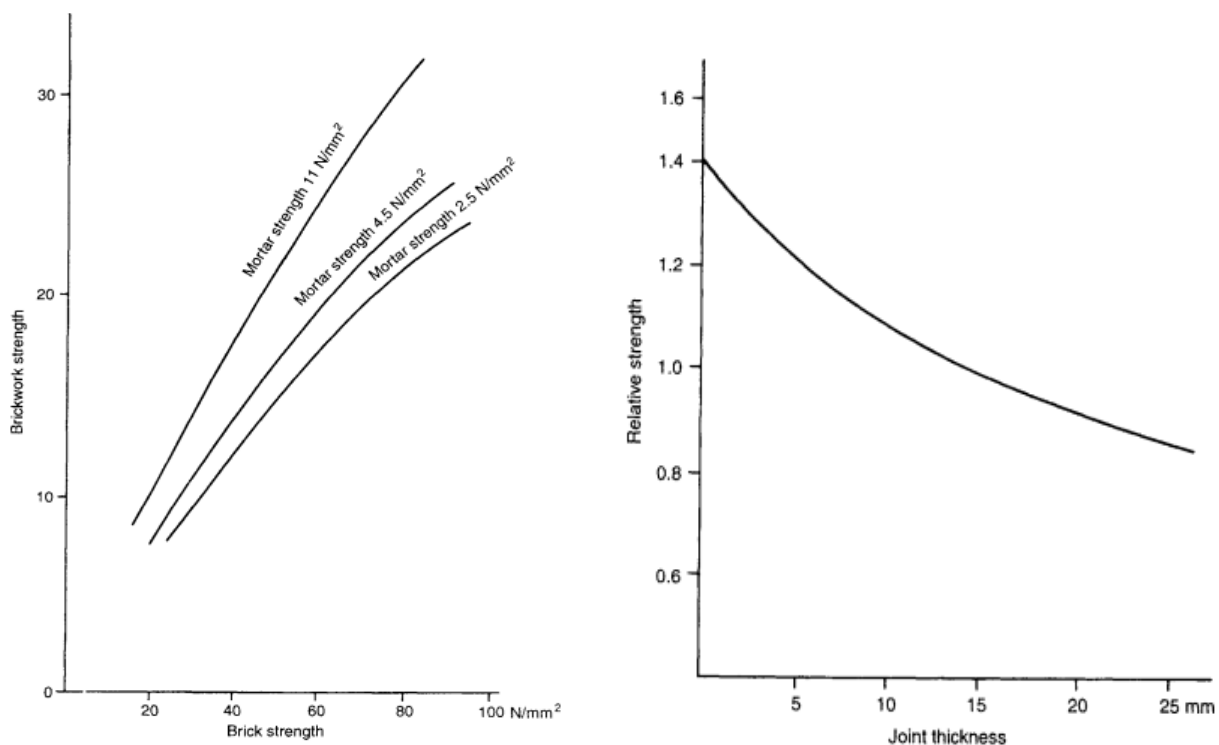


Figure 1-6: Effect of brick strength at different mortar strength (on the left) and the Effect of thickness on brickwork strength (on the right)

The strength of masonry in combined shear and compression is of importance in relation to the resistance of buildings to lateral forces. Many tests on masonry panels subjected to this type of loading have been carried out with a view to establishing limiting stresses for use in design. Typical results are shown in the figure below. It is found that there is a Coulomb type of relationship between

shear strength and precompression, i.e. there is an initial shear resistance dependent on adhesion between the units and mortar augmented by a frictional component proportional to the precompression. This may be expressed by the formula:

$$\tau = \tau_0 + \mu\sigma_c$$

Where τ_0 is the shear strength at zero precompression, μ is an apparent coefficient of friction and σ_c is the vertical compressive stress

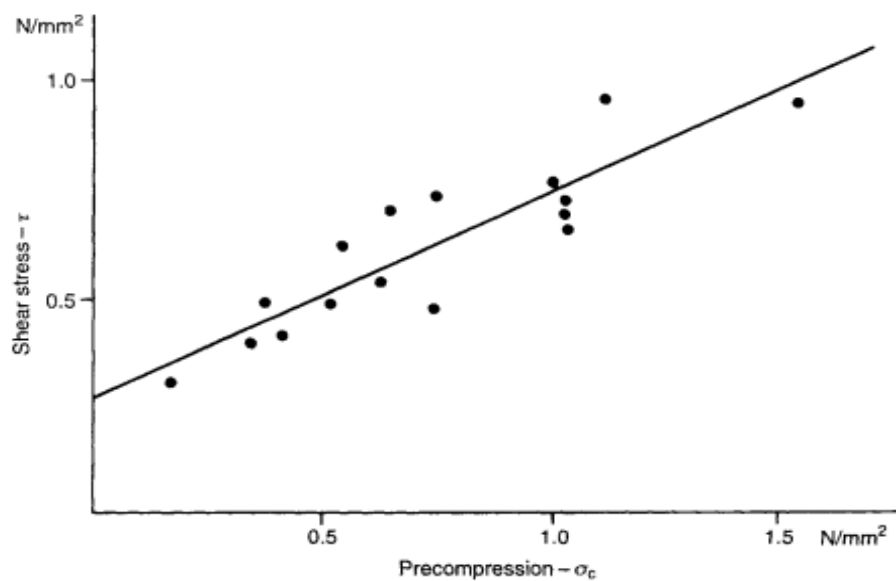


Figure 1-7: Graph of shear stress against precompression of a masonry.

1.1.3.2. The tensile strength of masonry

i. Direct tensile strength

Direct tensile stresses can arise in masonry as a result of in-plane loading effects. These may be caused by wind, by eccentric gravity loads, by thermal or moisture movements or by foundation movement. The tensile resistance of masonry, particularly across bed joints, is low and variable and therefore is not generally relied upon in structural design. Nevertheless, it is essential that there should be some adhesion between units and mortar, and it is necessary to be aware of those conditions, which leads to the development of mortar bond on which tensile resistance depends.

It is known that the grading of the mortar sand is important and that very fine sands are unfavourable to adhesion. In the case of clay brickwork, the moisture content of the brick at the time of laying is also important: both very dry and fully saturated bricks lead to low bond strength. This diagram below indicates the great variability of tensile bond strength and suggests that this is likely

to be greatest at a moisture content of about three-quarters of full saturation, at least for the bricks used in these tests. Direct tensile strength of brickwork is typically about 0.4N/mm², but the variability of this figure has to be kept in mind, and it should only be used in design with great caution.

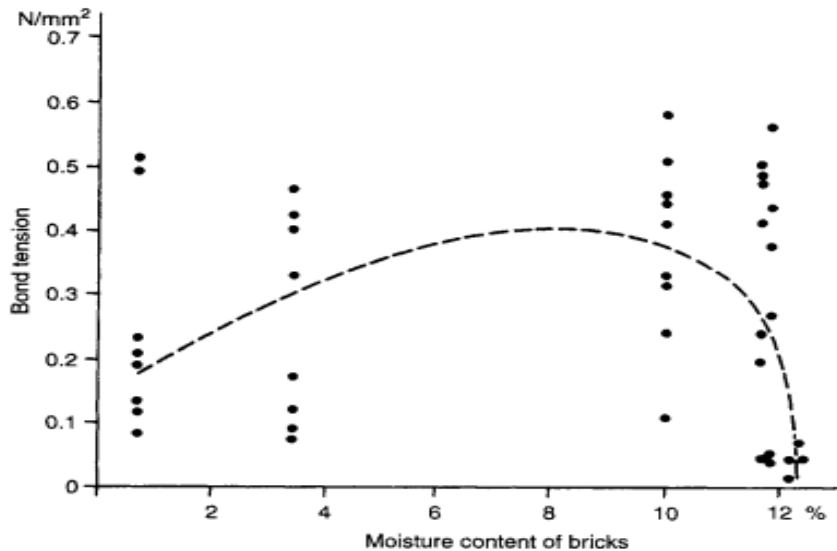


Figure 1-8: Direct tensile strength graph

ii. Flexural tensile strength

Masonry panels used primarily as building cladding must withstand lateral wind pressure and suction. The self-weight of a wall provides some stability, but it is generally insufficient to provide the necessary resistance to wind forces, so reliance must be placed on the flexural tensile strength of the masonry. The same factors that influence direct tensile bond development that were discussed in the preceding section apply to flexural tensile strength development.

1.1.3.3. Stress-strain properties of masonry

Although tests show that the stress-strain relationship in masonry is approximately parabolic, as shown in the figure below, it is generally treated as a linearly elastic material. Because masonry is stressed only up to a fraction of its ultimate load under service conditions, the assumption of a linear stress-strain curve is acceptable for calculating normal structural deformations. For calculating Young's modulus, several formulas have been proposed. This parameter, however, is rather variable even for nominally identical specimens, and it can be assumed as a rough approximation that:

$$E = 700\sigma'_c$$

Where σ_c is the crushing strength of the masonry. This value will apply up to about 75% of the ultimate strength.

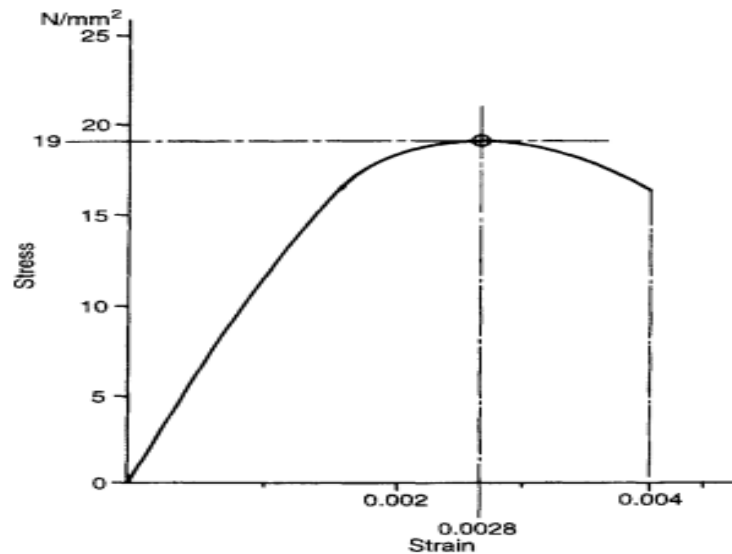


Figure 1-9: Typical stress-strain curve of brick masonry

1.1.3.4. Effects of workmanship on masonry strength

It is critical for engineers designing and constructing in masonry to understand the workmanship factors that are important in developing a specified strength. This information was obtained by conducting tests on walls with known defects and comparing the results to corresponding tests on walls without defects. In practice, these flaws will be present to some extent, and a combination of them may result in a wall that is only half as strong in compression as it should be. Some of these flaws are as follows:

- a. Failure to fill bed joints
- b. Bed joints of excessive thickness
- c. Deviation from verticality or alignment
- d. Exposure to adverse weather after laying
- e. Failure to adjust suction of bricks
- f. Incorrect proportioning and mixing of mortar.

1.2. Guidelines in national codes due to effect of masonry infill panels

The principle of calculation according to these codes consists in assimilating the assembly formed by the masonry panel and the reinforced concrete frame to a triangulated system whose diagonal elements are made up of active rods likely to form in masonry. Masonry walls act as

connecting rods diagonals subjected to compression, whereas reinforced concrete ties subjected to traction or compression, depending on the direction of the lateral loads.

Masonry infill is defined in the Eurocodes as a secondary element (non-structural element) of the structure, for a first analysis, but the participation of the walls in the resistance to lateral forces and energy dissipation can be taken into account. Dispositions specifications and prescriptions are also proposed to model the behavior of masonry fillings.

The various national codes can be grouped into two categories, those that consider the masonry Infill (M.I) and those that do not take into account the M.I.

- Very few codes recommend isolating the infill from the reinforced concrete frame, such as the stiffness of the M.I play no role in overall frame stiffness (NZS-3101 1995,). Consequently, the M.I are not considered in the analysis and the design. The isolation makes it possible to avoid the problems associated with irregularities and the fragile behavior of the infill.

- Another group of national codes prefers to take advantage of certain characteristics of infills such as their high initial lateral stiffness; in this case, the infill is rigidly connected with the frame. These codes require that the beneficial effects of infill be properly included in the analysis procedure and that adverse effects are mitigated. In other words, these codes tend to maximize the role of the M.I as the first line of defence against seismic actions, and to minimize their harmful effects through proper disposal and rigorous control of work to ensure good quality of execution

Summary of national codes on reinforced concrete frame with masonry infill.

Table 1.4: Summary of national codes on reinforced concrete frame with masonry infill.

Country / code	D	T _a	irregularity		K	Displacement	Infill			Out of plane
			plane	elevation			σ	Ki	O	
Algeria(1988)	yes	yes	x	x	1.42	x	x	x	x	x
Columbia(NSR-98 1998)	yes	yes	x	x	x	yes	x	x	x	x
Eurocode 8 (2003)	yes	yes	yes	yes	1.2	yes	x	x	yes	yes
USA (IBC 2003)	x	x	x	x	x	x	X	x	x	x
India (IS-1893 2002)	yes	yes	x	yes	x	x	x	x	x	x
FEMA- 306	yes	x	x	x	x	yes	Yes	yes	yes	yes

China(GBJ 11-98 1998)	yes	x	x	x	x	yes	X	x	x	x
Philippines (NSCP 1992)	yes	x	x	x	1.5	x	X	x	x	x

D is the need for dynamic analysis for irregular buildings, high-rise buildings, and buildings located in seismic zones.

Ta is the fundamental vibration period for the frameworks of frame with M.I

K is the ratio between the design seismic loads for frames in reinforced concrete with M.I and the design seismic load for frames without M.I.

Ki, σ are the stiffness and resistance of the M.I simultaneously.

O if we take into account the presence of openings.

For the purpose of this work, we are concerned with the following codes:

1.2.1 Eurocode 8 (EC 8)

It considers the masonry infills as non-structural elements and tends to inhibit any frame structural connection with the masonry infills through shear connectors or other ties. If structural connection is not avoidable, then considers the structure as one consisting of confined masonry and not as a RC frame with masonry infills. EC 8 requires avoiding strongly irregular, unsymmetrical or non-uniform arrangement of infills in plane and elevation. Moreover, if infill panels are irregular in plane and in elevation this irregularity shall be taken into account. EC 8 requires doubling the eccentricity in the analysis of structural systems with an asymmetric distribution of the infills in plane.

Structures on the sides with fewer infills in plane should be given more attention. They will deform more severely than the side with more infill panels. In this case, 3D structural models should be used for structure analysis, and infills should be included in the model. Elevation irregularities may result in a soft story due to the story's reduced stiffness in comparison to other stories. This type of failure can cause a building to collapse, and it appears to be the most common cause of damage for structures with infill panels. The inelastic deformation demand on the columns of the story with the reduced infills increases when the infills in the story are reduced relative to the adjacent ones. The interstory drift ratio in the story with infill panels (relative horizontal displacement of two floors divided by story height) is lower than in the story without or with reduced infills. Furthermore, EC 8

limited the interstory drift ratio or masonry infilled frames to about 1%. Large openings must be framed with reinforcement elements the entire length of the walls under this code.

Part three (3) of EC 8 (the seismic assessment and retrofitting of existing building) do not consider the masonry infills and there are no rules to consider the infill masonry panels. However, several problems are considered by the retrofitting of exiting building and not by designing new building. Hence, there is a need to extend the scope of the Part 3 of EC 8 and to consider the infill panels in the analysis of structures, providing the strength and stiffness of infill panels and to profit from the beneficial effect in the existing building.

1.2.2 Fema 273, Fema 306

In Fema 273, the masonry infills are considered as primary elements of a lateral force-resisting system. The solid infill can be modelled as equivalent strut to assess the stiffness and strength of the structure. This code recommends the following equation to compute the effective width of diagonal compression strut, w , which was developed by Mainstone (1974): The angle is computed from the equation below:

$$\theta = \arctan\left(\frac{L_m}{H_m}\right)$$

$$w = 0.175[\lambda_1 H]^{-0.4} D$$

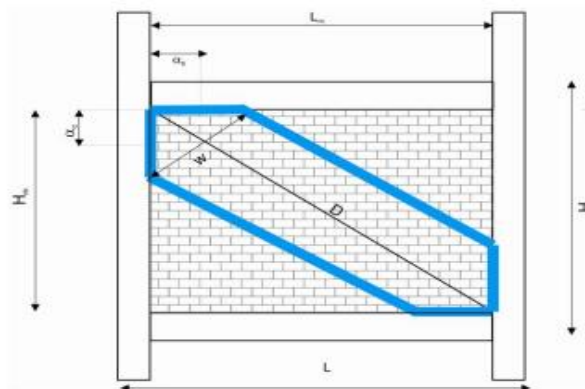


Figure 1-10: Diagonal Strut modelling

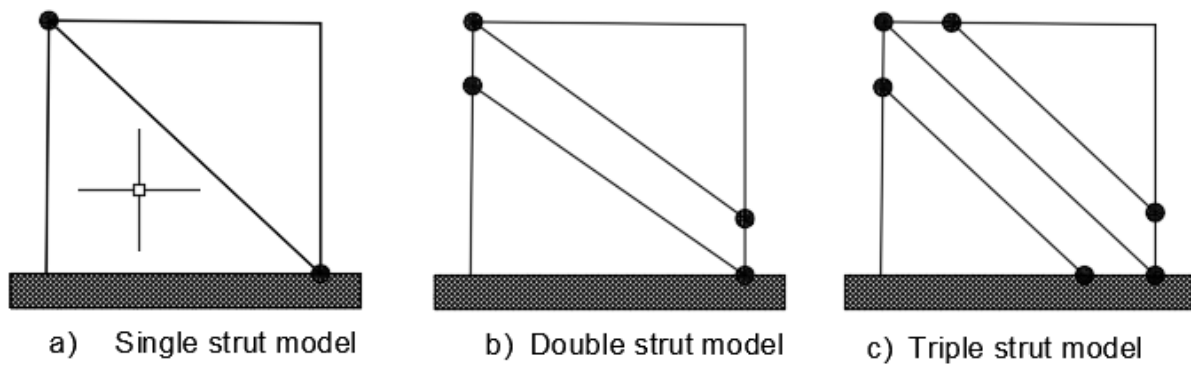


Figure 1-11: Strut Models

λ_1 is given by:

$$\lambda_1 = \left[\frac{E_m t_{inf} \sin 2\theta}{4E_{fe} I_{col} H_m} \right]^{0.25}$$

Where

- ❖ E_{me} and E_{fe} are modules of elasticity of masonry (secant modulus of elasticity between 5% and 33% of masonry prism strength) and frame material,
- ❖ D and t_{inf} are the diagonal length and actual thickness of masonry infill,
- ❖ H and H_m are the column and masonry infill height and
- ❖ θ is the inclination of diagonal strut.

For masonry infill, Fema 306 proposed four possible failure modes: sliding-shear failure, compression failure, diagonal failure, and diagonal tension failure of panel. This code contains equations that calculate the strength capacity or shear force demand of an infill panel. Furthermore, Fema 306 takes into account three distinct failure modes for RC frames: flexural failure of beam and/or columns due to reinforcement yielding, shear failure of beam and/or columns, and shear failure and bond failure of beam-column joints. Furthermore, Fema 306 specifies an interstory drift limit for different solid panels: 1.5% for brick masonry, 2% for grouted concrete block masonry, and 2.5% for ungrouted concrete block masonry. It is expected that these values are too large and these codes recommends experimental studies to verify these limit states.

1.3. Failure modes of the masonry infills

The experience of earthquakes and laboratory research produced during five decades (Thomas 1953; Wood 1958; Mainstone 1962; Liauw and Kwan 1983; Mehrabi and Shing, 1997) have highlighted various failure mechanisms of masonry infill walls. Rupture of masonry panels can develop through detachment of joints in mortar, cracking or crushing of masonry units or a

combination of these phenomena. The appearance of the different types of failure depends on the properties of the material and the state of stress induced in the panel, the resistance of the frame and the wall to the action of external stresses.

1.3.1. Failure parallel to the plane of the infill wall (In-plane)

Due to the action of the lateral force, the concrete frame and the masonry panel undergo different deformations, which leads to a state of stress which results in the rupture of the masonry. Three distinct in-plane failure mode categories are typically identified in the infilled frames (Asteris et al. 2011).

1.3.1.1. Shear Failure mode

Cracking of filler panels as a result of the action of shear force is the most frequent failure mechanism observed in both earth and laboratory tests. The failure mechanism is controlled by resistance to shear of the mortar layer, the tensile strength of the bricks and the ratio between shear stresses and normal stresses. Depending on the combination normal and tangential stresses, cracks can affect the panel either through the bricks, or by breaking away along the mortar joints.

i. Horizontal sliding along the mortar joint

Infill sliding shear failure mode in which the panel experiences horizontal sliding through multiple bed joints. It can occur when the mortar has poor mechanical properties and the infill aspect ratio is quite low, implying a significant horizontal component of the truss action. A factor contributing to the formation of horizontal cracks is the ratio between the size actual brick size and masonry panel dimensions. This type of failure has been mainly observed in non-integral infilled frames with low normal forces and with low to medium aspect ratios (height to the length of infill). This failure mode indicates a short-column behaviour and plastic hinges can generate at the mid-height of the column.



Figure 1-12: Horizontal cracks on masonry wall

ii. Stepped cracking along the mortar joints

When the mortar joints are weak in compression with the masonry units diagonal cracking can occur from one loaded corner to the other. This type of failure has been observed consistently in laboratory test and is the common failure mode of the infilled masonry.



Figure 1-13: Step cracking along mortar joint on masonry wall.

1.3.1.2. Compressive Failure Mode

The compression failure of the masonry panel can follow two different mechanisms resulting from the stresses that develop along the compressed diagonal and in corner areas.

i. The Diagonal compression mode

Infill diagonal compression failure mode, which consists of crushing of the panel centre. This failure mode usually occurs in slender infills, placed eccentrically with respect to the axis of the frame, and is accompanied by out-of-plane deformations and eventually collapse; in this mechanism, diagonal cracks occur from one loaded corner to the other. In this case, the infill develops a diagonal strut with a compressive strength conditioned to masonry thickness, compressive strength of masonry and the length and height of infill. This type of failure occurs as a result of diagonal tension cracking. If the masonry is horizontally reinforced or if the solidarity with the concrete frame is very good (the situation confined masonry, where concrete elements poured after the execution of the masonry), the cracks are small and spread over a large area in the masonry panel. In the other cases, the degradation is concentrated in a few cracks with large openings.



Figure 1-14: Diagonal cracks due to compressional forces on wall

ii. The Corner-crushing mode

Infill corner crushing failure mode, which consists of crushing in a loaded corner area of the infill panel due to a biaxial compression state. This normally occurs when the structure has a weak infill panel surrounded by strong columns and beams with weak infill-frame interface joints. The corner crushing occurs in the loaded corner due to a biaxial compression-compression stress. This failure indicates often a distinct diagonal strut mechanism with two distinct parallel cracks



Figure 1-15: Corner-crushing occurring on masonry wall.

1.3.1.3. Flexural Failure Mode

i. Flexural cracking

In this case, flexure effects are predominating (multi-storey infilled frames), the columns are very weak and a low reinforcement ratio induces the yielding of flexural steel in the windward column.

1.3.2. Failure in the plane perpendicular to the wall (out of plane)

Due to the action of forces in the direction perpendicular to the plane of the panel, it can be detached from the concrete frame. Some standards distinguish the bending failure in two distinct situations.

Out-of-plane effects cause failure in which damage occurs in the central region of the filler panel due to the arching action of the infill wall. This failure mode can occur for two reasons: inertial forces in the direction perpendicular to the plane of the wall, or the out-of-plane buckling instability of the filling associated with a relatively thin infill (Mosalam and Günay 2012). In the first circumstance, the combined effect of out-of-plane and in-plane forces reduce the infill resistance in both directions, which increases the likelihood of both out-of-plane and in-plane failure. A failure due to the second reason is rarely observed: it requires a high slenderness ratio of the infill, which results in out-of-plane buckling of the infill under loading in the plan. This phenomenon is however

very rarely encountered in very thin panels. (Infill panels are designed to meet acoustic insulation requirements and fire protection.) with a height / thickness ratio of value medium, a high lateral force being necessary to cause the disintegration of the masonry.

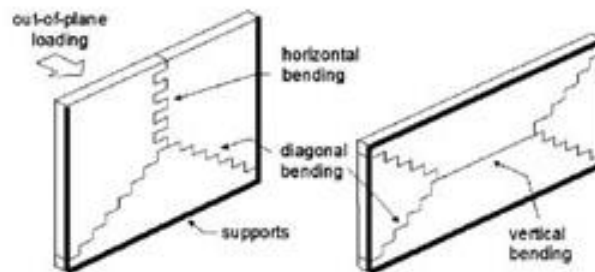


Figure 1-16: Usual crack pattern for a wall under bi-axial bending.

It should be noted that the out-of-plane failure of the infill walls creates a risk of mortal danger due to falling debris. Among the experimental tests, we can cite those carried out by Abrams (1994) and Mander (1994). As a result of tests carried out at the University of Tennessee, several factors have been identified that influence the ability to resist a perpendicular action: stiffness in the plane (determined by the size of the frame elements), the normal pre-existing stresses, the general properties of the wall and the eccentricity of the wall in relation to the frame.

Eurocode 8 defines measures to avoid failure by bending of the wall, in particular for walls with a slenderness coefficient (the ratio between the value maximum of the length and respectively of the height and thickness of the panel) of more than 15. These include, among other things, anchoring the wall in the frame that borders it to avoid the collapse.

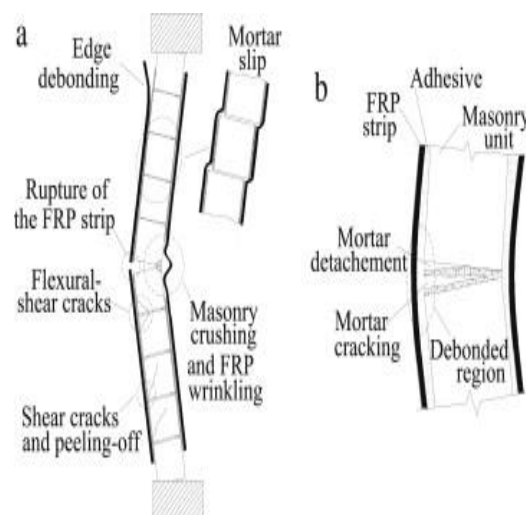


Figure 1-17: Possible out of plane cracks on a masonry wall.

1.4. Failure modes of the reinforced frame structure

Different failure mechanisms can develop in the surrounding setting by depending on the properties of the structural components, the frame and the panels of filling, and the interaction between them.

1.4.1. Flexural Collapse

When plastic hinges are developed at the ends of the columns with maximum bending moment, flexural collapse may occur in infilled frame. The plastic hinges in the columns do not always cause the collapse of the structure because the system behaves as a braced system until the masonry panel fails. The sliding shear in masonry infill can develop plastic hinges in the middle height of columns. This effect is named as knee-braced frame.

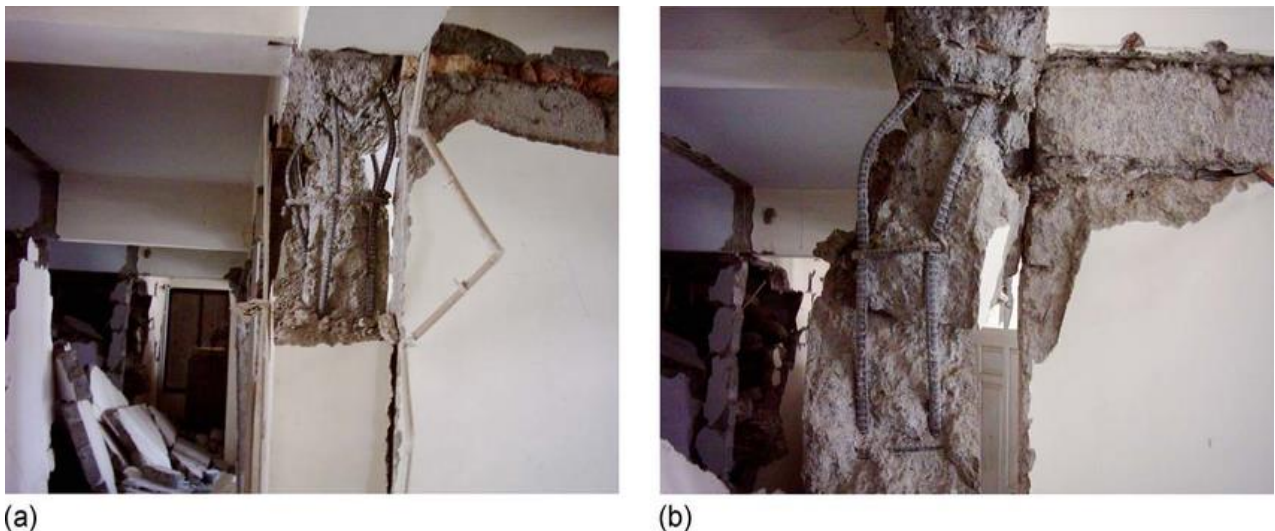


Figure 1-18: Flexural collapse on a column with the development of a plastic hinge.

1.4.2. Failure due to axial load

Gravity loads and the truss mechanism produce axial compressive forces in the columns. Buckling of the longitudinal reinforcement may occur due to severe cyclic loading and resulting in a compressive failure. However, this failure mode is not very common because of high compressive strength of the columns.

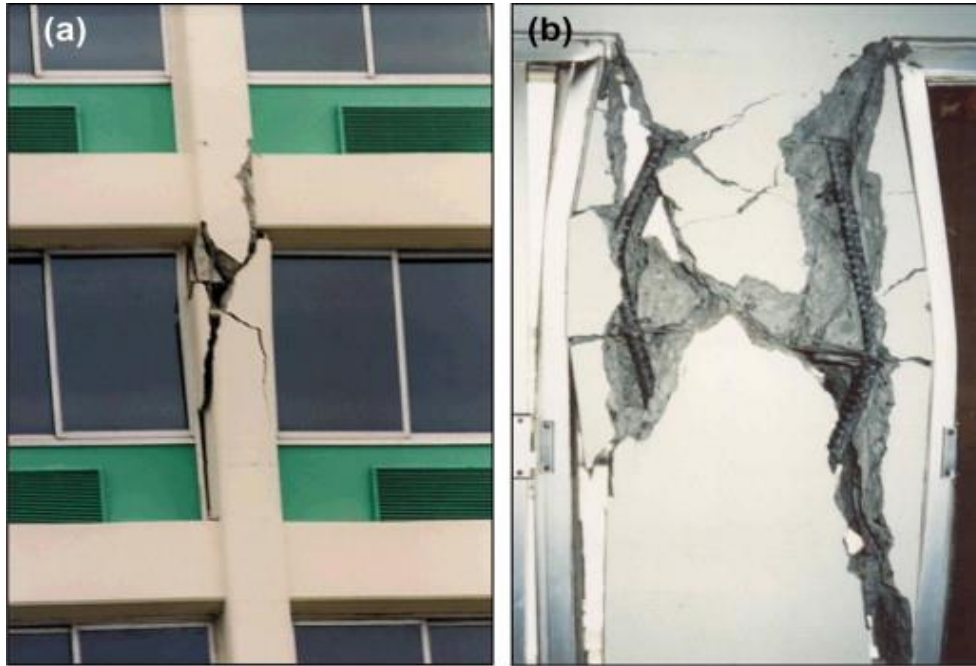


Figure 1-19: Column failure due to axial load.

1.4.3. Shear failure of the column

The shear forces in the columns may exceed the maximum along the contact length, near the loaded corner. One or more diagonal cracks appear in columns. Horizontal Sliding along mortar joints expedite the shear failure of the column due to develop a short column effect. This type of failure can be avoided by providing a sufficient amount of transverse reinforcement and length of concrete shear.



Figure 1-20: Shear failure on column

1.4.4. Beam-column joint failure

Large shear forces and bending moment in the loaded corner and along the contact length in the zones near loaded corner can develop wide diagonal cracks running across the from the interior to exterior corner.

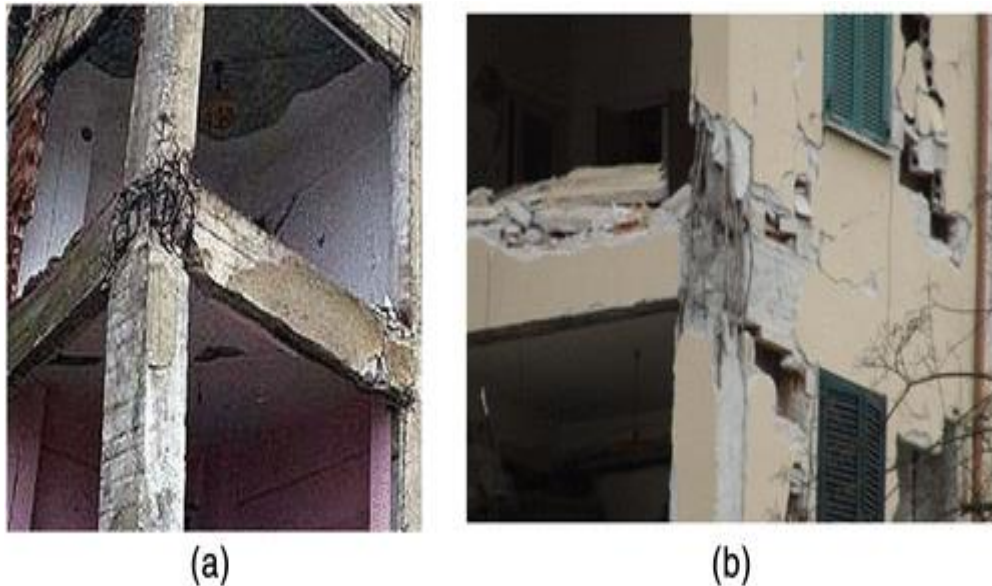


Figure 1-21: Failure at the beam-column joint due to large shear forces and bending moment in the loaded corner

1.5. Failure of the frame-infill composite

Infill panel influence on the structural response of frames. The in-plan and in-elevation geometrical distributions of the infill panels play a major role on the global response of structures subjected to lateral loads. A plan-irregular infill distribution may cause strong torsional effects, especially in the elastic domain, leading to larger-than-expected demands in the perimeter elements. Fardis et al. (1998) performed a shake table test on a single bay, two-storey, in-plan square RC frame structure with an eccentric arrangement of masonry infills. The frame was subjected to bidirectional ground accelerations. They clearly showed that the infills generated torsion on the structure. A common example of an in-elevation irregular distribution encountered all over the world is a frame structure with all storeys infilled, except for the base storey, typically used as commercial or parking space. This irregular configuration, when unaccounted for during design, may lead to the well-known and too-often observed soft-storey mechanisms with large lateral drifts in the base columns, with the upper floors displacing predominantly as a rigid body.



Figure 1-22: Soft-storey mechanisms due to absence at the first floor of the building.

In other cases, when the frames are partially infilled with a stiff material or when the column height is partially restrained, a short column effect may take place. This configuration may trigger shear failures in the columns. However, if the infills are well distributed and present in all storeys, those may provide most of the earthquake resistance and prevent collapse of relatively flexible and weak RC structures (Decanini et al. 2004, Fardis 2000, Kakaletsis and Kalayannis 2008).

1.6. Brief notes from experimental test on infill influence on the structural response of frames

➤ Fardis et al. (1998) [09] performed a shake table test on a single bay, two-storey, in-plan square RC frame structure with an eccentric arrangement of masonry infills. The frame was subjected to bidirectional ground accelerations. They clearly showed that the infills generated torsion on the structure. A common example of an in-elevation irregular distribution encountered all over the world is a frame structure with all storeys infilled, except for the base storey, typically used as commercial or parking space. This irregular configuration, when unaccounted for during design, may lead to well-known and too-often observed soft-storey mechanisms with large lateral drifts in the base columns, with the upper floors displacing predominantly as a rigid body. In other cases, when the frames are partially infilled with a stiff material or when the column height is partially restrained, a short column effect may take place. This configuration may trigger shear failures in the columns.

➤ However, Decanini et al. 2004, Fardis 2000, Kakaletsis and Kalayannis 2008 showed that if the infills are well distributed and present in all storeys, those might provide most of the earthquake resistance and prevent collapse of relatively flexible and weak RC structures.

➤ Infills give a significant contribution to the energy dissipation capacity, reducing the dissipation energy demands in frame elements and decreasing significantly the maximum displacements (Liberatore et al. 2004). It was experimentally proven that infills affect the response of the entire system through their strength and its correspond drift, but not always through their stiffness (Fardis 2000, Hashemi and Mosalam 2006, Griffith 2008, Baran and Sevil 2010).

➤ Kappos and Ellul (2000) shows that at serviceability level over the 95% of the energy dissipation is given by the infills, while at higher demand levels those dissipate around 40% of the total energy, being the rest dissipated by the RC frames. Therefore, infills represent the first line of resistance under moderate and strong motions and should be considered in both analysis and design to avoid a brittle collapse.

➤ Given the complexity of the frame-infill interaction, the overall lateral frame capacity cannot be Masonry infilled frame structures: state-of-the-art review of numerical modelling computed as the mere sum of the frame and infill contributions (Shing and Mehrabi 2002). The relative stiffness and the relative strength between infill panels and columns govern the overall system failure sequence (Stafford Smith 1967).

➤ The presence, size and position of the openings lead to a reduction of the panel stiffness and strength (Syrmakezis and Asteris 2001, Mondal and Jain 2008, Mohebkhah et al. 2007, Papia and Cavaleri 2001, Asteris 2003, Fiorato et al. 1970) and the load pattern within the panel is modified. Mosalam et al. (1998) identified strut-and-tie models that can reproduce the behaviour of panels with openings. However, predicting the strength of an infill with openings by means of simplified trusses remains a difficult task.

➤ If the panel is stiff with respect to the frame and the columns are not ductile, a shear failure in the frame may suddenly occur (Fig. 1.23 (b)). On the other hand, when the frame elements are flexible, the panel infill is expected to fail, and the overall behaviour is ductile (Fig.1.23 (c)). In some cases infill panels work as shear walls, despite not being designed for this purpose, and prevent collapse of non-ductile concrete frames (Patel and Pindoria 2001).

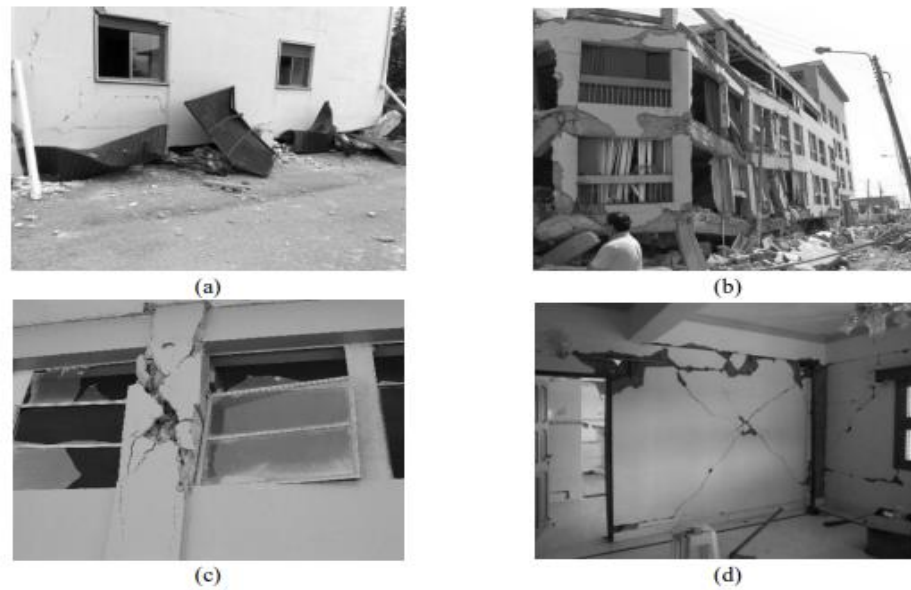


Figure 1-23: Failure of masonry wall and reinforced concrete frame

1.7. Design and calculation of reinforced concrete structures with masonry infill

The high cost of experimental campaigns and the need for accounting for the infills' contribution to the overall frame response led to the development of several numerical procedures, which are particularly important for the seismic assessment and retrofit of existing RC buildings. Three main approaches are identified for the infill models and in general immerse in the finite element method: micro-modelling (Fig 1.24(a)), meso-modelling (Fig 1.24(b)) and macro-modelling (Fig 1.24(c) and (d)). The first considers the detailed micro-modelling and the simplified micro-modelling; between the micro and macro-modelling, another technique level called meso-modelling could be considered. All the above approaches mainly differ in the degree of modelling detail of the infill panel, more specifically as (Lourenço 1996):

- Detailed micro modelling: Bricks and mortar joints are discretized using continuum (smeared) elements, with the brick-mortar interface represented by discontinuous elements.
- Simplified micro modelling: The bricks are modelled as continuum elements, while the behaviour of the mortar joints and of the brick-mortar interface are lumped in discontinuous elements.
- Meso-modelling: Bricks, mortar and brick-mortar interface are smeared out and the masonry is treated as a continuum, which means a new equivalent material representing the entire infill panel

obtained by a homogenization process. Contact, gap or spring elements can be considered for modelling the interface infill-frame.

- **Macro-modelling:** It refers to analyses that use frame elements and typically considers the infill presence through equivalent strut models. This approach – faster and easier to apply with today’s computational tools and speeds - is of greater interest for designers and engineers.

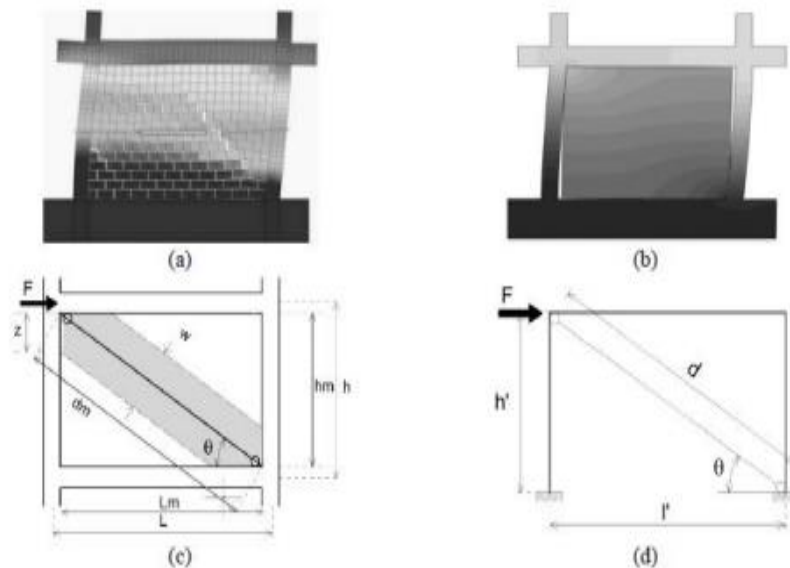


Figure 1-24: Finite element models for infill panels adapted respectively (Crisafulli, al.2000, Amato and al.2008)

1.7.1. Methods based on the finite element theory (micro modelling technic)

Over the last two decades, powerful computational platforms and faster computers have eased the development of refined micro-models. This term properly refers to the representation of each single element belonging to the system, such as the bricks and the mortar layers of the masonry infill panel or the concrete and reinforcement of the RC frame (e.g. detailed micro-modelling). Typically, such a detailed discretization is obtained by means of the finite element method (FEM) or the discrete element method (DEM). Micro-modelling are in general more precise than macro-models and can trace several possible failure mechanisms (for example, they can explicitly compute the contact zones between infill and frames and their evolution during a time history analysis).

However, these techniques require calibration of a high number of parameters for the material constitutive laws and proficiency in the use of finite element procedures, hence resulting today more suitable for research purposes or calibration of simplified strut models.

1.7.1.1. Equivalent method (macro modelling technic)

Several simplified models are proposed to reproduce the major aspects of the infill-frame interaction mechanisms. Polyakov (1960) first observed that the panel could be considered as a bracing diagonal. Here the panel was represented by a diagonal strut element that took into account the lateral stiffness and eventually the strength and post-peak behaviour of the panel.

For monotonic loads, one strut in the compression diagonal is needed, while two struts along the two diagonals are typically used for cyclic loads. The proposed models vary from single to multiple struts, from concentric to eccentric, from linear elastic to non-linear hysteretic.

The diagonal strut is usually connected to the intersection points of the beam and column centrelines, which implies that the numerical strut length is greater than the physical diagonal infill length. Multiple strut models have been proposed to at least partially address this issue. When openings are present, the problem complicates further. For the strut geometric properties the cross area is typically given by the panel thickness times an equivalent width, w . The length of the diagonal of the panel gives the length of the strut, d . The width can be computed considering the relative stiffness between the infill and the frames or indirectly evaluating the contact length between them. Recently, the influence of vertical loads has been incorporated into the width evaluation (Amato et al. 2008).

The typical equations to compute the equivalent width are presented in Table 1.5 in chronological order.

Table 1.5: Summary of expressions proposed to compute w/d

Author (year)	Equation	Observation
Holmes (1961)	$w/d = 1/3$	$\lambda_h < 2$,
Stafford Smith (1967)	$0.10 < w/d < 0.25$	The value graphically depends on λ_h
Mainstone (1971)	$w/d = 0.16 \lambda_h^{-0.3}$	For λ_h see Eq. (1)
Mainstone (1974)	$w/d = 0.17 \lambda_h^{-0.4}$	Adopted by FEMA-274 (1997), FEMA-306 (1998)
Bazan & Meli (1980)	$w = (0.35 + 0.022\beta)h_m$	$0.9 \leq \beta \leq 11$ For β see Eq. (3)

Hendry (1981)	$w = \frac{1}{2} \sqrt{z_b^2 + z_c^2}$	For z_b and z_c see Eq. (5)
Tassios (1984)	$w/d = 0.20\beta \cdot \sin\theta$	$1 \leq \beta \leq 5$
Liau & Kwan (1984)	$w/d = \frac{0.95 \sin 2\theta}{2\sqrt{\lambda_h}}$	$25^\circ \leq \theta \leq 50^\circ$
Decanini & Fantin (1987) For uncracked panels	$w/d = 0.085 + \frac{0.748}{\lambda_h}$	$\lambda_h \leq 7.85$
	$w/d = 0.130 + \frac{0.393}{\lambda_h}$	$\lambda_h > 7.85$
Decanini & Fantin (1987) For cracked panels	$w/d = 0.010 + \frac{0.707}{\lambda_h}$	$\lambda_h \leq 7.85$
	$w/d = 0.040 + \frac{0.470}{\lambda_h}$	$\lambda_h > 7.85$
Paulay & Priestley (1992)	$w/d = 1/4$	$\lambda_h < 4$
Durrani & Luo (1994)	$w/d = \gamma \cdot \sin 2\theta$	$\gamma = 0.32 \sqrt{\sin 2\theta} \left(\frac{h^4 E_m t}{m E_c I_c h_m} \right)^{-0.1}$ $m = 6 \left(1 + \frac{6 E_b I_b h}{\pi E_c I_c L} \right)$
Flanagan & Bennet (1999)	$w = \frac{\pi}{C \cdot \lambda_h \cos\theta}$	C is an empirical value dependent on the in-plane drift displacement For λ^* see Eq (6)
Cavaleri <i>et al.</i> (2005) Amato <i>et al.</i> (2008)	$w/d = \frac{k \cdot c}{z (\lambda^*)^\beta}$	c and β are coefficients that takes into account the Poisson module, k takes into account the vertical load and z is a geometrical parameter.

The relative stiffness between the infill and the column may be evaluated through the dimensionless parameter λ_h , first proposed by Stafford Smith (1967)

$$\lambda_h = h \left[\frac{E_m * t * \sin 2\theta}{4 E_c I_c h_m} \right]^{1/4}$$

Where t and h_m are the thickness and height of the infill panel, respectively; E_m and E_c are the masonry and concrete moduli of elasticity, respectively; θ is the inclination of the panel diagonal; I_c is the column moment of inertia and h is the column height to the beam centrelines. λ_h decreases as the column becomes stiffer than the masonry panel.

Furthermore, Stafford Smith (1967) proposed an expression to compute the contact length z between panel and frame. It stems from the analogy between the panel-frame contact problem and beam on elastic foundation subjected to a concentrated load

$$z = \frac{\pi}{2\lambda_h} h$$

From this formula, it can be seen that the interaction between the frame and the panel is governed by the stiffness of the column and infill

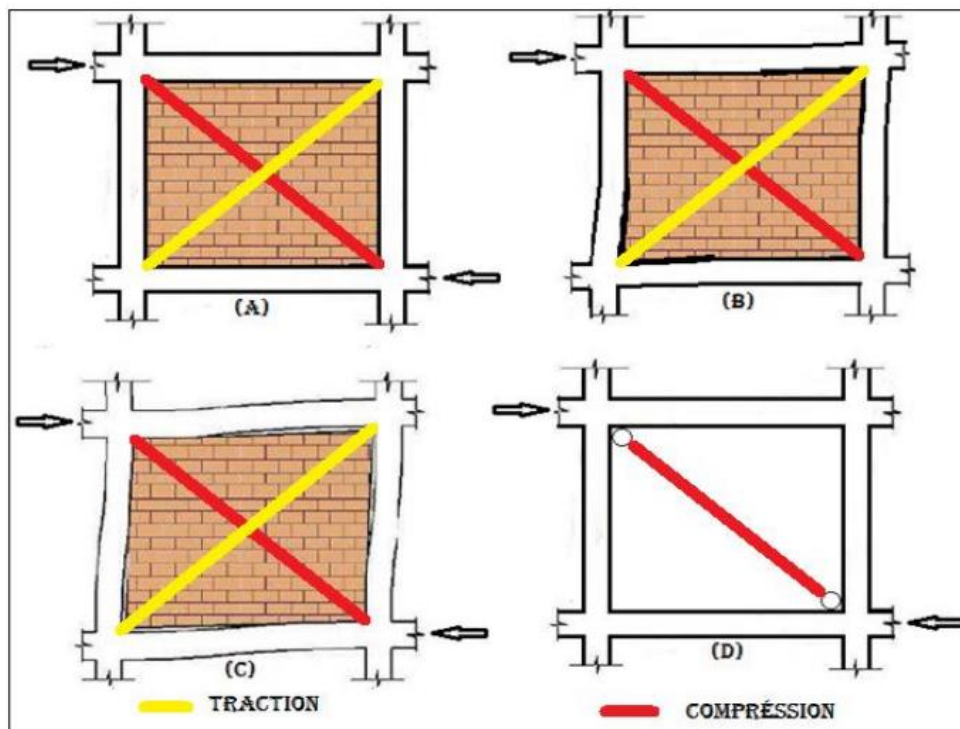


Figure 1-25: Behaviour of the filled frame under horizontal loading.

Conclusion

The infill-frame interaction has been studied experimentally, analytically and numerically especially in seismic prone countries. Some of the results show that uniformly and regularly distributed infill panels may improve the structural behaviour due to a generalized increment of the lateral stiffness and strength at the early loading stages and due to the energy dissipation capacity. However, irregular infill distributions, or no uniform infill cracks and failures may trigger undesired soft storeys and/or torsional behaviour and partial infills may also trigger short column phenomena. In this chapter, contribution of infill walls on the performance of framed structures were investigated and an overview of the modelling methods of infill walls in reinforced concrete frames is presented widely. Various researchers proposed different analytical models to describe the behaviour of the frames with infill walls. There are two main different approaches on modelling infill panels have been used. Micro model based on the finite element techniques while macro model is the equivalent strut method. One of the analytical models –macro modelling- has been used widely due to simple and efficient computational process. On the other hand, macro modelling is not capable of giving any further information about the failure mechanism of the frame and wall-frame interaction, which is provided in the micro-modelling approach. The next chapter will be dedicated to the methodology adopted for the task to be done in this work.

CHAPTER 2: METHODOLOGY

Introduction

In order to study the contribution of masonry infill wall in the behavior of a reinforced concrete framed building, a nonlinear dynamic analysis and a modal analysis are performed on the building. By analyzing the entire structure with the masonry infill included, the contribution of infill walls is demonstrated globally. To achieve plausible results, it is also necessary to define the contribution and behavior of each structural element. This work will be completed in the following steps: The first step is to identify the site through documentary research, followed by data collection. The second and third steps will be the designing and modeling of structural elements of the structural, followed by the analysis.

2.1. Site recognition

The site recognition will be achieved out through documentary research, with the primary goal of learning the location of the site, as well as the climate, geology and hydrology parameters in the region.

2.2. Site visit

The goal of this activity is to describe a building description based on observations and presentations of the building category, dimensions, floor plans, and elevation configuration.

2.3. Data collection

Two types of information will be collected namely those related to the site's topography (topographic data) and those related to the structure (structural data).

2.3.1. Topographic/relief data

The topographic data will be obtained from documentary researches on the region of our case study.

2.3.2. Structural data

Structural data are related to the structural plan of each level and include the position of structural elements like the beams, columns, and foundations, as well as the concrete core and material characteristics.

2.3.2.1. Design codes

For our work, the codes and standards norms that will be used for the design of elements are:

- EN 1990 Eurocode 0: Basis of Structural Design
- EN 1991 Eurocode 1: Actions on structures
- EN 1992 Eurocode 2: Design of concrete structures
- The FEMA 356 for infill walls modelling

These standards define the loads and the combination of loads for the design.

2.3.2.2. Applied loads

To carry out the analysis, the different type of loads applied on the structure should be considered. There are permanent loads and variable loads.

a. Permanent loads

It is the sum of structural and non-structural members' self-weight. The structural elements' self-weight is calculated by multiplying the specific weight of concrete by the cross - sectional area of the elements, and the self-weight of the secondary element is specified in the Eurocode. The self-weight is considered in action combinations as a single action.

b. Variable loads

They are loads caused by the building's occupancy and can differ from one area to the next. If an area is subjected to different imposed loads, the most critical should be considered for design and analysis. The magnitude of the imposed loads is determined by the building categories, as shown in tables A2 and A3 of the annex.

2.3.2.3. Load combination

As the name implies, a combination of actions consists of a set of load values applied to the structure at the same time to verify its structural reliability for a given limit state (design limit states). When designing a building, the sign "+" means "combined with"; different load combinations are defined as follows.

a. Fundamental load combination

The fundamental load combination at ultimate limit state (ULS) is written as follow:

$$\sum_{i \geq 1} \gamma_{G, j} G_{k, j} + \gamma_{Q, 1} Q_{k, 1} + \sum_{i > 1} \gamma_{Q, i} \Psi_{0, i} Q_{k, i}$$

The coefficients $\gamma_{G, j}$ and $\gamma_{Q, i}$ are partial factors or safety coefficients, which minimize the action which tends to reduce the solicitations and maximize the one which tends to increase it. The values of these partial factors recommended by the Eurocode 0 for the structural and Geotechnical (STR and GEO) verifications are:

$$\gamma_G = 1.35 \text{ when unfavorable}$$

$$\gamma_G = 1 \text{ when favorable}$$

$$\gamma_Q = 1.50 \text{ When unfavorable or } 0 \text{ when favorable.}$$

b. Rare load combination

The characteristic combination (rare), used for non-reversible serviceability limit states (SLS) to be used in the verifications with the allowable stress method is:

$$\sum_{j \geq 1} G_{k, j} + Q_{k, 1} + \sum_{j > 1} \Psi_{0, j}$$

2.4. Design of Structural Elements

Each element in the structural frame serves a specific purpose and behaves differently when subjected to loading. The concrete cross section, steel reinforcement section, and spacing are all determined by structural element design.

2.4.1. Durability and concrete cover

Concrete cover is the least distance between the surface of embedded reinforcement and the outer surface. It is crucial to protect the steel reinforcement from corrosion caused by environmental effect. It also protects the structural reinforcement from fire. For concrete structures, Eurocode 2 ensures this protection by the definition of a concrete cover taking into account the structural class of the structure and the exposure class. The concrete cover is illustrated below.

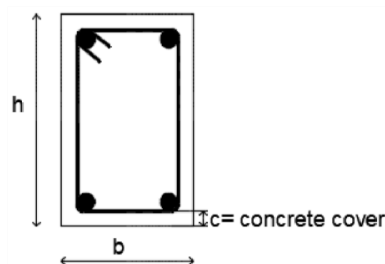


Figure 2-1 Illustration of the concrete cover

The nominal value of the concrete cover is defined as a minimum cover C_{min} plus an allowance in the design for deviation. The minimum cover C_{min} is defined in equation below as:

$$C_{min} = \max(C_{min,b}; C_{min,dur} + \Delta C_{dur,\gamma} - \Delta C_{dur,st} - \Delta C_{dur,add}; 10mm)$$

Where:

$C_{min,b}$: the minimum cover due to bond requirement, equal to the diameter of the bars or the equivalent diameter in the case of bundled bars

$\Delta C_{dur,\gamma}$: the additive safety element with a recommended value of 0 mm

$\Delta C_{dur,st}$: reduction of minimum cover for use of stainless steel

$\Delta C_{dur,add}$: the add reduction of minimum cover for use of additional protection

$C_{min,dur}$: the minimum cover due to environmental conditions obtain from the table of the annex A1 gives the concrete cover in function of the exposure and the structural class of the building.

The annex A1 gives the concrete cover in function of the exposure and the structural class of the building.

The nominal value of the concrete cover is then expressed by:

$$C_{nom} = C_{min} + \Delta C_{dev}$$

Where:

ΔC_{dev} is the allowance in design for deviation with a recommended value of 10 mm.

2.4.2. The Beams

Reinforced concrete beams are structural elements intended to support transverse external loads. Across their length, the loads generate bending moments, shear forces, and, in some cases, torsion. The rectangular cross section is the most common type of concrete cross section. Certain assumptions must be made before the design of a reinforced concrete beam can begin. To obtain the solicitation parameters and curves, materials, section properties, loads, load combinations, restraints and constraints, and other design parameters are defined and assigned to the beam. For each solicitation parameter, the envelop curve is then calculated. This calculation is performed using the working width corresponding to the section being calculated.

2.4.2.1. Ultimate Limit State design

Under ULS, the beam will be verified for bending moment and shear force solicitations as there are no axial forces on the beam.

a. Bending moment design

Design for bending moment is done with the envelope curve of the bending moment solicitation parameter. Provisions given by Eurocode 2 recommend moment reduction at the support as shown in the figure below. For continuous beams, the value depends on the connection between the beam and the support

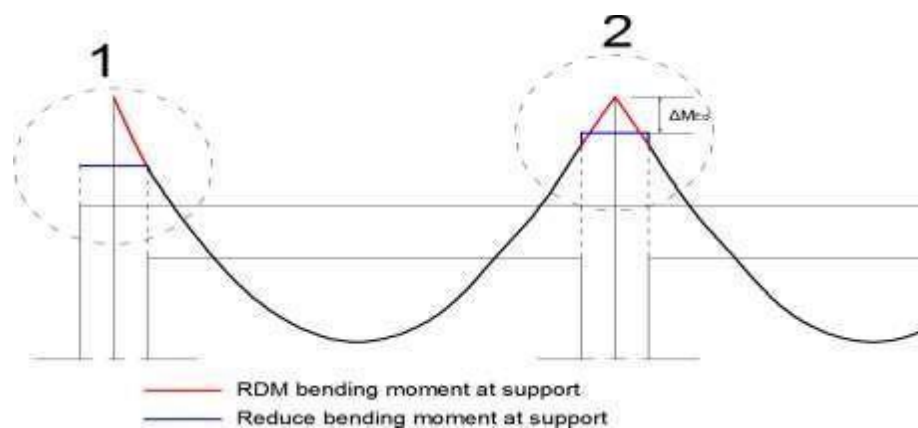


Figure 2-2: Moment reduction at supports (Djeukoua 2019)

When a beam is monolithic with its supports, the critical design moment at the support should be assumed to be that at the support's face. As illustrated in Figure 2.2(1).

If, on the other hand, the beam is continuous over a support (Figure 2.2(2)), the analysis is performed with the assumption that the support does not provide any rotational restraint. The amount of this reduction is given by:

$$\Delta M_{Ed} = F_{Ed} * t / 8$$

Where:

t: is the breadth of the support

F_{Ed} , is the design of the support

The curve used for design is obtained by doing a shift of the moment curve a distance of a_i in the worst direction as it is illustrated in Figure 2.3 below, accounting for the additional tensile force.

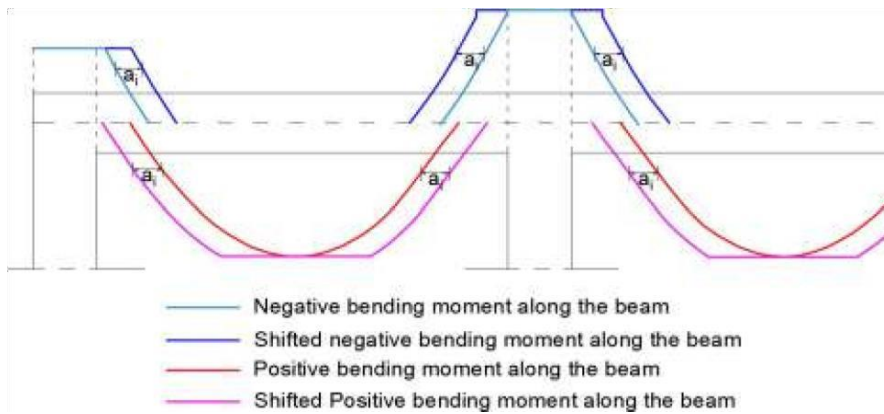


Figure 2-3: Shifting of the moment curve representation (Djeukoua 2019)

The value of a_i is computed as thus;

$$a_i = (\cot\theta - \cot\alpha)/2$$

Where:

z : Is the inner lever arm

θ : Angle of concrete compression strut to the beam axis

α : Is the angle between shear reinforcement and the beam axis perpendicular to the shear force.

i. Longitudinal steel reinforcement

The quantity of longitudinal reinforcements is then determined with values of bending moment obtained in the shifted curve. The section of the beam is a rectangular one. The longitudinal steel reinforcement is computed using.

$$A_s = \frac{M_{Ed}}{0.9 * d * f_{yd}}$$

According to the Eurocode 2, the maximum and the minimum steel reinforcement are given by the equations below:

$$A_{s,min} = \max\left(0.26 \frac{J_{ctm}}{f_{yk}} b_t d; 0.0013 b_t d\right)$$

$$A_s = 0.004 A_c$$

Where:

b_t is the mean width of the tension zone

d is the effective depth of the section

f_{ctm} is the tensile strength of the concrete

A_c is the concrete section.

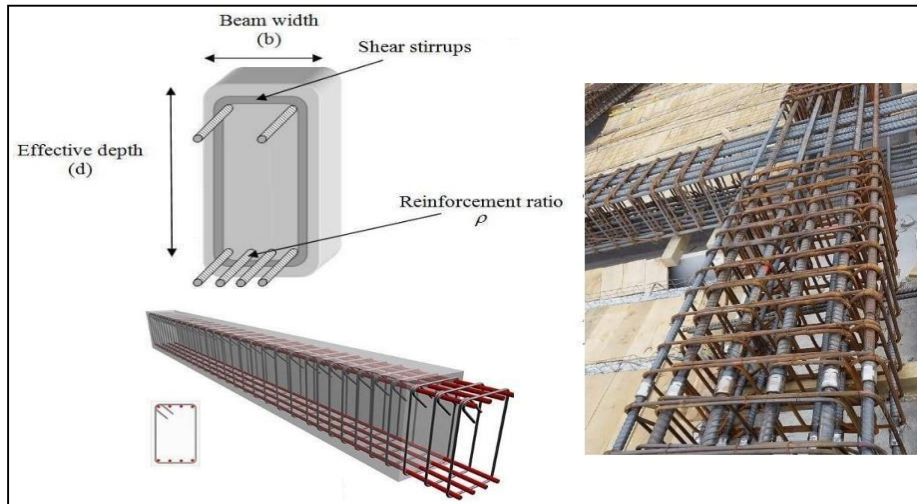


Figure 2-4: Example of a beam with reinforcements.

ii. Verification of the steel reinforcement

We calculate the number of reinforcement bars required and the area of reinforcement required. The section is checked by calculating the section's resisting bending moment using the position of the neutral axis within the section.

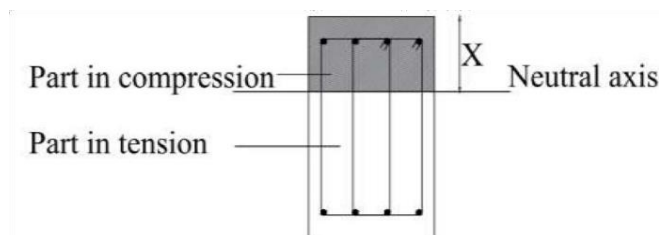


Figure 2-5: Neutral axis position in the beam section

The computation of the neutral axis is given by this formula:

$$X = \left(\frac{d}{2\beta_2} \right) - \sqrt{\left(\frac{d}{2\beta_2} \right)^2 - \frac{M_{ed}}{\beta_1 \beta_2 b f_{cd}}}$$

Where:

d : Effective depth of the section

b: Width of the section

f_{cd} : Design concrete compressive strength

β_1 and β_2 : Correction factor equal to 0.81 and 0.41 respectively

The resisting moment is given by equation below;

$$M_{Rd} = A_s \cdot f_{yd} \cdot (d - \beta_2 \cdot x)$$

Where:

$A_{s,real}$: is the effective area of the steel section

f_{yd} : is the design yielding strength of the steel

a. Shear verification

Shear reinforcement is required for the beam to resist shear. The amount of transversal reinforcement required is determined by the maximum shear V_{ed} . The value of V_{ed} must be greater than the design resistance without shear reinforcement, as calculated by the equation below.

$$V_{Rd,c} = \{ [C_{Rd,c} k (100 \rho_l f_{ck})^{1/3} + k_1 \sigma_{cp}] b_w d; (V_{min} + k_1 \sigma_{cp}) b_w d \}$$

With;

f_{ck} : is the characteristic strength of the reinforcement

d: is the effective depth of the section

$$\sigma_{cp} = \frac{N_{Ed}}{b_w d} < 0.2 * f_{cd} \left[\frac{N}{mm^2} \right]$$

b_w : is the smallest width of the cross section in the tensile area

N_{Ed} : Axial force of the cross section due to loading or prestressing

$b_w d$: Concrete cross-sectional area

$$K = 1 + \sqrt{\frac{200}{d}} \leq 2.0$$

With d in mm

$$\rho_l = \frac{A_{sl}}{b_w d} \leq 0.02$$

Minimum shear reinforcement is provided where, according to the provision above, no shear reinforcement is required.

For members where the design shear reinforcement is required, the shear resistance is the minimum between V_{rds} and V_{rdmax} defined by the following equations:

$$V_{Rd} = \alpha_{cw} b_w z v_1 f_{cd} / (\cot\vartheta + \tan\vartheta)$$

$$V_{Rd,S} = \frac{A_{sw}}{S} z f_{ywd} \cot\vartheta$$

Where:

f_{ywd} is the design yielding strength of the shear reinforcement

v_1 is a reduction factor for concrete cracked in shear ($v_1 = 0.6$ for $f_{ck} \leq 60 \text{ N/mm}^2$)

α_{cw} is a coefficient taking account of the state of stress in the compression cord $\alpha_{cw} = 1$ for non- pre-stressed structures is the cross sectional area of the shear reinforcement with a maximum value given by the relation

$$\frac{A_{swmax} f_{ywd}}{b_w S} \leq \frac{1}{2} \alpha_{cw} b_w v_1 f_d$$

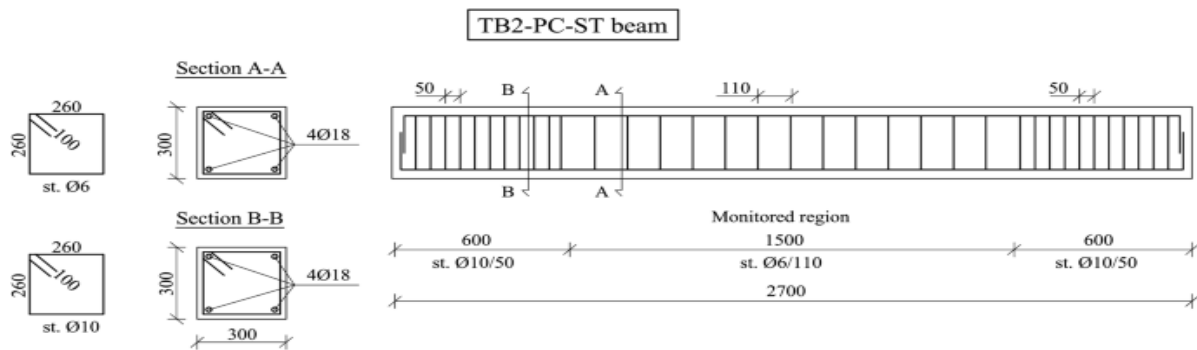


Figure 2-6: Longitudinal spacing and transversal spacing of a beam.

The obtained design shear reinforcement must validate the detailing of members. It defines the maximum longitudinal spacing of the shear assembly, the maximum transversal spacing of the legs in a series of shear links, and the minimum shear reinforcement ratio in the case of the beam, as shown in figure 2.6. The spacing is given by equation:

$$S_l = 0.75(1 + \cot\alpha)$$

$$S_t = 0.75d \leq 600\text{mm}$$

$$\rho_{w,min} = (0.08\sqrt{f_{ck}}) / f_{yk}$$

Where reinforcement ratio is given by equation below.

$$\rho_w = A_{sw} / (s \cdot b_w \cdot \sin\alpha)$$

2.4.2.2. Serviceability Limit State

The stress constraints, crack, and deflection control are the parameters of interest in this section. The stress verification uses the unusual combination discussed previously in the preceding sections because it prevents inelastic deformation of the reinforcement and longitudinal cracks in concrete.

i. Stress verification

The stress value is function of the modular ratio in short terms and long terms expressed in the equations below:

$$n_0 = \frac{E_S}{E_C}$$

$$n_{\infty} = n_0(1 + \varphi_L \times \rho_{\infty})$$

Where $\varphi_L = 0.55$ for shrinkage of concrete and the parameter $\rho_{\infty} = 2 \div 2.5$. For an uncracked concrete section, the neutral axis is computed thus:

$$x = \frac{-n(As + As') + \sqrt{(n(As + As')^2) + 2bn(Asd + As'd')}}{b}$$

Where A_S' and A_S are the upper and lower steel reinforcement inside the section respectively. The variables b , d' and d , are the geometrical characteristics of the section presented in the Figure 2.7

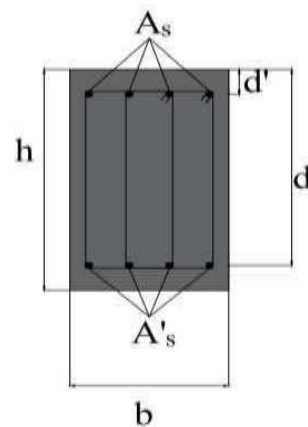


Figure 2-7: Geometric characteristics of a transversal beam section

The equation below is used to obtain the moment of inertia of the uncracked beam section.

$$J_{cr} = \frac{bx^3}{3} + nAs(d - x)^2 + nAs'(x - c)^2$$

The stresses in the concrete and steel can be computed using the relations below;

$$\sigma_s = \frac{M_{Ed}(d - x)}{J_{cr}} * n_{\infty}$$

$$\sigma_s = \frac{M_{Ed}(x)}{J_{cr}}$$

The verifications of these stresses for the obtained cross section as provided by Eurocode 2 are given by these equations:

$$\sigma_c \leq k_1 * f_{ck}$$

$$\sigma_s \leq k_3 * f_{yk}$$

With $k_1 = 0.6$ and $k_3 = 0.8$.

ii. Deflection verification

The deflection of a loaded beam is the vertical movement of a point. According to Eurocode 2, a member's or structure's deformation must not impair its correct function or appearance. If the equations below are satisfied, Eurocode 2 permits you to avoid calculus.

$$l/d \leq K \left[11 + 1.5 \cdot \sqrt{f_{ck}} \frac{\rho_0}{\rho} + 3.2 \cdot \sqrt{f_{ck}} \left(\frac{\rho_0}{\rho} - 1 \right)^{3/2} \right] \quad \text{if } \rho < \rho_0$$

$$l/d \leq K \left[11 + 1.5 \cdot \sqrt{f_{ck}} \frac{\rho_0}{\rho - \rho'} + 1/12 \cdot \sqrt{f_{ck}} \sqrt{\frac{\rho'}{\rho_0}} \right] \quad \text{if } \rho > \rho_0$$

Where:

l/d is the limit span/depth

K is the factor to take into account the different structural systems (see Annex 4)

ρ_0 is the reference reinforcement ratio = $\sqrt{f_{ck}} 10^{-3}$

ρ is the required tension reinforcement ratio at mid-span to resist the moment due to the design loads (at support for cantilevers)

ρ' is the required compression reinforcement ratio at mid-span to resist the moment due to design loads (at support for cantilevers)

f_{ck} is in MPa units

2.4.3. The Column design

A column or pillar is a structural element that transfers the weight of the structure above to the structural elements below by compression. The most commonly utilized columns for framed structures are reinforced concrete columns. As a matrix, they are made of concrete. The concrete

supports the steel structure. The compressive load is carried by concrete, whereas the tensile load is born by reinforcing. Steel, polymers, or alternative composite materials can be used as reinforcing materials. In the case of the column, ULS is taken into account, as are the axial force, bending moment, and shear force verifications. The shear force verification process for the column is the same as for the beam. As a result, the technique will no longer be detailed, but rather will be shown.

2.4.3.1. Axial load resistance of the section

The axial force is assumed to be taken over by 60% of the concrete resistance in the column's preliminary design. Then, using the relation below, we can calculate the column's minimal area section.

$$N_{Rd} = 0.6 \times f_{cd} \times A_c \geq N_{sd}$$

Where:

N_R is the design axial compression force

A_c is the concrete section area;

N_{sd} is the axial load computed using the recovery area of the column. The axial load is computed using the relation

$$N_{sd} = q \times S_r \times n$$

Where:

q is the uniform distributed loads on each floor computed at ULS;

S_r is the recovery area of the column;

n is the number of stories above the considered column.

2.4.3.2. Bending moment-axial force verification

For a column line, from the ground floor to the roof, the envelope curve is derived. Shear forces put aside, each column at each level is subjected to moment and axial force; these solicitations are obtained from the respective envelope curves. Each couple of points, M-N (moment-axial force) should belong to the section M-N interaction diagram.

The interaction is a diagram that represents all of the computational section failure limit possibilities and is computed by determining points that will be drawn to obtain the curve. Points within the diagram must adhere to the design criteria; otherwise, failure will occur. The computation

of the points is done as stated in the following sections while considering a rectangular section as illustrated in the figure 2.8 below.

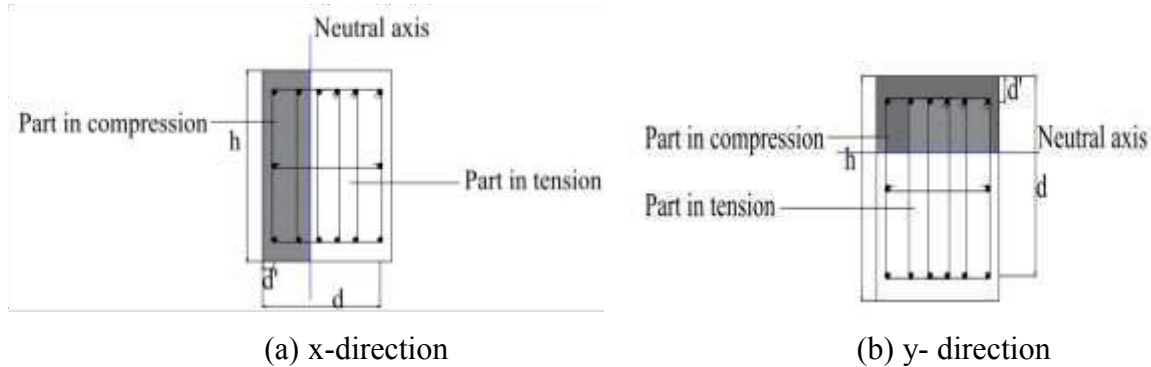


Figure 2-8: M-N diagram computation of a rectangular column section in both loading directions

a. First point

At this point, the section is completely subjected to tension, thus, the concrete is not reacting (concrete does not work under tension). We impose $\epsilon_s = \epsilon_{su}$, $\epsilon_s' = \epsilon_{syd}$. The stress inside the element corresponds to the design yielding strength of the steel reinforcement and the limit axial force and bending moment are obtained using the equations below

$$N_{Rd} = f_{yd} \cdot A_s + f_{yd} \cdot A'_s$$

$$M_{Rd} = f_{yd} \cdot A_s \cdot \left(\frac{h}{2} - d'\right) - f_{yd} \cdot A'_s \cdot \left(\frac{h}{2} - d'\right)$$

b. Second point

At the second point, the section is completely subjected to tension. We impose that; the strains, $\epsilon_s = \epsilon_{su}$, $\epsilon_c = 0$. The upper steel yielding condition is verified. If the steel has not yielded, then ϵ_s' is determined. For the computation of the axial force and the bending moment, we use the following relations

$$N_{Rd} = f_{yd} \cdot A_s + f_{yd} \cdot A'_s$$

$$M_{Rd} = f_{yd} \cdot A_s \cdot \left(\frac{h}{2} - d'\right) - f_{yd} \cdot A'_s \cdot \left(\frac{h}{2} - d'\right)$$

c. Third point

Here failure is due to concrete and the lower reinforcements have yielded. It's assumed that $\epsilon_s \geq \epsilon_{syd}$, $\epsilon_c = \epsilon_{cu2}$ and the position of the neutral axis is determined. Yielding condition of the upper steel reinforcement is verified. If the steel is yielded or not we proceed by determining ϵ_s' in order to

determine the corresponding stress.

$$N_{Rd} = -\beta_1 \cdot b \cdot x \cdot f_{cd} + f_{yd} \cdot A_s - f_{yd} \cdot A'_s$$

$$M_{Rd} = f_{yd} \cdot A'_s \cdot \left(\frac{h}{2} - d'\right) + f_{yd} \cdot A_s \left(\frac{h}{2} - d'\right) + \beta_1 \cdot b \cdot x \cdot f_{cd} \left(\frac{h}{2} - \beta_2 \cdot x\right)$$

d. Fourth point

To compute the coordinate of this point, the failure is due to concrete and the lower reinforcement reaches exactly $\varepsilon_s = \varepsilon_{syd}$. Likewise, we determine the neutral axis position and the strain ε'_s .

e. Fifth point

At this state, $\varepsilon_s = 0$ and failure is due to concrete. The lower reinforcement is considered to have yielded and the position of the neutral axis is the same as that of the effective depth.

$$N_{Rd} = -\beta_1 \cdot b \cdot x \cdot f_{cd} - f_{yd} \cdot A'_s$$

$$M_{Rd} = f_{yd} \cdot A'_s \cdot \left(\frac{h}{2} - d'\right) + \beta_1 \cdot b \cdot d \cdot f_{cd} \left(\frac{h}{2} - \beta_2 \cdot x\right)$$

f. Sixth point

We impose that concrete is uniformly compressed and assume the strain. Axial force and bending moment are computed as below.

$$\varepsilon_s = \varepsilon_c \geq \varepsilon_{c2}$$

$$N_{Rd} = -b \cdot h \cdot f_{cd} - f_{ywd} \cdot A'_s - f_{yd} \cdot A_s$$

$$M_{Rd} = f_{yd} \cdot A'_s \cdot \left(\frac{h}{2} - d'\right) - f_{yd} \cdot A_s \left(\frac{h}{2} - d'\right)$$

An example of an M-N interaction diagram is shown in the figure 2.9 below. The figure shows the M-N diagram in red for positive and negative loading directions with the couple of points (solicitation M_{Ed} and N_{Ed}), in blue, which lie within it, thereby respecting the design criteria. Provisions of Eurocode with regards to the steel reinforcement of the column.

$$A_s = 0.04A_c$$

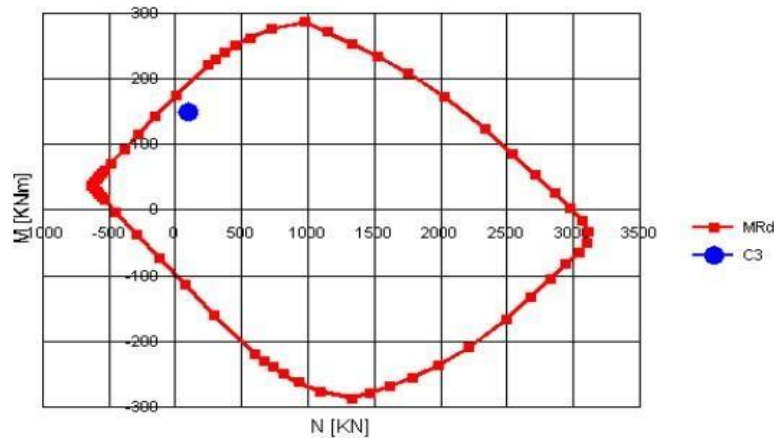


Figure 2-9: Example of M-N diagram (D'Antino et al., 2016)

The steel reinforcement of the column is considered taking into account the limitations of the Eurocode 2 defined by equation.

$$A_{s,min} = \max\left(\frac{0.10N_{Ed}}{f_{yd}}\right); 0.002Ac$$

Where:

N_{Ed} is design axial compression force;

f_{yd} is design yield strength of the longitudinal reinforcement.

2.4.3.3. Shear verification

The Eurocode 2 requires a minimum diameter of 6mm or one quarter of the maximum diameter of the longitudinal bars. The maximum spacing of the transverse reinforcement is given by the equation below.

$$S_{cl} = \min (20\phi_{l, n}; b; 400\text{mm})$$

Where:

ϕ is the minimum diameter of the longitudinal bars b is the lesser dimension of the column

The factor of 0.6 is used to reduce the maximum spacing in sections within a distance equal to the larger dimension of the column bars.

2.4.3.4. Slenderness verification

The need for slenderness verification arises from whether or not second order effects are to be accounted for. Eurocode 2 recommendations are out-lined below:

$$\lambda_{lim} = 20ABC/\sqrt{n}$$

With:

$$A = \frac{1}{1+0.2\varphi_{ef}} : \varphi_{ef} \text{ is the effective creep ratio; If not known, } A=0.7)$$

$$B = \sqrt{1 + 2\omega} \quad (\omega = A_s f_{yd} / A_c f_{cd} : \text{mechanical reinforcement ratio})$$

$$C = 1.7 - r_m \quad (r_m = M_{01} / M_{02} : \text{the moment ratio; equal to one (1) for unbraced system})$$

$$n = N_{Ed} / A_c f_{cd} \quad : \text{relative normal force}$$

The expression below is the one used for the estimation of slenderness λ .

$$\lambda = l_0 / i$$

Where:

i: The gyration radius of the uncracked concrete l_0 : Effective length of the element ($l_0 = 0.7l$)

$$i = \sqrt{\frac{I}{A}}$$

I: Moment of inertia and A is the area of the section.

2.5. Numerical Analysis

Analytical studies will be conducted through linear models using the finite element method which uses the ABAQUS CAE software, in order to evaluate the suitability of the dynamic behavior of the building. For numerical modelling, it is critical to comprehend which components and materials of the structure have structural importance. In our work, depending on the physical and mechanical properties of the building elements, the program is utilized to observe and evaluate the influence of masonry infill on the building's behaviour. In order to acquire precise outcomes from the finite element model, all components in the model will be deliberately relegated to two mesh sizes (100 for RC frame and 50 for concrete block), which ensures every two distinct materials share the same node.

2.5.1. Geometrical Modelling (part module)

This involves the modelling of the structural elements; the column, beam, bricks and reinforcement.

2.5.1.1. Brick element (C3D8R):

The three-dimensional C3D8R brick reduced integration element is used to represent masonry walls, reinforced concrete slab, brick and mortar in the models. This element has the capability of representing large deformation, geometric and crushing in compressive and cracking in tension. It is defined by 8 nodes, each node has three translational degrees of freedom X, Y, and Z directions as showed in figure 2.10 (a) The name of each element in ABAQUS identifies its main aspects. C means continuum element, 3D means three-dimensional element, 8 Indicates the number of nodes required to create the element and R reduced integration (Daniel and Dubey, 2014)

2.5.1.2. Truss element (T3D2):

When loading of the slender member on the center line or along it, we select the truss element (T3D2) that supports this type of loading for 3D or 2D modelling as shown in figure 2.10(b). The truss element (T3D2) two noded in this study is used to represent the reinforcing steel of the roof, slab, and lintels (Daniel and Dubey, 2014)

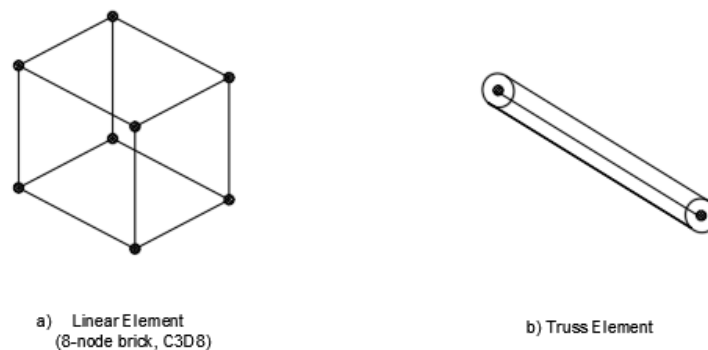


Figure 2-10: Geometrical elements in Abaqus CAE

Due to the complexity of the masonry construction, because it consists of several differentiated materials, its study requires the adoption of effective representation techniques. Therefore, Researchers presented several techniques for the purpose of simulating the construction wall, there are three techniques that can be applied in the specific elements method, namely, macro modelling, simplified modelling, and micro modelling as shown in the figure 2.11 below.

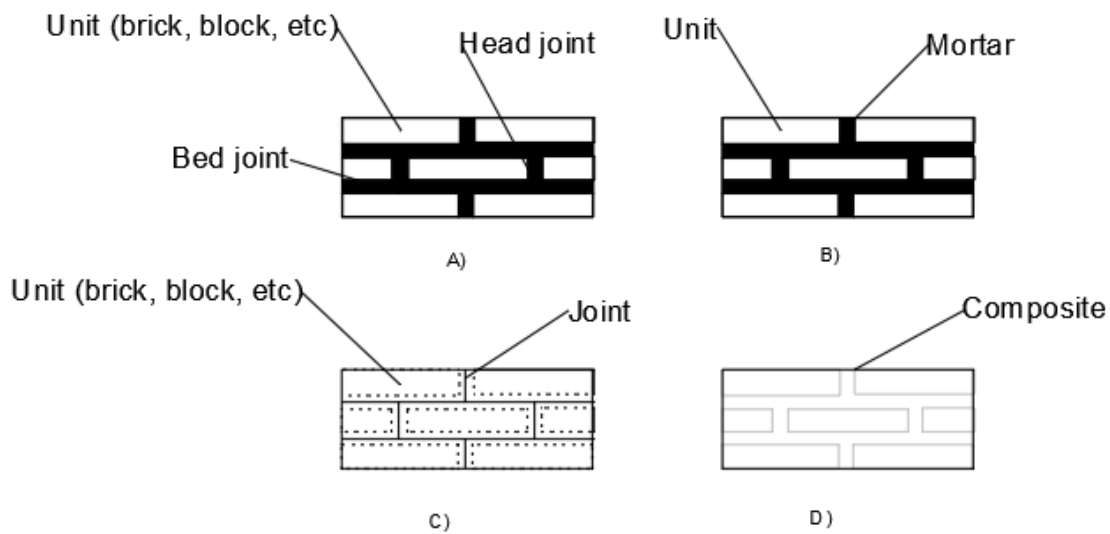


Figure 2-11: Numerical models of masonry wall; (a) prototype masonry wall, (b) detailed micro modelling, (c) semi-micro modelling and (d) macro modelling

1- Micro-modelling: It means complex modelling where both the blocks and the joint of mortar are represented by a separate element with an interface element for the purpose of linking the two elements together. This modelling is often used for small models because of the complexity of the details and the need for more variables than the other types as well as taking a lot of time for representation and analysis, but gives more accurate and reliable results and used when the need to study cracks and failures and stresses.

2- Simplified micro-modelling: In this approach, brick is modelled as a continuum element, but the mortar joint and its interface with brick is modelled together as an interface elements. However, in this instance the mortar is not defined as a solid element but rather as an interface between the solid brick elements. These interface element represent the preferential crack locations where shear and tensile cracking occurs.

3- Macro modelling: This type of modelling is the most common and especially in large models, where both the bricks and the mortar are modelled for one piece that possesses part of the properties of the bricks and the mortar in one. The material properties are introduced through mathematical equations whose variables are the compressive strength of both materials found by researchers or through the experimental test of brick and mortar samples. This technique is used when there is a need to reduce the time of analysis or the breakdown of storage memory and large size model.

For our work, we shall adopt the simplified micro-modelling method. The materials is represented by using brick element C3D8R for masonry brick, and concrete, while the truss element T3D2 using to represent the steel reinforcement.

2.5.2. Material property Modelling

As precised above the modelling method used for this work is the simplified micro modelling. This method makes use of two structural components: the structural frame and the masonry infill (hollow concrete blocks). The mechanical properties of concrete members (i.e., columns, beams, and concrete masonry unit) and reinforcing rebars were considered depending on the experimental results, which were conducted by Al-Chaar et al. (2002). However, some missing properties were calculated based on relevant design codes and the ABAQUS users' manual (ABAQUS, 2012). Table 2.1 illustrates the concrete, reinforcing rebars, and the concrete masonry properties of specimens tested by Al-Chaar et al. (2002).

Table 2.1: Properties of concrete, rebars and masonry units (Al-Chaar and al (2002))

Concrete (MPa)		Reinforcing Rebars (MPa)		Concrete masonry unit (MPa)
Compressive Stress (σ_c')	Young's modulus (E_o)	Yield Stress (σ)	Young's modulus (E)	Compressive Stress (σ_c')
38.438	29,992	338.5	200,000	12.907

The plasticity for concrete behavior has been applied in ABAQUS by utilizing the concrete damage plasticity (CDP) model for simulating the concrete behavior in beams, columns, and the concrete masonry unit. CDP followed Lubliner et al. proposed models (Lubliner et al., 1989), in addition to Lee and Fenves (1998). This model can simulate the behavior of each compressive strength, as well as the tensile strength of concrete, which is exposed to external pressures. The compressive stress-strain ($\sigma_c - \epsilon_c$) curves were obtained following Eurocode 2 (EN-1992-1-1, 2005a) provisions as shown in figure 37. This relationship is described in Eq. (1), (2), (3), and (4) (EN-1992-1-1, 2005a). The concrete strains at maximum stress (ϵ_{c1}) were assumed as 0.0017 and 0.0025 for concrete members and concrete masonry unit, respectively, while 0.0035 for the maximum strain at failure (ϵ_{cu1}) for all concrete parts. The resulting relationship between σ_c and ϵ_c for concrete members and concrete masonry unit is shown in figure 2.12. In this study, the CDP parameters, which are used to simulate concrete in ABAQUS, are shown in Table 2.2.

$$\sigma_c = \sigma_c' \frac{k\eta - \eta^2}{1 + (k-2)\eta} \quad (1)$$

$$\eta = \frac{\varepsilon_c}{\varepsilon_{c1}} \quad (2)$$

$$\varepsilon_{c1} = 0.0007\sigma_c'^{0.31} \quad (3)$$

$$k = 1.05E_0 \varepsilon_{c1} / \sigma_c' \quad (4)$$

Where σ_c is the compressive stress, k is the material coefficient, and η is the strain coefficient.

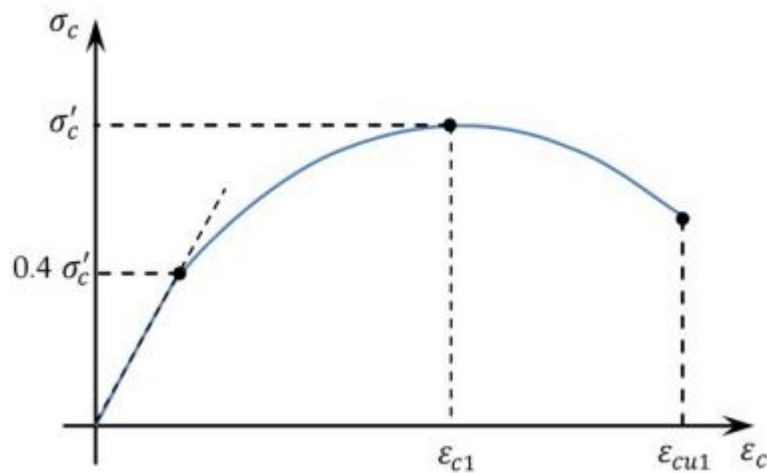


Figure 2-12: Representing the schematic of the compressive stress-strain curve for structural analysis

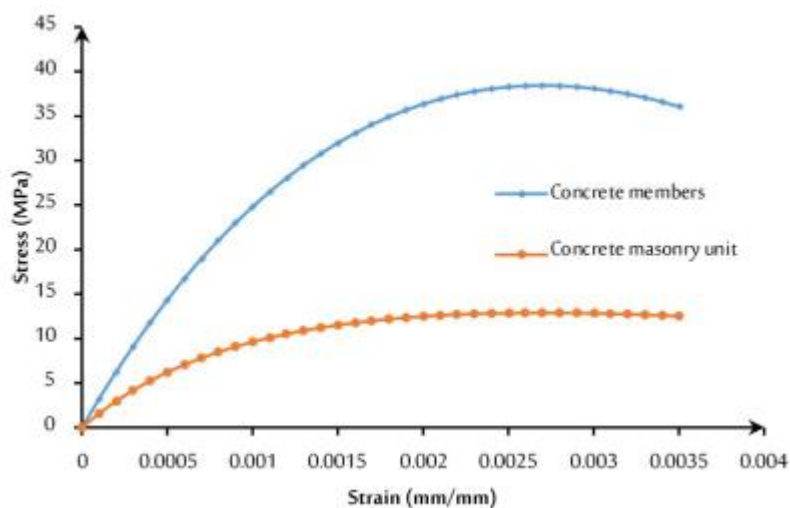


Figure 2-13: Stress-strain curve of concrete in compression

Table 2.2: Concrete implemented material parameters

Parameter	Value	Definition	Denotation
ϵ	0.1	Flow potential eccentricity	(ABAQUS, 2012)
ψ	35	Dilation angle	(Malm, 2009)
σ_{b0}/σ_{c0}	1.16	Ratio of biaxial to uniaxial compressive	(ABAQUS, 2012); (Lubliner et al., 1989)
K_c	0.7	Second stress invariant ratio	(ABAQUS, 2012)
μ	0.00025	Viscosity	(ABAQUS, 2012)
Elasticity	$\nu = 0.2$	Poisson's ratio for concrete members	Widely utilized in FEM simulations
	$\nu = 0.15$	Poisson's ratio for concrete masonry unit	
	$E_o = 4700\sqrt{\sigma'_c}$	Young's modulus	acc. (ACI, 2011)

The elastic region in the stress-strain curve of reinforcing rebar was modelled with typical values of 210,000 MPa, in addition to 0.3 for the modulus of Young and the ratio of Poisson, respectively. The plastic region has been defined following the specified test results provided by (Al-Chaar et al., 2002) by using the idealized curves as shown in Figure 2.14. The remainder key parameters were obtained based on Eurocode 3 (EN-1993-1-2, 2005b) provisions.

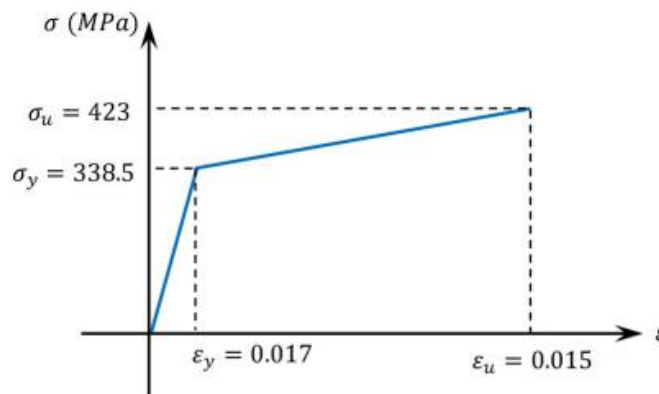


Figure 2-14: The idealized stress-strain curve for reinforcing rebars

2.5.3. Assembly modelling

The assembly module as its name indicates is the module in which the different parts of our model are put in the same global coordinate system. This is done by creating part instances. For our work the analyses are performed on four construction cases (models)

2.5.3.1. Empty frame

In this case, we have a structural frame comprise of reinforced concrete. The beam element is 4.8m long with a cross section of 20X40 cm and the column element is 2.6m high with a cross section of 20X40

cm. The reinforcement used for both elements are 6 longitudinal bars of diameter 12mm and transversal bars of diameter 6mm as illustrated in the figure 2.15 below. There is a footing added with dimensions: 30X60cm as cross section and 6m long.

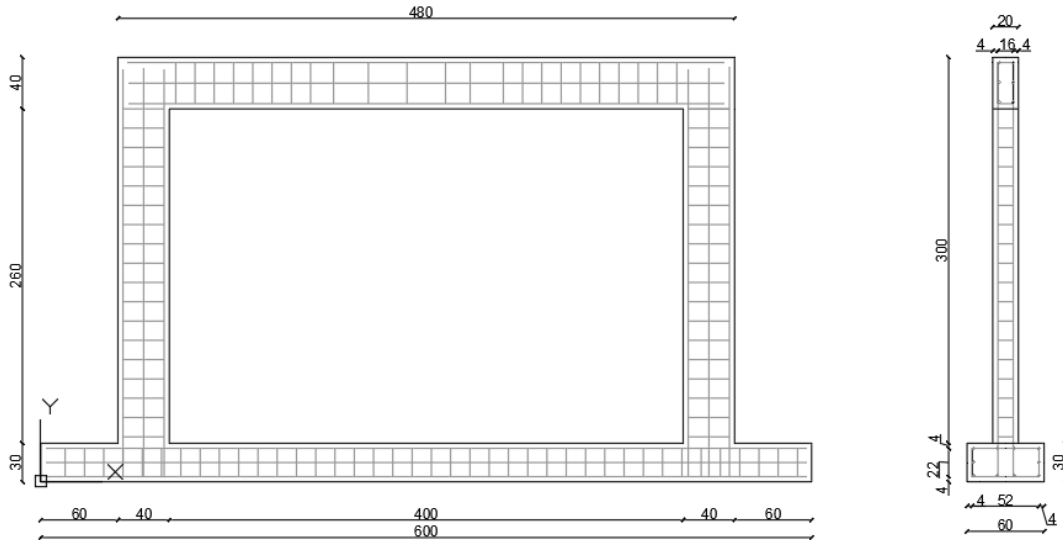


Figure 2-15: Empty frame model

2.5.3.2. Infilled frame

We have the same configuration of the structural frame. In addition, we introduce a masonry wall made of concrete blocks of dimension 20X20X40 cm. We have 13 row of concrete blocks as illustrated in figure 2.16 below.

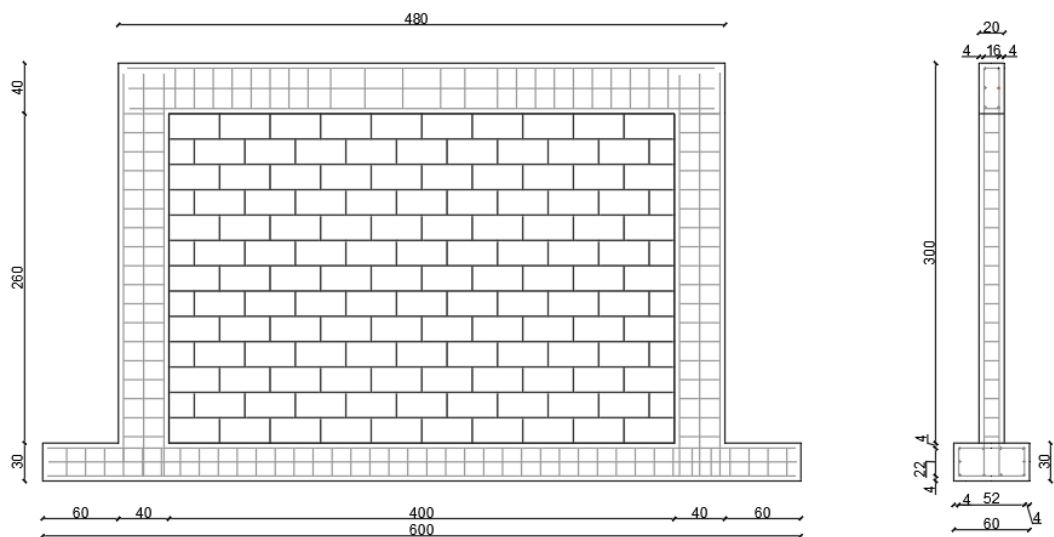


Figure 2-16: Infilled frame model

2.5.3.3. Infilled frame with opening (door)

In this case, a door is introduced in the previous configuration (infilled frame). The door is of dimensions: 1.2m large and 2.0m high. This is illustrated in figure 2.17 below.

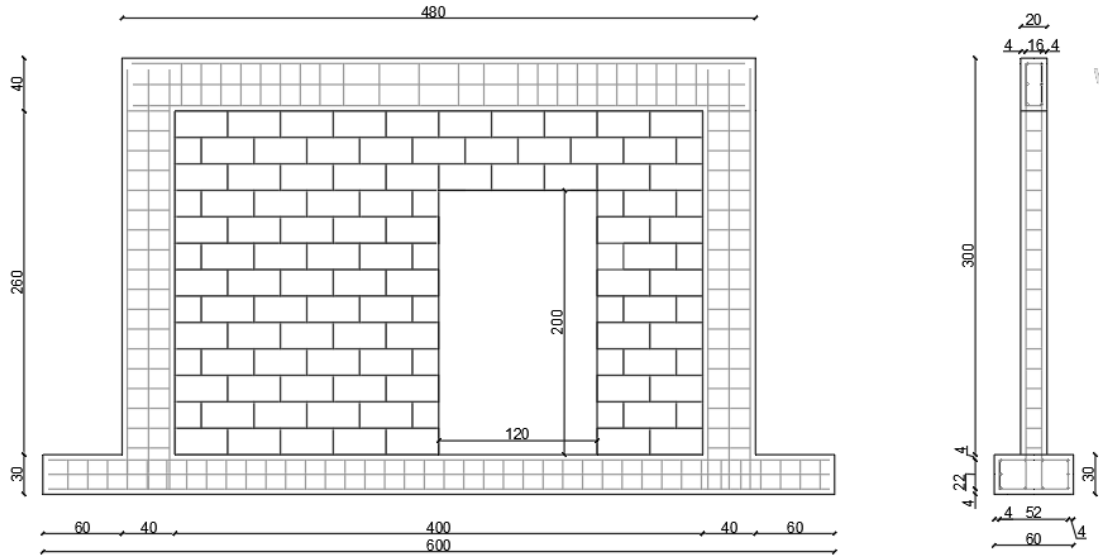


Figure 2-17: Infilled frame with opening (door)

2.5.3.4. Infilled frame with opening (window)

Here a window is introduced in the infilled frame configuration. The window is of dimension 1.4m large and 1.0m high. This is illustrated in figure 2.18 below.

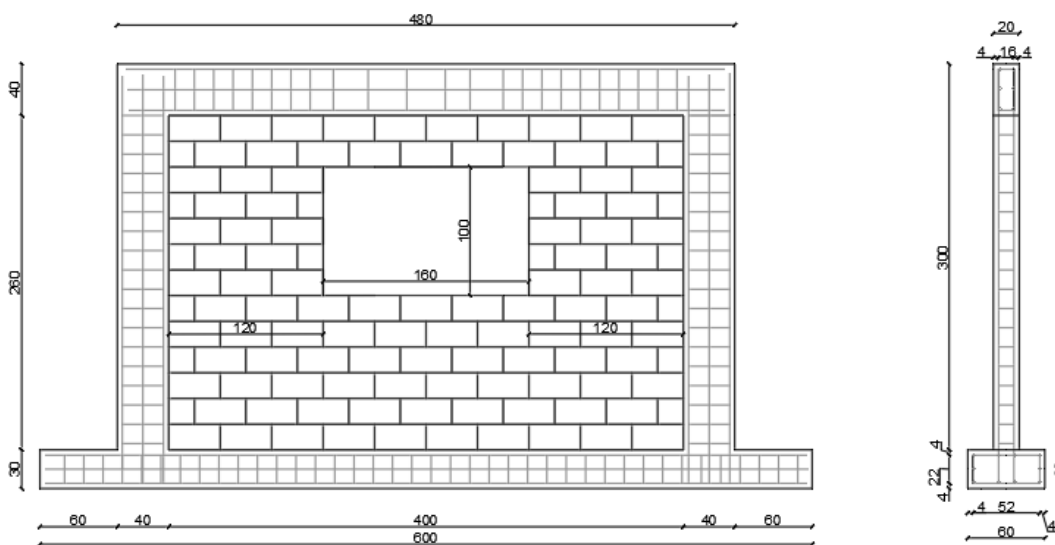


Figure 2-18: Infilled frame with opening (window)

2.5.4. Step modelling

The step module is the next module in the process. It is where the analysis steps are created. Steps permit to define the type of analysis we want to carry out, define the procedure of the analysis, and describe how the output data should be presented. Two steps were created for the dynamic explicit analysis of the four (04) models created above.

2.5.5. Interaction Modelling

In order to be able to properly describe the contact between bodies (FE meshes). For each case, a privacy connection is taken into consideration. . To set up this functionality, the frame and the wall are connected by interface/constraint elements that can transfer normal and shear stresses.

a. **Frame interaction (beam-column-reinforcement):** Tie constraint is used to connect different model parts with the same material properties. In order to assume an ideal bond between the reinforcement and concrete, an embedded connection was used. 3-D truss elements representing the reinforcement are the embedded region, while the concrete (foundation, beams and slabs) is the host region.

b. **Masonry interaction:** Ordinarily, the brick walls are connected to RC frames using mortar joints, by these articulations, the interaction between the wall and the frame is fulfilled. The traditional node-to-surface discretization, as well as the approach of the small sliding tracking has been utilized to model interaction, which resulted from mortar located amid the block units. Moreover, to define the friction model between the contact surfaces, the coefficient of friction amid the units of the concrete masonry is equivalent to 0.44. In ABAQUS, cohesive behavior is referred to as a fragment of interaction properties assigned to contact surfaces. In ABAQUS, the interface elements' properties can be identified based on the characteristics of the mortar and masonry unit of the experimental test conducted by Al-Chaar et al. (2002). The normal and shear stiffness (in first and second directions), which are essential for defining the mortar joints, as well as the masonry unit, and the mortar interface's behavior, are described in the equations below (Lourenço, 1994). The normal, and shear stiffness (in first and second directions) value are shown in Table 2.3.

$$k_{nn} = \frac{E_u E_m}{h_m (E_u - E_m)}$$

$$k_{ss} \text{ and } k_{tt} = \frac{G_u G_m}{h_m (G_u - G_m)}$$

where k_{nn} , k_{ss} , and k_{tt} are joint stiffness for the normal direction and first shear direction, as well as second shear direction, correspondingly, E_u and E_m are Young's modulus for masonry unit,

as well as mortar, respectively, G_u and G_m represent the shear modulus of the masonry unit, in addition to the mortar, correspondingly, while hm signifies the joints' actual thickness.

Table 2.3: Joint stiffness for the brick-mortar interaction

k_{nn} (MPa/mm)	$k_{ss} = k_{tt}$ (MPa/mm)
16020	11856

2.5.6. Load Modelling

It is where the loads are created and managed. The boundary conditions are equally created and assigned in this module. We have two loading cases: a vertical pressure of 0.3 N/mm² is applied on the beam, and a horizontal force of 50KN is applied on one end of the beam. The wall was fixed at the end by “encastre”.

2.5.7. Meshing modelling

The meshing here is important to analyse de detail behaviour of elements. For uniformity, we shall take mesh element to be square elements of size 100mm.

2.5.8. Job module (Numerical analysis of the structure)

In order to evaluate the contribution of infill wall on the mechanic behavior of the structure, different analysis will be performed. Firstly, overall structural system of the building with and without infill walls(using SAP2000) and secondly using micro modelling method (using ABAQUS CEA 2020), local analysis would be performed on reinforced concrete frames with and without infill wall.

2.5.8.1. Modal analysis

Modal analysis will eventually be performed with the aim of observing the building vibration modes. Modal analysis is used to determine the vibration modes of a structure. These modes are useful to understand the behavior of the structure. They can also be used as the basis for modal superposition in response-spectrum and modal time-history Load Cases. We shall use the software SAP2000 to perform this analysis

The following time- properties are printed for each Mode:

- ❖ Period, T , in units of time
- ❖ Cyclic frequency, f , in units of cycles per time; this is the inverse of T

2.5.8.2. Dynamic analysis.

The dynamic (explicit) analysis is performed on a structural model on ABAQUS CAE. The displacement and principal stress of the building model elements (frame and infill) are obtained here on various construction stage for both the vertical and horizontal loading cases. The obtained displacement, may be used to compute the stiffness K of the frame structure for each case. Stiffness is a measure of how much force is require to displace a building by a certain amount.

2.5.9. Visualization module

The output data is viewed and analyzed in this module. The deformation, the stresses and plastic strains are shown in this module. In this module, we can see the stresses caused in the wall by the vertical and horizontal loads acting on it. Different types of stresses can be visualized in this module. Below, a brief explanation on when to consider the value of the different stresses is given

- The Von Mises stress is used for ductile materials such as steel, to see if the material will yield or fracture.
- The equivalent plastic strain attained by the structural element due to the loads.
- Deflection is given by the symbol U . It can be U_1 , U_2 and U_3 , which represent the deflection in the 3 principal directions.

Conclusion

The aim of this chapter was to present in details the methodology of the different analysis that will be perform on the building. The site recognition and the different data collection procedure were first presented, secondly the design steps of different structural elements, and then the modelling specification and parameters were defined for the conception of the structural frame of the buildings. Analysis procedure, description and searched parameters were stated. The result of these analyses will be displayed and discussed in chapter 3 for the understanding of the influence of infill walls on the behavior of RC buildings.

CHAPTER 3: RESULTS AND INTERPRETATIONS OF THE ANALYSIS

Introduction

This chapter presents various responses to the methodology studied in Chapter 2 in order to support our research on the role of infill walls in the structural behavior of an RC building. In the meantime, a comparison study will be conducted between brick walls, drywall walls, and masonry walls to determine which infill wall has the greatest impact on the structure. The ABAQUS CAE software will be used for all analysis, and Excel will be used to present the results.

3.1. General presentation of the site

The building under consideration is a residential reinforced concrete structure in Nomayos (total Nomayos) a village in Cameroon's Central Region, located in the town of Mbankomo and the department of Méfou-et-Akono. The building's total height is 11.4 meters, with each storey measuring 3.00 meters in height and a water tank of 2.4m high. It is consistent in both plane and elevation. The slab is assumed to be reinforced concrete with 16cm thick hollow blocks. The floor plan of the structure is identical for all the levels, as shown in the elevation view in figure 3.1 and figure 3.2. The architectural plan is shown in Annex A5.

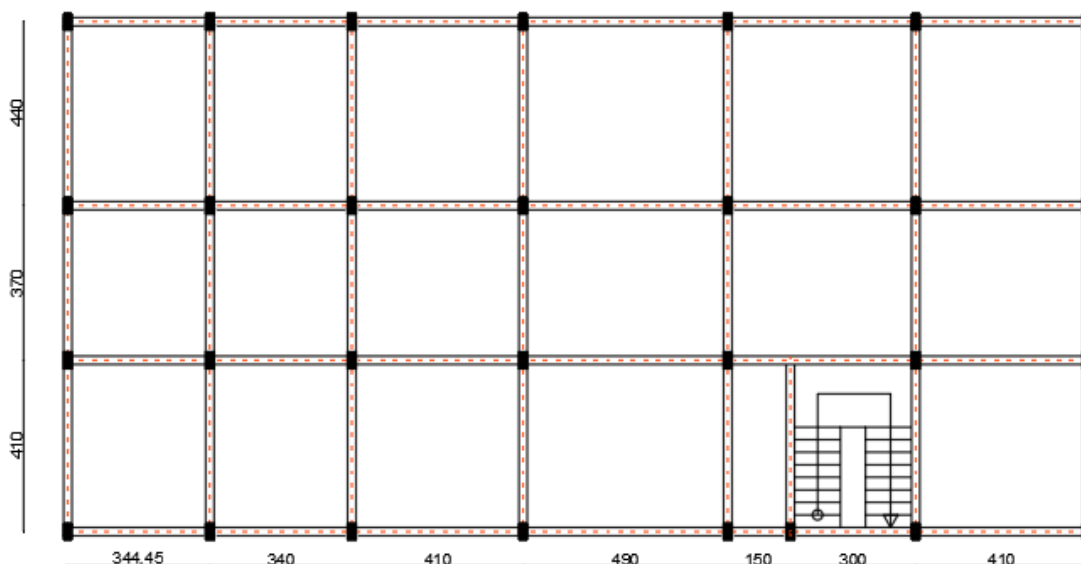


Figure 3-1: Structural plan of case study

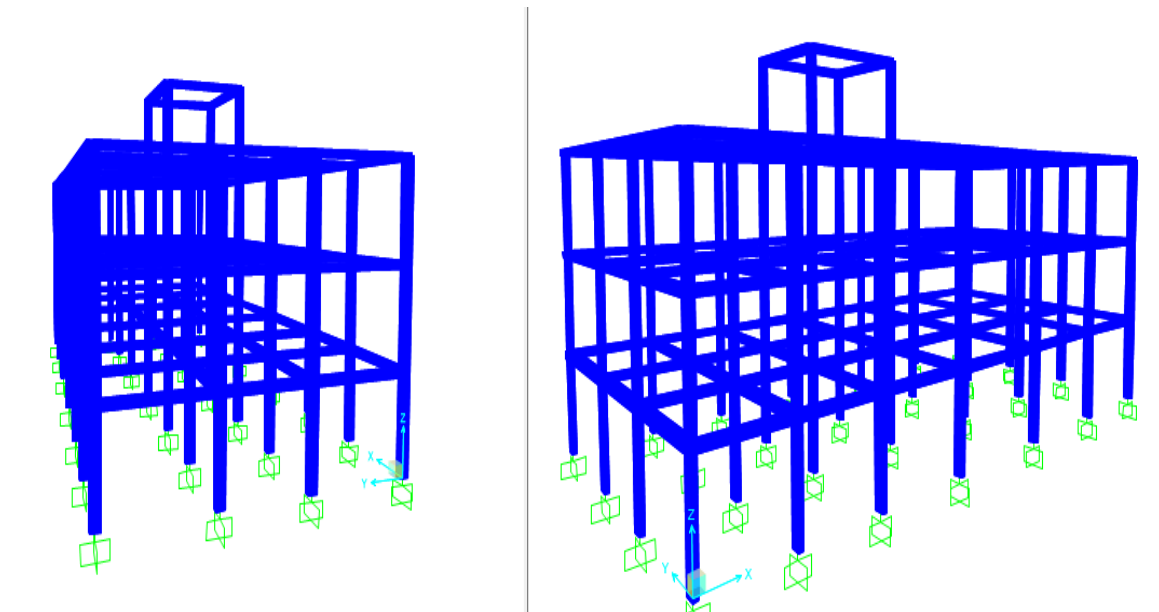


Figure 3-2: 3D model of the building (SAP2000)

3.2. Topographic/Relief data

The current topography of the site shows that the building is located on a field with a negligible slope. The site belongs to the sedimentary basin of Yaounde area and rest on a plinth of crystalline. The basin is made up of thick continental and luvio marine formation separated by some fossiliferous arine intercalation.

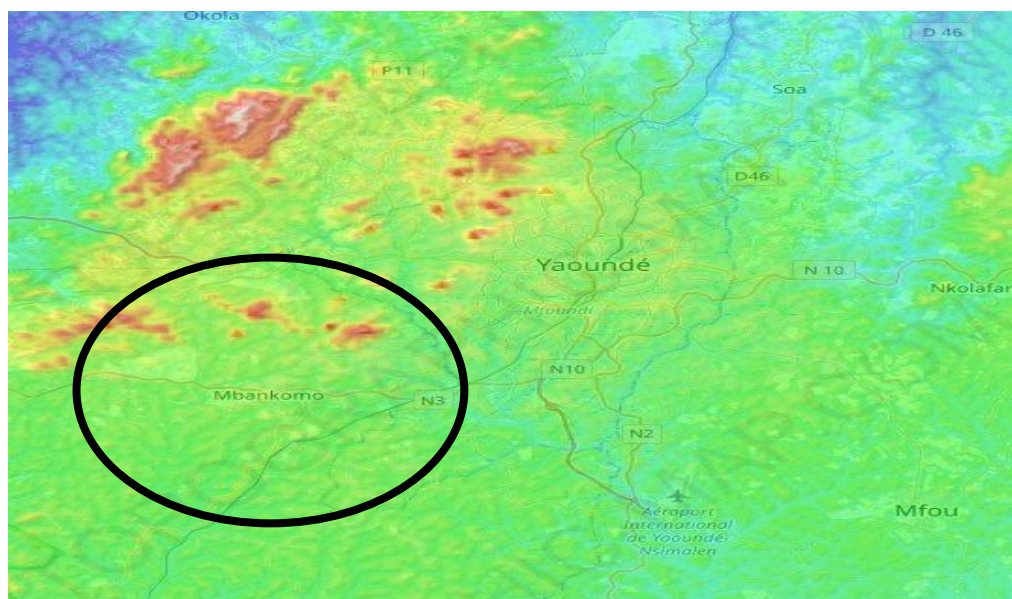


Figure 3-3: Topographic view of Mbakomo town

3.3. Geographic and Climatic data

The city of Yaoundé is located in the south of the Center Region and is 250 km east of the coast of the Gulf of Biafra. This mountain site³ is broken down into three topographic units inscribed in a rocky base of Precambrian gneiss: the barrier of inselbergs to the northwest dominated by the Mbam Minkom mountains (1,295 m) and the Nkolodom mountain (1,221 m) and southwest with Mount Eloundem (1,159 m), a set of hills 600 to 700 m high and plateaus; the valleys also called élobis.

Yaounde is located in a tropical savannah climate with numerous months of heavy rain. The dry season lasts from late November to early February. Rainfall decreases in July and August during the rainy season.

3.4. Structural Element Design

The structural elements to be designed for our study are the beam and column. It was assumed that in the conventional structural design method, soil–structure interaction (SSI) effects were not considered.

3.4.1. Imposed Load

A residential building is the subject of our case study. According to the eurocode, variable load for residential buildings ranges from 1.5KN/m² to 2.0KN/m², so 1.5KN/m² was chosen. Table 3.1 displays the various applied loads.

Table 3.1: Applied loads on structure

Nature	Description	Value	Unit
G _{1k}	Hollow body slab	2.85	KN/m ²
G _{2k}	Secondary element load	0.22	KN/m ²
Q _k	Variable load	1.5	KN/m ²

3.4.2. Load Combinations

The load combination in the equation below provides for the verification of the structure at Ultimate Limit State.

$$1.35G_k + 1.5Q_k$$

$$G_k = G_{1k} + G_{2k}$$

For non-reversible Serviceability Limit State (SLS), the verification is done using the following equation.

$$G_k + Q_k$$

3.4.3. Material properties

The chosen concrete class is C25/30, and the longitudinal steel reinforcement is B450. For the transversal reinforcement, we assume a characteristic yield strength of 235 MPa. Table 3.2 shows the main properties of concrete, and table 3.3 shows the properties of steel used as reinforcement in the design of structural elements.

Table 3.2: Concrete Properties.

Property	Value	Unit	Definition
Class	C25/30	-	Concrete class
Rck	30	MPa	Characteristic cubic compressive strength
fck	25	MPa	Characteristic compressive strength of concrete at 28 days
$f_{cm} = f_{ck} + 8$	33	MPa	Mean value of concrete cylinder compressive strength
γ_c	1.5	-	Partial factor for concrete
$f_{ctm} = 0.3 \times (f_{ck})^{\frac{2}{3}}$	2.56	MPa	Mean value of axial tensile strength of concrete
$f_{ctd} = 0.7 \times \frac{f_{ctm}}{\gamma_c}$	1.2	MPa	Design resistance in traction
$E_{cm} = 22000 * \left(\frac{f_{cm}}{10}\right)^{0.3}$	31476	MPa	Secant modulus of elasticity
N	0.2	-	Poisson's ratio
G	13115	MPa	Shear modulus
γ	25	KN/m ³	Specific weight of the concrete

Table 3.3: Reinforcement rebars

Property	Value	Unit	Definition
Class	B450C	-	Steel class
f_{yk}	450	MPa	Characteristic yield strength
γ_s	1.15	-	Partial safety factor for steel
γ	78.5		Specific weight of the steel
v	0.3	-	Poisson's ratio

3.4.4. Durability and Concrete Cover Determination

Using a concrete structural class of S4 and an exposure class of XC1, as well as the Eurocode 2 provision outlined in section 2.5.1, the concrete cover obtained is $C_{min} = \max(14,15,10) = 15$ mm.

Using the nominal cover equation, $C_{nom} = 15 + 10 = 25$ mm.

As a result, the concrete cover for the upper structural elements will be $c=30$ mm

3.4.5. Beam Design Results

The beams that support the slab are the horizontal structural elements of the building under consideration. Figure 3.4 shows the main beam that was chosen for the design. It is the most heavily loaded beam, and its section will be used for all other beams.

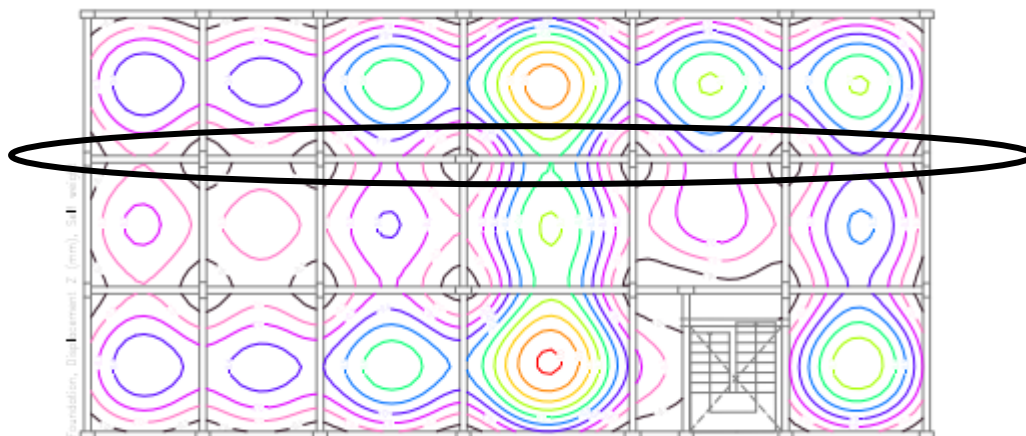


Figure 3-4: Most solicited beam to design (load distribution)

The predesign of the cross section is obtained by assuming the value of the section height and the section depth. The section height is obtained from the maximum span as:

$$h \geq \frac{4.72}{12} = 0.3933 \text{ m}$$

And the section width b , given by;

$$b \geq \frac{h}{2} = 0.1966 \text{ m}$$

We will take as initial value $h = 40$ cm and $b = 20$ cm. This section is modelled in the software as frame element with the different restraints as supports as shown in the figure 3.5.

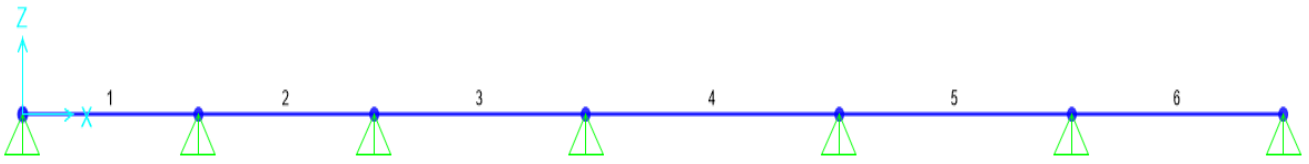
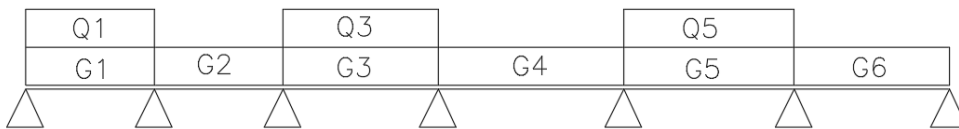


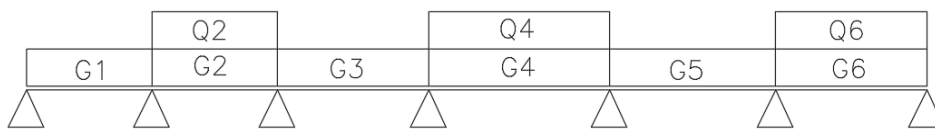
Figure 3-5: Simple support model

From this model, loads combinations for maximum moment at mid span and maximum shear are presented on figure 3.6 below.

Combination ULS 1



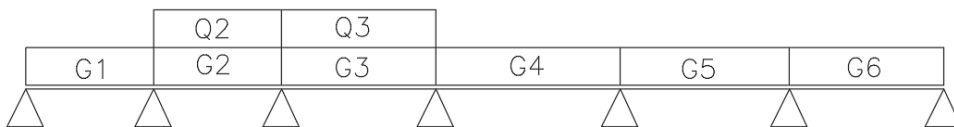
Combination ULS 2



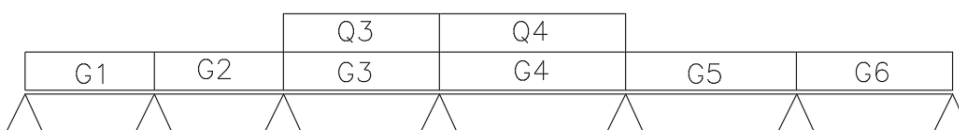
Combination ULS 3



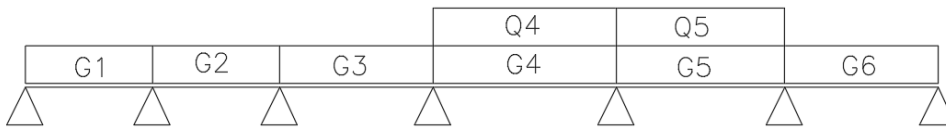
Combination ULS 4



Combination ULS 5



Combination ULS 6



Combination ULS 7

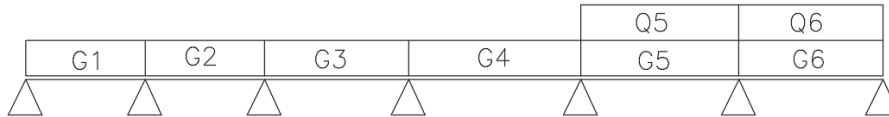


Figure 3-6: Applied Load Combinations

3.2.5.1. Ultimate limit state design

The above load arrangements inserted in the software SAP 2000 allow for the easy generation of solicitation curves along the beam for the bending moment and shear force depicted in figures 3.7 and 3.8.

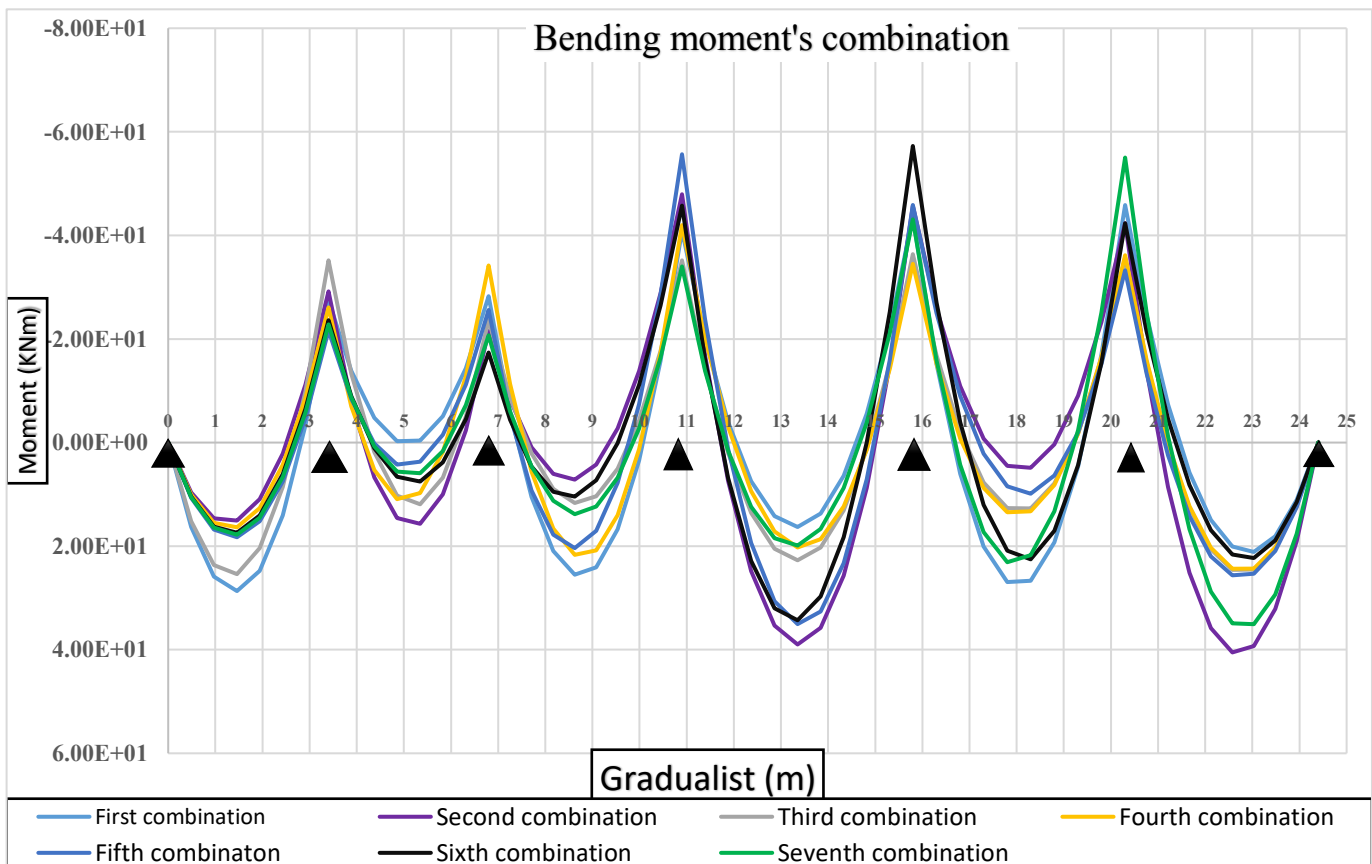


Figure 3-7: Bending moment Diagram for the load combinations

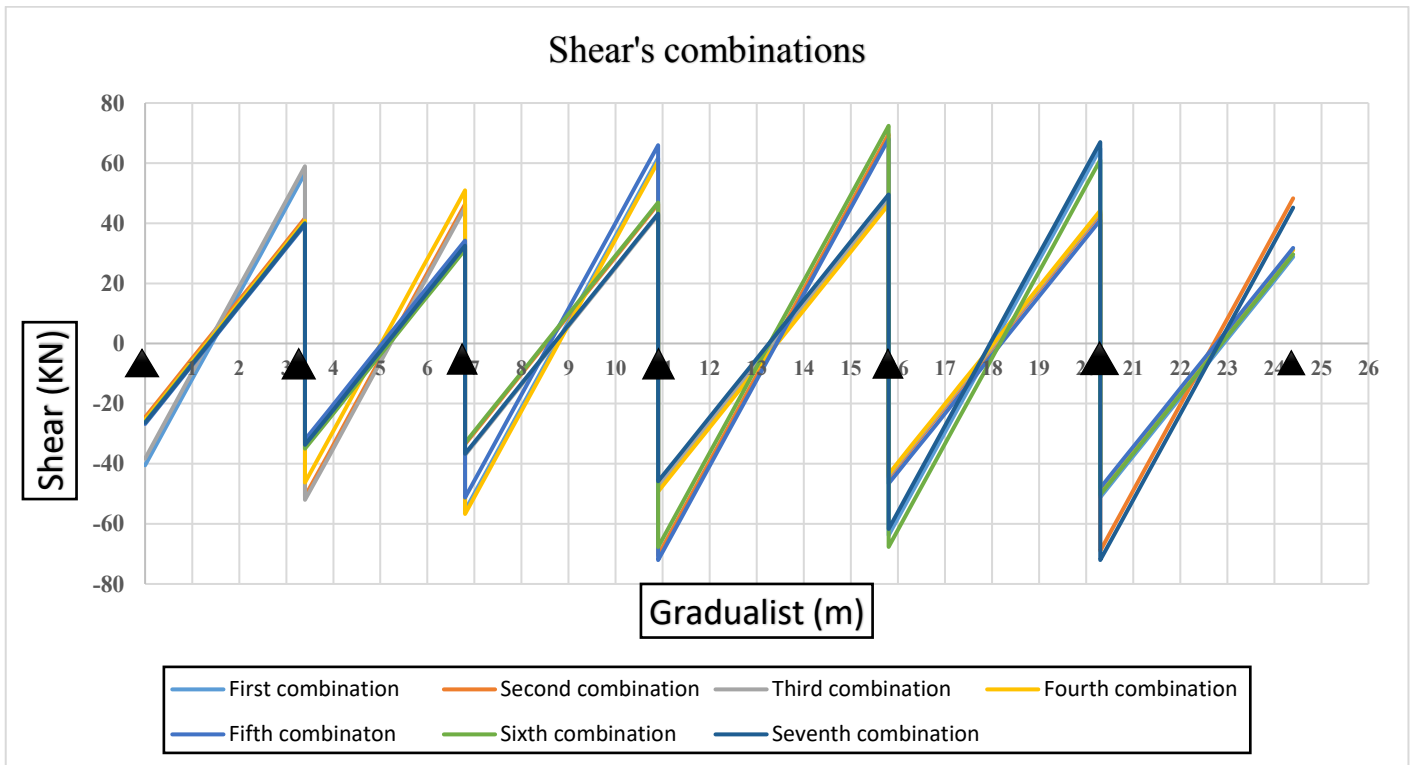


Figure 3-8: Shear diagram for the loads combinations

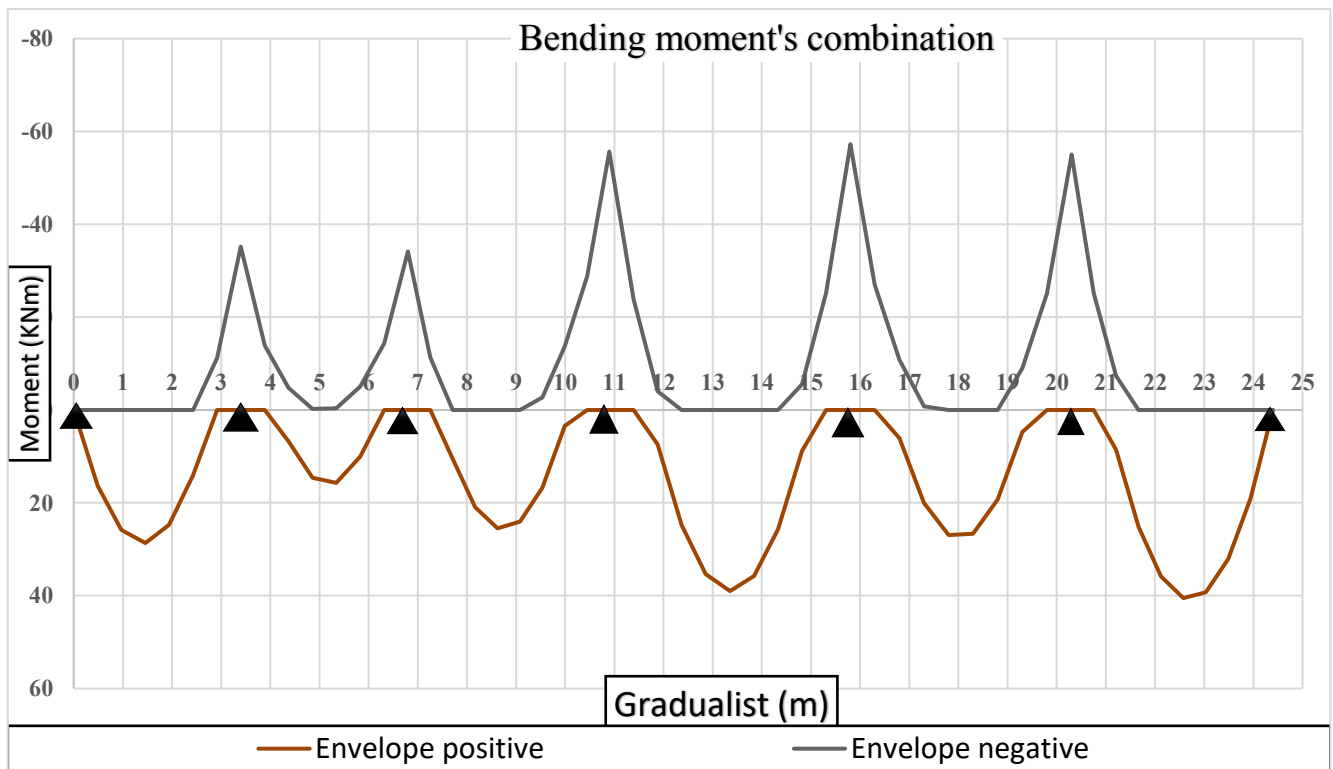


Figure 3-9: Envelop of moment diagram

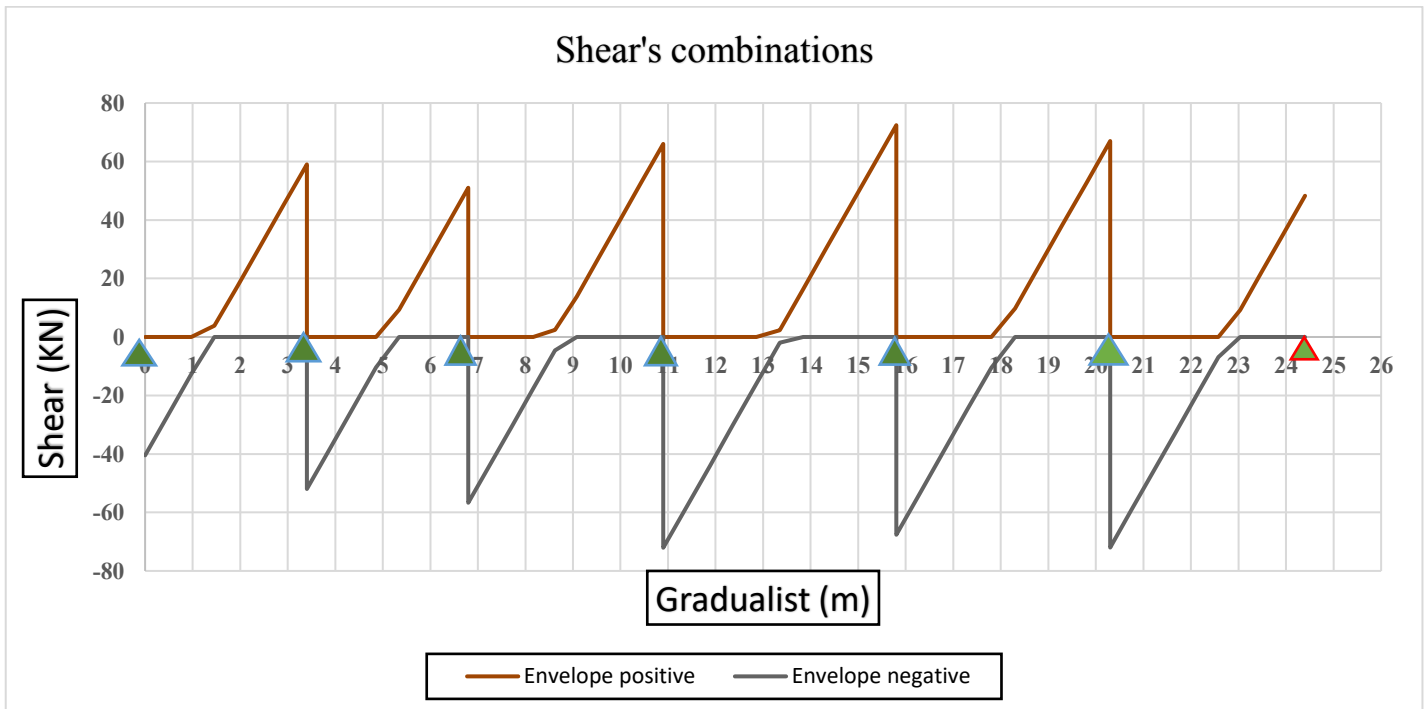


Figure 3-10: Envelop of the shear diagram

From this graph the steel reinforcement is computed and presented in table 3.4 below

Table 3.4: Longitudinal steel reinforcement of the beam

Longitudinal steel reinforcement						
	Span	Support2	Support3	Support4	Support5	Support6
Position of the neutral axis X (mm)	52.75	45.41	44.04	74.37	76.72	73.43
As calculated (mm ²)	305.53	263.04	255.13	430.77	444.39	425.35
As adopted (mm ²)	339.29	339.29	339.29	452.39	452.39	452.39
Med (KNm)	40.52	35.18	34.18	55.6688	57.2646	55.0301
Mrd (KNm)	44.99	45.38	45.46	58.46	58.30	58.53
Number of rebars (n)	3φ12	3φ12	3φ12	4φ12	4φ12	4φ12

The designed shear value for transversal reinforcement is $V_{ed} = 72.409 \text{ kN}$. The use of the criteria presented in the previous chapters, allows for the calculation of design shear resistance without reinforcement. $V_{Rdc} = 59.220 \text{ kN}$. Since V_{Rdc} is greater than V_{ed} we do not need to provide for shear reinforcement. However, we shall use a minimum amount of shear reinforcement based on V_{ed} .

Thus, with a 6 mm diameter, the design procedure presented on the section allows for the spacing of the stirrups required to resist the envelope of shear solicitations to be 200 mm at mid span and 120 mm at the support. Annex 6 illustrates the distribution of shear reinforcement.

3.3.5.2. Serviceability limit state design

The seven load arrangements inserted in SAP 2000 at the characteristic rare combination permit to obtain the solicitation curves presented in the figure 3.11

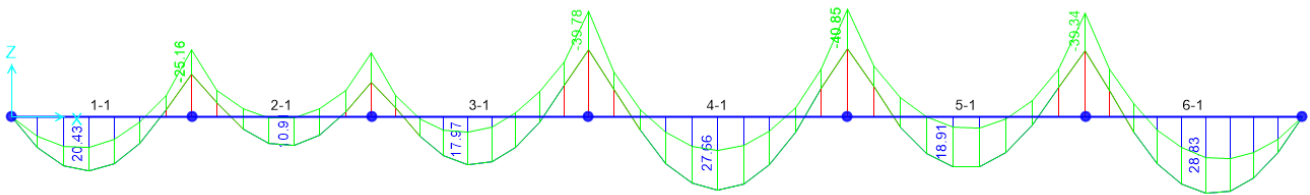


Figure 3-11: Bending moment envelop curve at SLS

The maximum bending moment with this load configuration is $M_{ed} = 28.83 \times 10^6$ Nmm. The stress and deflection verifications were obtained using the equations cited in the previous chapter and the results obtained.

i. Stress verification

The values of the stress values of steel and concrete at serviceability limit state was calculated and obtained as in the table 3.5 below. Their values were verified according to the Eurocode 2.

Table 3.5: Stress verification of beam

STRESS VERIFICATION		
Quantities	Values	Units
Modular ratio short term(n_0)	6.6717499	-
Modular ratio long term(n_∞)	14.0106748	-
Neutral axis(x)	83.3258031	Nm
Moment of inertia I_r	249101577	Nm^4
Steel stress σ_s	448.637814	N/mm^2
Concrete stress σ_c	9.64378841	N/mm^2
Check		
Steel stress	VERIFIED	
Concrete stress	VERIFIED	

ii. Deflection verification

The deflection was verified using the beam section and reinforcement section provided. Using the Eurocode 2 we obtained a verified section of beam.

Table 3.6: Beam deflection verification

DEFLECTION VERIFICATION	
Reference reinforcement ratio(ρ_0)	0.005
Allowable span/depth(l/d)	29.810
Actual span/depth	12.25
K(interior span of beam)	1.5
$\rho=As/Ac$	0.0042
DEFLECTION CHECK	OK

3.4.6. Column design results

The column designed is showed in figure 3.12.

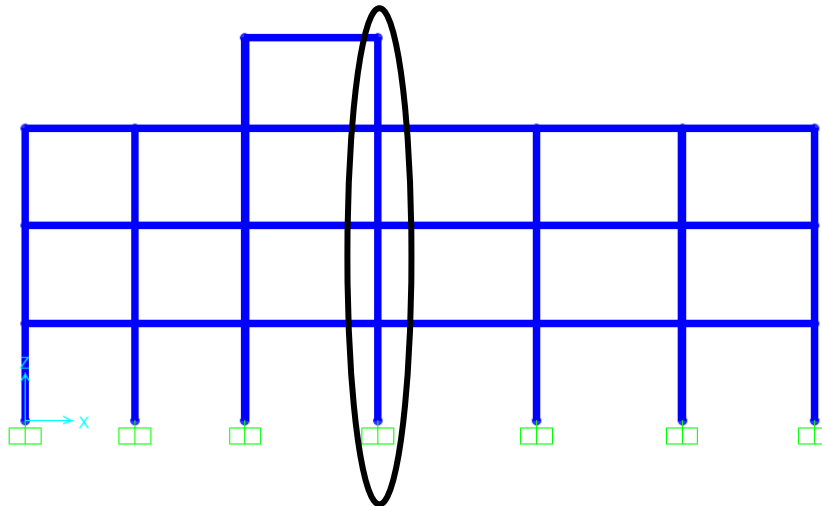


Figure 3-12: Most solicited column

According to the equations

$$N_{Rd} = 0.6 \times f_{cd} \times A_c \geq N_{sd} \text{ and } N_{sd} = q \times S_r \times n$$

The value of A_c is given by the formula

$$A_c \geq q \times S_r \times n / 0.6 f_{cd} = 34\,963.96 \text{ mm}^2$$

$$\text{With } q = 1.35G_k + 1.5Q = 6.395 \text{ kN/m}^2$$

The assumed crossed section of the column is 20x30 thus the area of the cross section is $A_c = 600\text{cm}^2$ and according to equations provided in the previous chapter, the values of A_{smin} and A_{smax} is given in table 3.7. The maximum axial force of the ULS envelop obtained shown that the maximum axial force is $N_{ed} = -491.33\text{ KN}$ as illustrated in the figure 3.13 below.

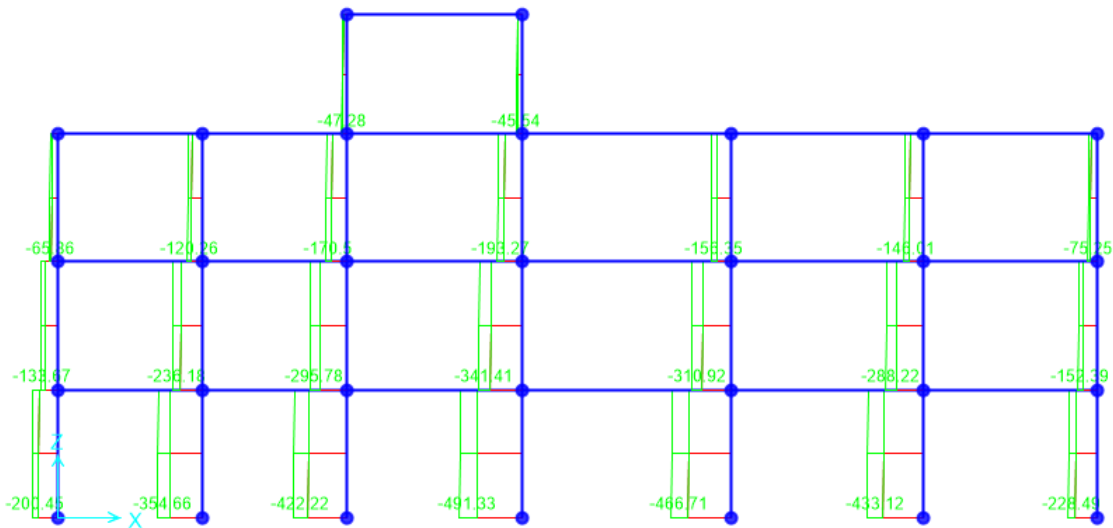


Figure 3-13: Axial force on most solicited column.

Table 3.7: Steel reinforcement section area

Steel reinforcement		
$A_{s\ min}$	125.56	mm^2
$A_{s\ max}$	2400	mm^2
$A_{s\ assumed}$	609.16	mm^2
N0 of bars	4 Φ 12 and 2 Φ 10	

The computed steel reinforcement value is $A_s = 609.16\text{ mm}^2$ which correspond to 4 Φ 12 and 2 Φ 10. The spacing of the bars is thus $s = 130\text{ mm}$ along x and $s = 172\text{ mm}$ along y which are less than the maximum spacing $s_{cl} = 280\text{ mm}$; Φ 6 will be use transversal reinforcement with a spacing of 180 mm at midspan and 150mm at the boundaries.

3.4.6.1 Bending moment-axial force verification

The designed column section is verified for each level because each couple of points M-N (moment-axial force) belongs to the M-N interaction diagram domain as shown in figure 3.14.

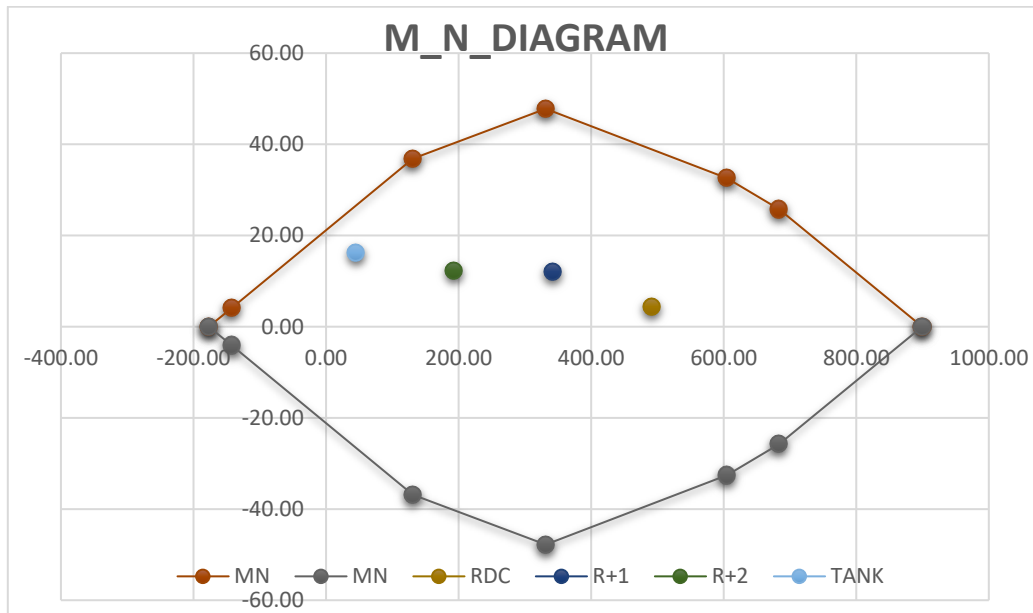


Figure 3-14: M-N interaction diagram

3.4.6.2 Shear verification

According to the Eurocode design of column, the maximum spacing of the transverse reinforcement is given by the equation below

$$S_{cl} = \min (20\phi_l, n; b; 400mm)$$

From this formula we obtained, using a 6mm diameter shear reinforcement, the maximum spacing of 240mm. Hence our spacing of 180mm is verified. The shear reinforcement distribution is represented in annex 6.

3.4.6.3 Slenderness verification

The slenderness verification for the most loaded column was obtained as in the table 3.8 below.

Table 3.8: Slenderness Verification of column

SLENDERNESS VERIFICATION	
A	0.7
B	1.2
C	0.7
N	0.3685
Critical slenderness ratio, λ_{lim}	19.3729
Effective height l_0 (mm)	2100
Radius of gyration i (mm)	115.4701
Slenderness ratio λ	18.1865

Since $\lambda < \lambda_{lim}$ column will NOT need to be designed for second order moments.

3.5. Analysis results and interpretation

The design of RC building only consider infill walls as distributed loads on the beams. The analysis performed aims to determine the influence of the masonry infill on how the RC frame respond. The comparative studies will be made between the simple frame and the frame with masonry infill. The infill material properties are presented in table 3.9.

Table 3.9: Infill material Properties

Material	Weight per unit volume (KN/m ³)	Elastic modulus E (MPa)	Poisson ratio ν	Dimensions (mm)	Compressive strength N/mm ²
Masonry (concrete blocks)	17.65	6681.6	0.2	200	7.2

The following results have been obtained after performing the different analysis describe in the methodology.

3.5.1. Modal analysis results

The modal analysis gives the modal period and natural frequencies of the building. The three first modes are translational along the X-axis, translational along the Y-axis and torsional around the Z-axis. For this analysis, two (02) construction configurations were considered and modelled on SAP2000: an empty frame configuration and an infilled frame configuration. From these setups, the different deformed shapes and the corresponding modes are obtained.

3.5.1.1. The Natural Frequencies

We obtained vibration frequencies for the first three modes of vibration for the two construction configurations. These frequencies are illustrated in table 3.10 below

Table 3.10: Natural frequencies and mode of vibration of the structure at different construction configuration

CONSTRUCTION CONFIGURATION	VIBRATION MODE	NATURAL FREQUENCIES
EMPTY FRAMED STRUCTURE	1	7.109
	2	3.831
	3	5.101
INFILLED FRAMED STRUCTURE	1	46.484
	2	44.400
	3	48.502

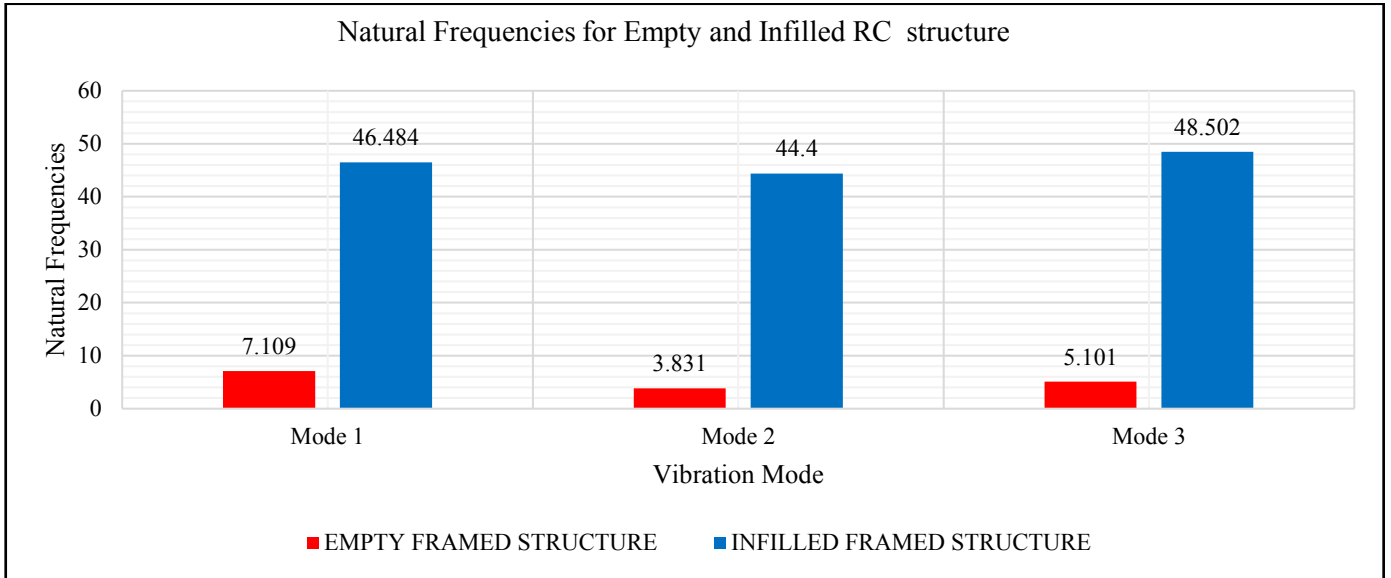


Figure 3-15: Natural Frequencies of Empty and Infilled RC framed structure

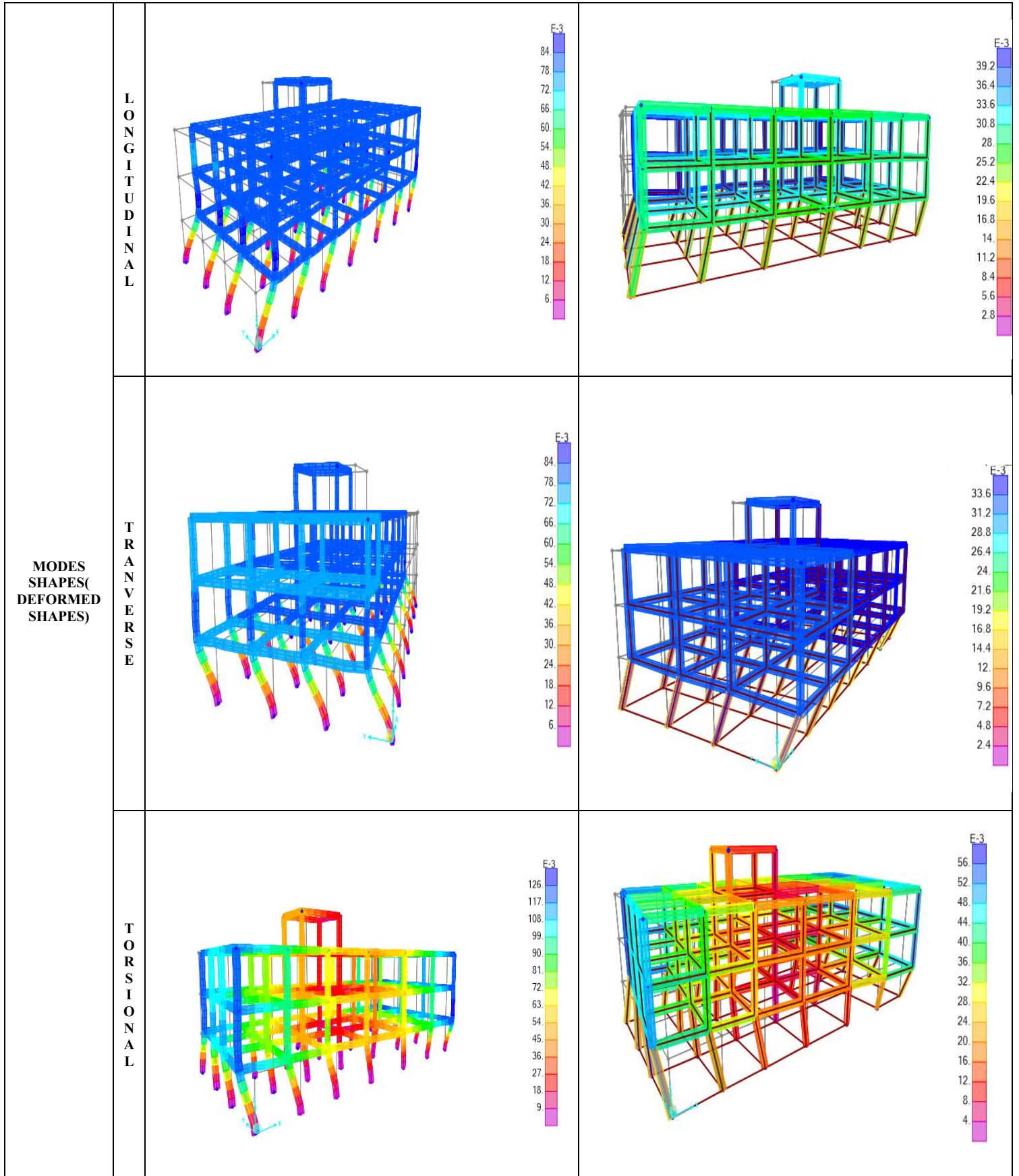
3.5.1.2. Modes Shape

Here our interest is on the shape of the different modes (longitudinal, transversal and torsional) of our construction configurations. These modes are illustrated in the table 3.11 below.

Table 3.11: Deformed shape at different modes of vibration

CONSTRUCTION CONFIGURATION	EMPTY FRAMED STRUCTURE	INFILLED FRAMED STRUCTURE
UNDEFORMED SHAPES		

INFLUENCE OF MASONRY INFILLS ON THE BEHAVIOR OF REINFORCED CONCRETE FRAMED STRUCTURES:
CONCEIVED CASE STUDY OF AN R+2 RESIDENTIAL BUILDING IN YAOUNDE



3.5.1.3. Interpretation of results

It can be seen in the table 3.10 and figure 3.15 that the greatest values of natural frequencies are manifest in the infilled framed structure case. Because of the masonry infill, the frequencies increase about 39Hz. However, in the analysis, the effect of the interaction between mortar and bricks of the infill walls of RC buildings is commonly neglected, even though it plays a significant role in the dynamic behavior of the structure.

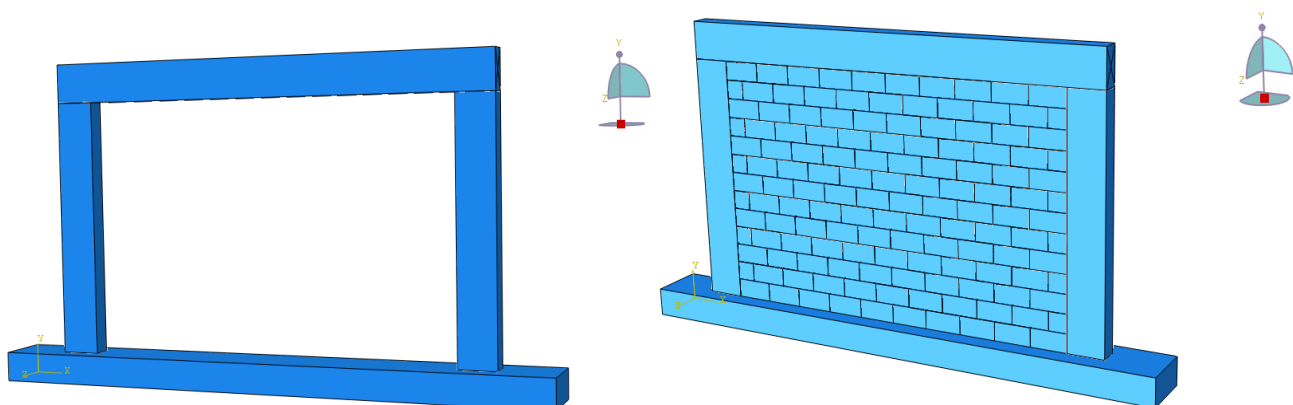
The modal behaviors of the structure (Table 3.11) are longitudinal, transverse and torsional. However, it can be seen that the mode shapes (longitudinal and transverse) of the infilled wall change significantly. The non-structural elements have contributed highly to the lateral stiffness, even changing the direction of the mode shape of a structure (Pan, T.C.; You, X.; Brown john, M.A.W.). It shows that the non-structural elements have contributed significantly to the lateral stiffness and the deformability of the structure.

3.5.2. Local Dynamic Analysis of infill walls

In order to understand the influence of the infill walls in the global behavior of the building, it is important to illustrate and evaluate the interaction between the infill wall and the frame structure. To do so, we considered four simple models; one with just an empty RC frame, the second being a completely infilled RC frame with masonry blocks, the third was an infilled frame with a window and lastly an infilled frame with a door. The characteristics of the elements are the following:

- Beam_ section: $b = 0.2\text{m}$; $h = 0.4\text{m}$; length= 4.8m ;
- Column_ section: $b = 0.2\text{m}$; $h = 0.4\text{m}$; height = 2.6 m
- Masonry block_ section: $b = 0.2\text{m}$; $h = 0.4\text{m}$; height = 0.2m

Figure 3.16 displays the different 04 models.



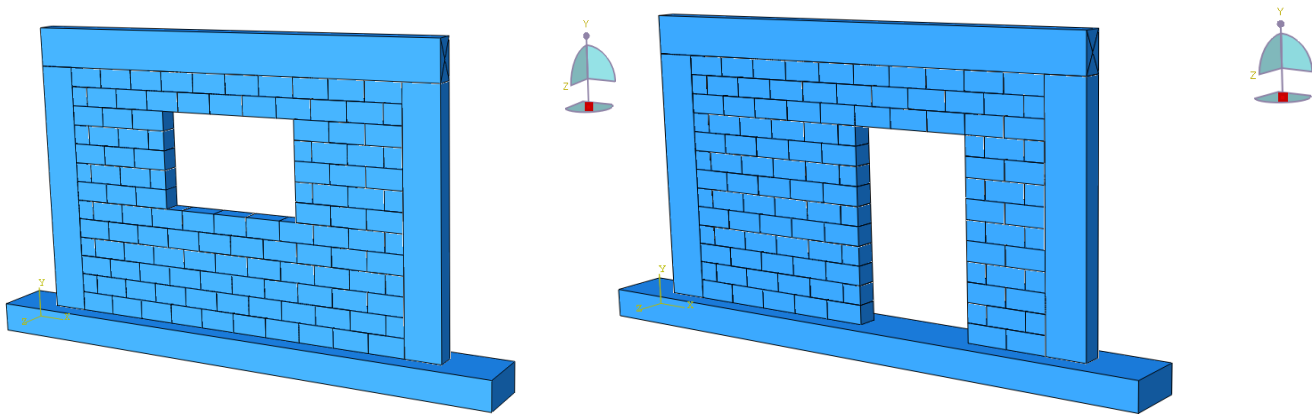


Figure 3-16: Models for the local dynamic analysis on Abaqus a) Empty RC frame b) Infilled RC frame c) Infilled RC frame with window and d) Infilled frame with door

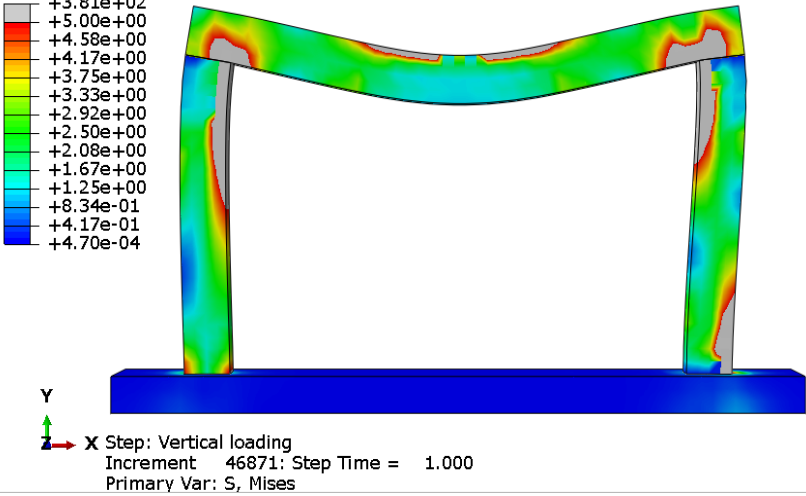
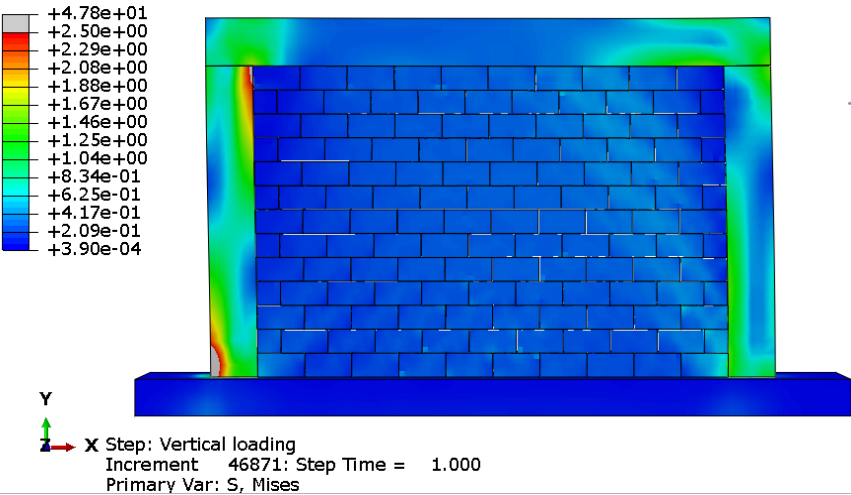
The micro model discretization of the elements is performed in a way that the boundary nodes of the infill frame correspond to the frame nodes. Afterward, a horizontal force $F=50\text{KN}$ is applied on one upper node on the beam element and a vertical pressure of 0.3KN/m^2 was applied on the beam of the models.

3.3.2.1. Stress integration of Von Mises Stress

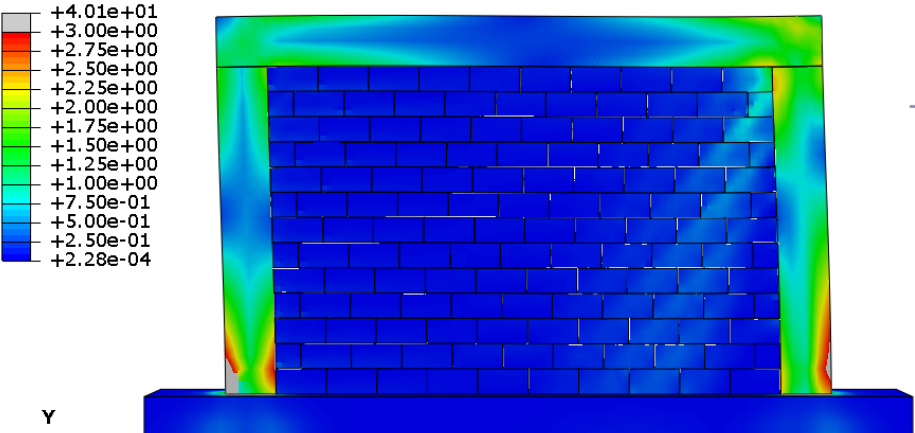

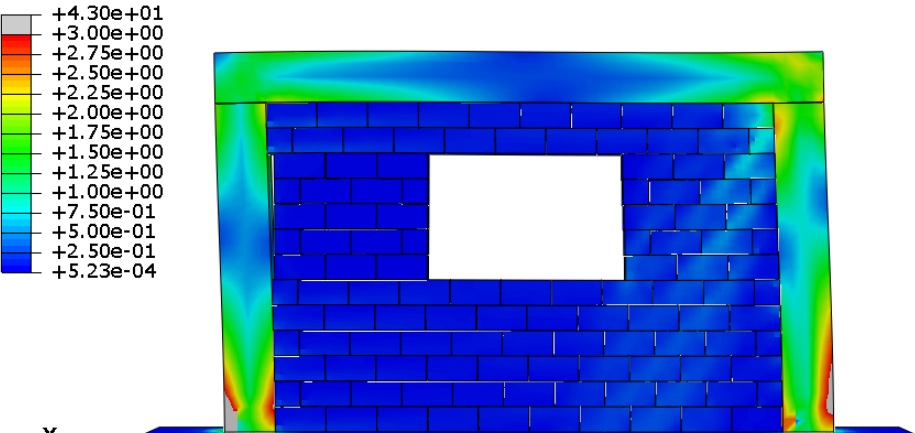

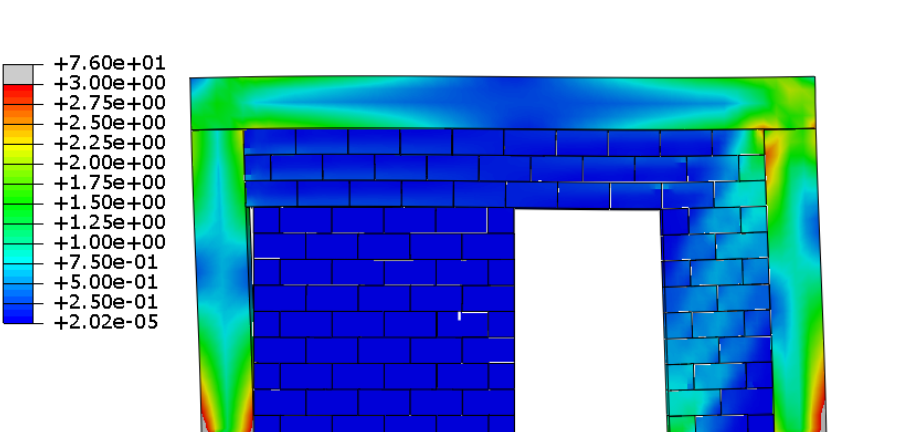

As a result of the horizontal and vertical loading on our models, a stress variation is noticed in the RC frame and the infill, and the highest stress is noticed in the diagonal range of the panel.

Table 3.12 shows the results (Von Mises) obtained after the analysis of the four models described earlier. As can be observed in figure 3.17, the maximum stress is recorded in the empty framed RC structure and the minimum is experienced in the infilled RC framed structure in both horizontal and vertical loading. This first observation leads to the understanding that the RC structure experienced a stress of 380 N/mm^2 and 197 N/mm^2 (vertical and horizontal loading respectively) when empty but now experiences a stress of 47 N/mm^2 and 40 N/mm^2 (vertical and horizontal loading respectively) hence a reduction of more than 300 N/mm^2 . This is due to the presence of non-structural elements (masonry infill) which increased the stiffness of the structure and participated as a first line of response to the external load.

Table 3.12: Von Mises Stress states for vertical and horizontal loading on different model configurations (illustrations scaling is of 150 on ABAQUS CEA)

LOADING STEPS	MODEL	VON MISES STRESS	
		MAXIMUM VALUE (N/mm ²)	ILLUSTRATION
VERTICAL LOADING	EMPTY FRAME	380.7	
	INFILLED FRAME	47.8	

	<p>INFILLED FRAME WITH WINDOW</p>	<p>51.7</p>	
	<p>INFILLED FRAME WITH DOOR</p>	<p>95.5</p>	
<p>HORIZONTAL LOADING</p>	<p>EMPTY FRAME</p>	<p>197.6</p>	

	INFILLED FRAME	40.13	 <p> $+4.01e+01$ $+3.00e+00$ $+2.75e+00$ $+2.50e+00$ $+2.25e+00$ $+2.00e+00$ $+1.75e+00$ $+1.50e+00$ $+1.25e+00$ $+1.00e+00$ $+7.50e-01$ $+5.00e-01$ $+2.50e-01$ $+2.28e-04$ </p> <p>  X Step: Horizontal loading Increment 46873; Step Time = 1.000 Primary Var: S, Mises </p>
	INFILLED FRAME WITH WINDOW	42.97	 <p> $+4.30e+01$ $+3.00e+00$ $+2.75e+00$ $+2.50e+00$ $+2.25e+00$ $+2.00e+00$ $+1.75e+00$ $+1.50e+00$ $+1.25e+00$ $+1.00e+00$ $+7.50e-01$ $+5.00e-01$ $+2.50e-01$ $+5.23e-04$ </p> <p>  X Step: Horizontal loading Increment 46873; Step Time = 1.000 Primary Var: S, Mises </p>
	INFILLED FRAME WITH DOOR	76.05	 <p> $+7.60e+01$ $+3.00e+00$ $+2.75e+00$ $+2.50e+00$ $+2.25e+00$ $+2.00e+00$ $+1.75e+00$ $+1.50e+00$ $+1.25e+00$ $+1.00e+00$ $+7.50e-01$ $+5.00e-01$ $+2.50e-01$ $+2.02e-05$ </p> <p>  X Step: Horizontal loading Increment 46873; Step Time = 1.000 Primary Var: S, Mises </p>

As we move from the horizontal loading step (0 to 1 seconds), we observed that the stress of the structure was first imposed on the RC frame elements but during the vertical loading step, the masonry infill carries a greater stress than the RC frame. This leads to the understanding that the masonry reduces considerably the total stress imposed by the external forces on the RC structure.

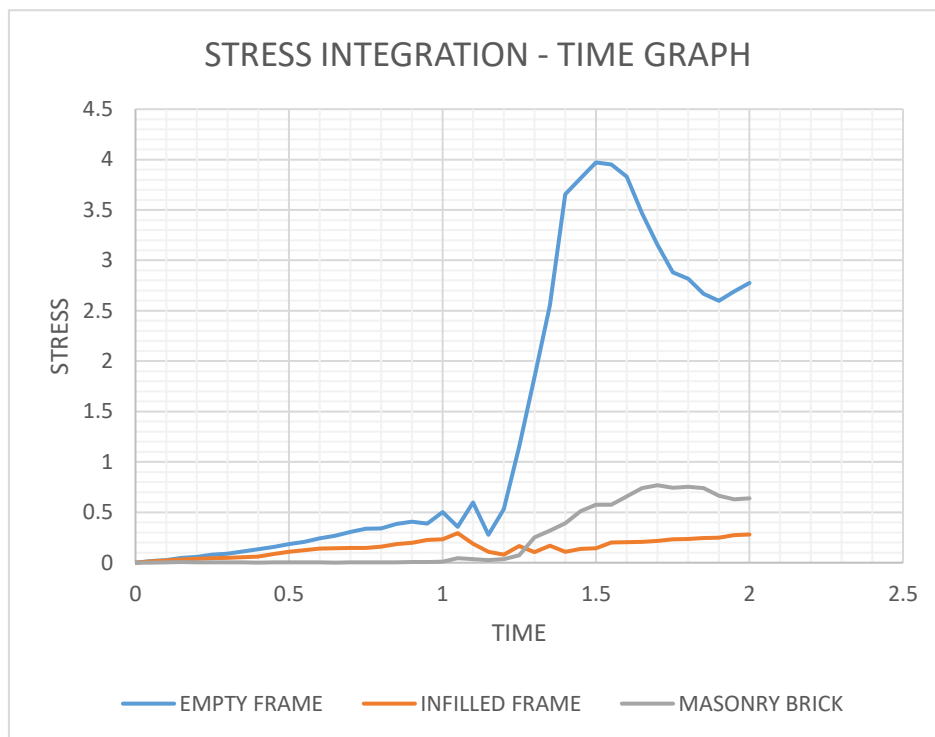


Figure 3-17: Von Mises stress- time graph for the vertical and horizontal loading

It is also observed in the section around the column-beam joint a higher concentration of stress which when not accounted for leads to the failure of the structure at these joints as in the figure (table 3.12). This stress is again reduced considerably after the addition of the masonry infill. Hence contributing to the positive influence of masonry infill on the behavior of RC structures.

A keen attention should be addressed on masonry infill with openings (door or windows). Since from the figures illustrated above, there is the occurrence of cracks around the openings, which are generally observed in our homes and buildings in Cameroon. This can be remedied by ameliorating the interaction between the masonry units (the mortar). Construction using good blocks having sufficiently high compressive and tensile strength and mortar ameliorates the firmness and rigidity of the masonry wall.

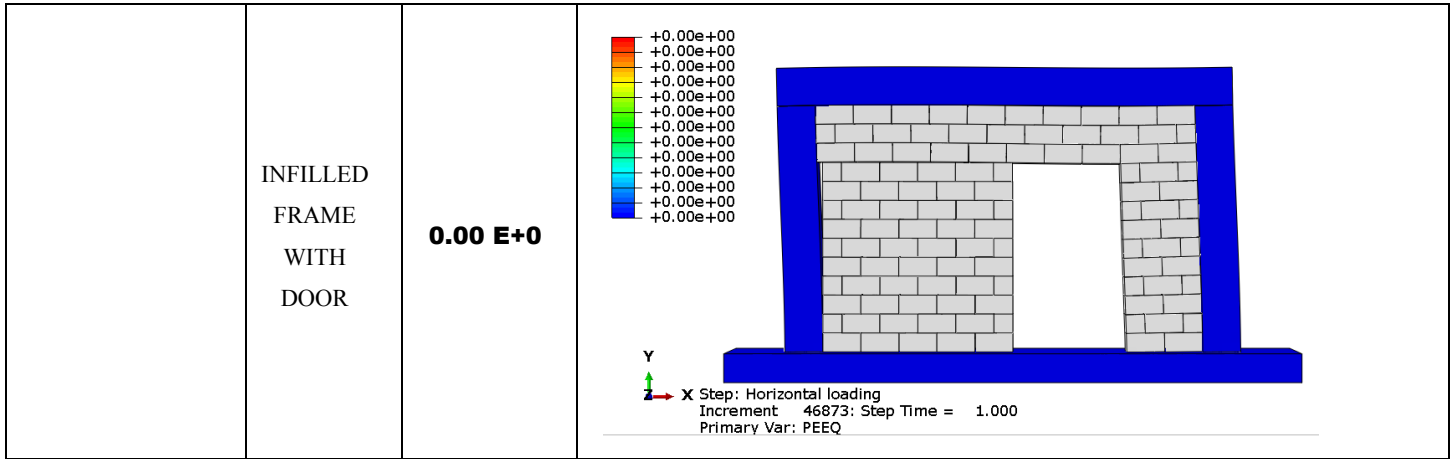
3.3.2.2. Equivalent Plastic Strain

The frame develops a plastic strain due to the loading steps of the horizontal force and the vertical pressure as illustrated in the table 3.13 below.

Table 3.13: Equivalent plastic strain

LOADING STEPS	MODEL	PLASTIC STRAIN	
		MAXIMUM VALUE	ILLUSTRATION
VERTICAL LOADING	EMPTY FRAME	8.05 E-5	
	INFILLED FRAME	0.00 E+0	
	INFILLED FRAME WITH WINDOW	0.00 E+0	

	INFILLED FRAME WITH DOOR	0.00 E+0	<p>Y X Step: Vertical loading Increment 46871: Step Time = 1.000 Primary Var: PEEQ</p>
	EMPTY FRAME	7.86 E-9	<p>Y X Step: Horizontal loading Increment 46872: Step Time = 1.000 Primary Var: PEEQ</p>
HORIZONTAL LOADING	INFILLED FRAME	0.00 E+0	<p>Y X Step: Horizontal loading Increment 46873: Step Time = 1.000 Primary Var: PEEQ</p>
	INFILLED FRAME WITH WINDOW	0.00 E+0	<p>Y X Step: Horizontal loading Increment 46873: Step Time = 1.000 Primary Var: PEEQ</p>



From the above table we can observe a clear disappearance of the plastic strain, which was initially developed at the column-beam joint. This strain is developed as a consequence of excess stress at those regions, which in a long run can lead to the structure defect (plastic hinge). Since the introduction of masonry infill considerably reduced the stress in the structure, a zero (0.00 E+0) strain developed in the structure (figure 3.18). Thereby validating the positive influence of masonry infill on the RC framed structure.

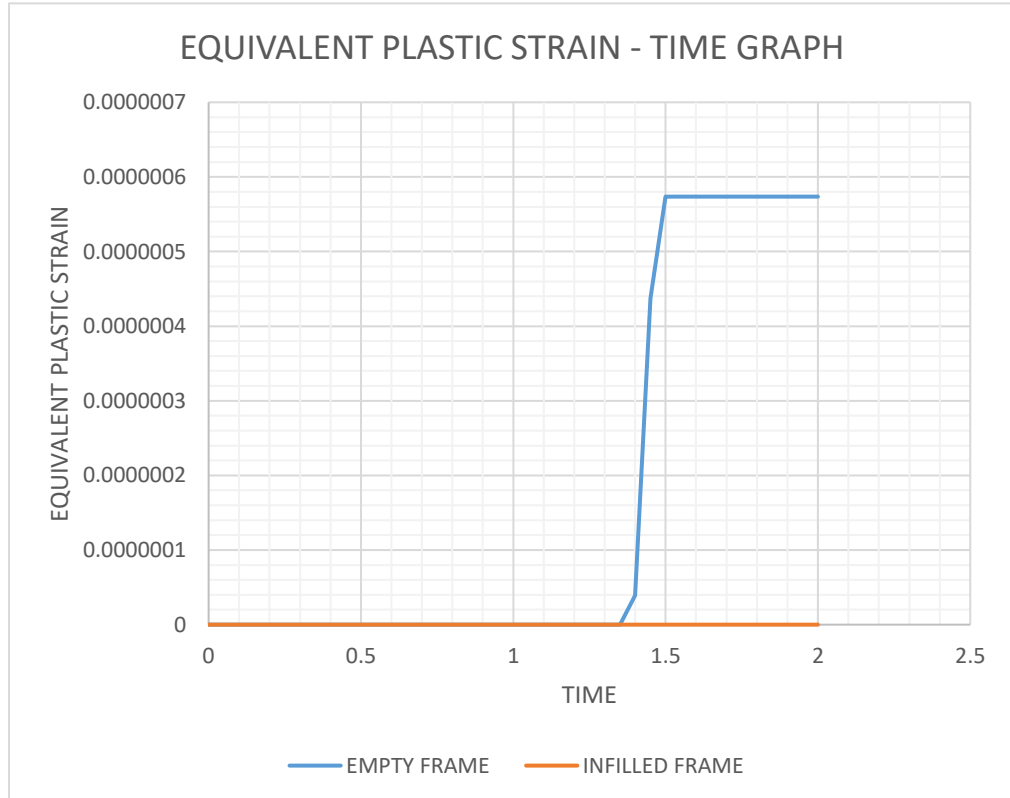


Figure 3-18: Equivalent Plastic strain - time graph of vertical and horizontal loading.

3.3.2.3. Deformation

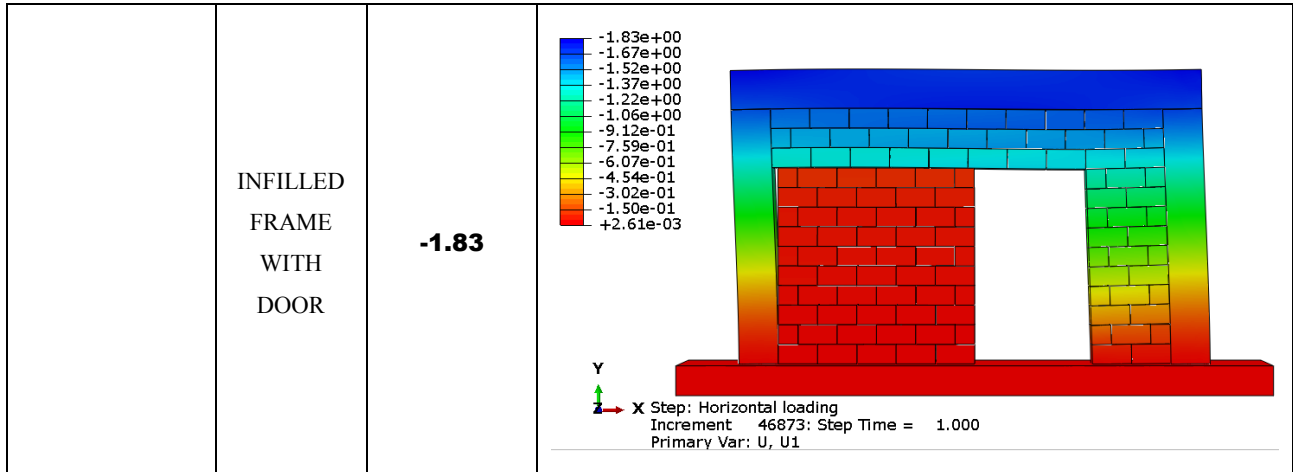
The application of the loads gives rise to a deformed shape of our structure hence displacement of the structure's elements. Table 3.14 illustrates the displacements obtained after analysis

Table 3.14: Displacement of structure under vertical and horizontal loading

LOADING STEPS	MODEL	DISPLACEMENT	
		MAXIMUM VALUE (mm)	ILLUSTRATION
VERTICAL LOADING	EMPTY FRAME	-7.28	<p>X Step: Vertical loading Increment 46871: Step Time = 1.000 Primary Var: U, U2</p>
	INFILLED FRAME	-0.147	<p>X Step: Vertical loading Increment 46871: Step Time = 1.000 Primary Var: U, U2</p>
	INFILLED FRAME WITH WINDOW	-0.669	<p>X Step: Vertical loading Increment 46871: Step Time = 1.000 Primary Var: U, U2</p>

**INFLUENCE OF MASONRY INFILLS ON THE BEHAVIOR OF REINFORCED CONCRETE FRAMED STRUCTURES:
CONCEIVED CASE STUDY OF AN R+2 RESIDENTIAL BUILDING IN YAOUNDE**

	INFILLED FRAME WITH DOOR	-1.05	<p>Y X Step: Vertical loading Increment 46871: Step Time = 1.000 Primary Var: U, U2</p>
HORIZONTAL LOADING	EMPTY FRAME	-3.00	<p>Y X Step: Horizontal loading Increment 46872: Step Time = 1.000 Primary Var: U, U1</p>
	INFILLED FRAME	-1.56	<p>Y X Step: Horizontal loading Increment 46873: Step Time = 1.000 Primary Var: U, U1</p>
	INFILLED FRAME WITH WINDOW	-1.69	<p>Y X Step: Horizontal loading Increment 46873: Step Time = 1.000 Primary Var: U, U1</p>



It is observed from the above table that the displacement caused by the vertical and horizontal loading decreases from 7.28mm and 3.00mm respectively without any infill to a displacement of 0.147 mm and 1.56mm with an infilled wall. Due to the compressive strength of the masonry units, the displacement reduces by a great amount. From this displacement the strain experienced by the models are illustrated in the figure 3.19 below.

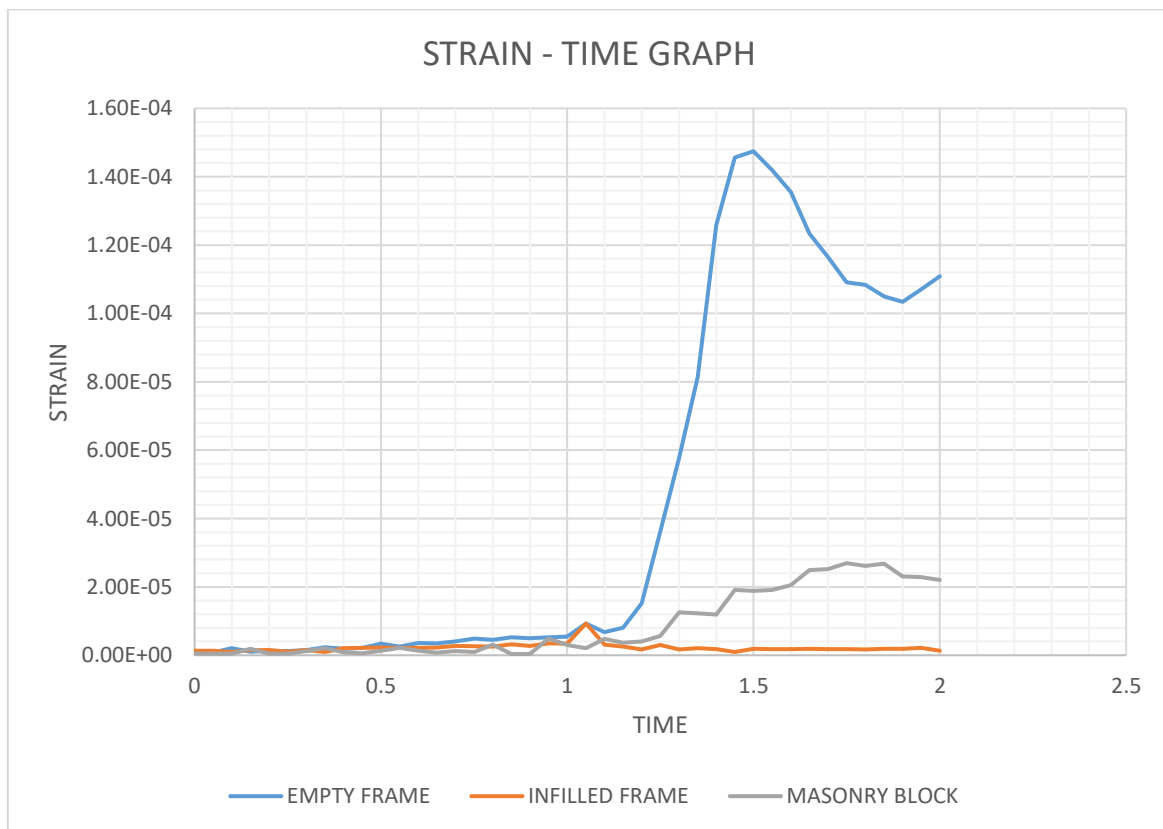


Figure 3-19: Strain-time graph of vertical and horizontal loading

Conclusion

The main objective of this chapter was the presentation and the interpretation of the result obtain from the analysis performed on the case study, by following the methodology described in chapter 2. The case study was first presented, and the design of the structural elements permit to obtain their respective cross sections and steel reinforcement. Afterwards, the analysis performed on the case study showed that the presence of infill wall reduce the lateral and the vertical deformability of the RC structure. In addition, the infill increases the rigidity and stiffness of the structure thereby decreases the stress and strain effects on the RC structure.

GENERAL CONCLUSION

The importance and influence of masonry infill wall on the daily progressive innovations and design of reinforced concrete structures is one of the most questioned and investigated problematic faced by engineers nowadays and has a significant role to play in future construction projects. It was revealed in the literature review important results of experiments made by scientists who proved the importance of masonry infill on seismic and lateral loading response on RC structures and also reveal some failure mechanisms that occurred on the infill.

In this study, numerical modelling has been conducted by using SAP2000 and ABAQUS software at each stage. The finite element model was described, and the main calculated results were presented. The different results were then compared to provide a better understanding of the building behaviour and the influence of masonry infill in the building. The main contribution of this work was to

- Present and propose a simple and efficient method of designing masonry infills in reinforced concrete framed structures
- Study the influence of masonry infills on the behaviour of reinforced concrete framed structures by: evaluating the dynamic characteristics of such structures with regard to the presence or absence of infills

Modelling techniques (detailed micro, simplified micro and macro modelling) demonstrate high effective in representing the masonry wall in general and the nonlinear properties of materials in particular. Simplified micro modelling was selected in this work because it provides enough important details for the analysis of the masonry wall with its different units (brick mortar). An analytical model analysis was performed on the three-dimensional finite element model developed using the SAP2000 and ABAQUS finite element software package

From the analyses conducted, we observed a net amelioration on the structure's behaviour to external perturbations; firstly, on the modal analysis we obtained a net increase of 39Hz in the structure's natural frequencies, which implies that the structure will need a greater external perturbation to experience any undesired vibration. In addition, it was shown that the structure's stiffness was improved considerably.

Then from the local dynamic analysis, we observed a great decrease in the principal stress, the plastic strain and displacement of the frame from 380 KN/mm², 8.05e-5, 7.28 mm respectively to 47

KN/mm², 0.00, 0.147mm respectively. Hence a decrease of about 300 N/mm² on the total stress component on the whole structure.

These results contribute to the conclusion that masonry infill influences positively on the behaviour of a reinforced concrete framed structure by increasing its rigidity and stiffness thereby reducing the defects on the RC structure elements (column and beam) which are the skeleton of the structure. The work also illustrated some defects on a typical masonry wall that usually occur in our building, a more detailed and meticulous study on the interaction (mortar) properties for masonry wall can be conducted to investigate on the best composition of mortar to reduce de defects (cracks) observed earlier. In addition, a more detailed micro modelling should be carried on a masonry infill to observe and study the crack pattern.

BIBLIOGRAPHY

- [1] 16th World Conference on Earthquake Engineering, 16WCEE 2017 Santiago Chile, January 9th to 13th 2017 Paper N° 3064 (Abstract ID) Registration Code: S-C1463230992 Investigation of the seismic behavior of infill masonry using numerical modelling approaches by Kubalski et al.
- [2] A Critical Review on Non-Load Bearing Wall Based on Different Materials by Dr. Jayeshkumar Pitroda , Krunalkumar A. Bhut , Hardik A. Bhimani , Sagar N. Chayani , Uday R. Bhatu , Nirav D. Chauhan.
- [3] Adil Rafiq, Muhammad Fahad, Mohammad Adil, 2020, November. Macro-Scale Numerical Modelling of Unreinforced Brick Masonry Squat Pier under In-Plane Shear. Advanced Design Examples of Seismic Retrofit Structure.
- [4] Ali Sahin Tasligedik, S. P. (2014). Low Damage Non-Structural Drywalls: Details and
- [5] Anecchiarico, M., F. Portioli and R. Landolfo, 2010, August. Micro and macro finite element modeling of brick masonry panels subject to lateral loadings. In Proc., COST C26 Action Final Conf, pp: 315-320
- [6] Bayraktar, A.; Turker, T.; Altunısık, A.C.; Sevim, B.; Sahin, A.; Ozcan, D.M. Determination of dynamic parameters of buildings by operational modal analysis method. Tek. Dergi 2010, 21, 5185–5205.
- [7] Behavior of Masonry-Infilled Nonductile Reinforced Concrete Frames by Ghassan Al-Chaar, M.ASCE; Mohsen Issa, M.ASCE; and Steve Sweeney, M.ASCE
- [8] Boudjamaa Roudane, Süleyman Adanur and Ahmet Can Altunısık, 8 August 2019, Numerical Modelling of Masonry Infilled Reinforced Concrete Building during Construction Stages Using ABAQUS Software.
- [9] Campilho RD, De Moura M, Domingues J. Using a cohesive damage model to predict the tensile behavior of CFRP single-strap repairs. Int J Solids Struct 2008; 45(5):1497–512.
- [10] Daniel, A.J. and R.N. Dubey, 2014. Finite element simulation of brick masonry building under shock loading. Tenth U.S. National Conference on Earthquake Engineering Frontiers of Earthquake Engineering, 21- 25.
- [11] Design of Structural Elements Third Edition Concrete, steelwork, masonry and timber designs to British Standards and Eurocodes Chanakya Arya, published in the Taylor & Francis e-Library, 2009.
- [12] DESIGN PROVISIONS FOR MASONRY-INFILLED RC FRAMES Michael N FARDIS
- [13] Dmytro Dizhur, R. P. (2016). Building typologies and failure in the 2015 Gorkha (Nepal) earthquake. Research Gate Engineering, 122(3), 228-237.

- [14] Eurocodes (0, 1, 2).
- [15] Fei Wang, K. Z. (2021). Influence of different types of infill walls on the Hysteretic Performance of Reinforced Concrete Frames. MPDI, Switzerland. Haag Engineering Co., 10.
- [16] J. Morton. (n.d.). The Design of Laterally Loaded Wall.
- [17] James Stevens, S. W. (2015). The Oxford Dictionary of Architecture. The Oxford University Press. Mehrabi, A. S. (1996). Experimental evaluation of masonry infilled RC frame. Journal of Structural
- [18] Kuang JS, Yuen Y. Simulations of masonry-infilled reinforced concrete frame failure. Proc Inst Civ Eng – Eng Compute Mech 2013; 166(4):179.
- [19] Kurdo F. Abdulla, Lee S. Cunningham, Martin Gillie, 12 August 2017, simulating masonry wall behavior using a simplified micro-model approach
- [20] Lourenço, P.J.B.B., 1997. Computational strategies for masonry structures. Ph.D. Thesis, Delft University, the Netherlands.
- [21] Masonry infilled frame structures: state-of-the-art review of numerical modelling Tarque Nicola , Candido Leandro , Camata Guido and Spacone Enrico
- [22] Mishra, G. (2014). Different Types of Failures in RCC Buildings with Case Studies. The Constructor. Mohammad Yekrangnia, H. S. (2019). Example of a Steel Frame Building with Masonry infill wall.
- [23] Mohammad H. Jinya, V. R. Patel, ANALYSIS OF RC FRAME WITH AND WITHOUT MASONRY INFILL WALL WITH DIFFERENT STIFFNESS WITH OUTER CENTRAL OPENING. IJRET: International Journal of Research in Engineering and Technology eissn: 2319-1163 | pissn: 2321-7308
- [24] Osman Fatih BAYRAK1, M. B. (JUNE 2018). ANALYZING THE EFFECT OF INFILL WALLS ON A RC STRUCTURE. DISASTER SCIENCE AND ENGINEERING.
- [25] P.G Asteris. (2008). Finite element micro modeling of infilled frame (Vol. 8). Electron.J.Struc.Eng. PG.Asteris, D. C. (2011). Failure mode of infilled frame. Electron. J Struck.
- [26] Pan, T.C.; You, X.; Brownjohn, M.A.W. Effects of infill walls and floor diaphragms on the dynamic characteristics of a narrow-rectangle building. Earthq. Eng. Struct. Dyn. 2006, 35, 637–651
- [27] S.V.Polyakov. (1956). On the Interaction between masonry filler walls and enclosing frame when loaded in plane on the wall, translation in earthquake engineering, Research Institute, Moscow.
- [28] Sedat Kömürcül *, Abdullah Gedikli1. Macro and Micro Modelling of the Unreinforced Masonry Shear Walls
- [29] Srisanthi, V.G., L. Keshav, P.P. Kumar and T. Jayakumar, 2014. Finite Element and Experimental Analysis of 3D Masonry Compressed Stabilised Earth Block and Brick Building

Models against Earthquake Forces. Periodica Polytechnica. Civil Engineering, 58(3): 255.
Their Performance. 2014NZSEE, (p.nd their). Auckland/New Zealand.civiljungle.com. (n.d).
[30] Timothy P.Marshall, S. M. (n.d.). On the performance of brick and concrete masonry in
windstorms

ANNEXES

ANNEXE 1. Values of minimum cover, $c_{min,dur}$, requirements with regard to durability for reinforcement (Eurocode 2)

Environmental Requirement for $c_{min,dur}$ (mm)							
Structural Class	Exposure Class according to Table 4.1						
	X0	XC1	XC2 / XC3	XC4	XD1 / XS1	XD2 / XS2	XD3 / XS3
S1	10	10	10	15	20	25	30
S2	10	10	15	20	25	30	35
S3	10	10	20	25	30	35	40
S4	10	15	25	30	35	40	45
S5	15	20	30	35	40	45	50
S6	20	25	35	40	45	50	55

ANNEXE 2. Building category (Eurocode 2)

Category	Specific Use	Example
A	Areas for domestic and residential activities	Rooms in residential buildings and houses; bedrooms and wards in hospitals; bedrooms in hotels and hostels kitchens and toilets.
B	Office areas	
C	Areas where people may congregate (with the exception of areas defined under category A, B, and D ¹⁾)	<p>C1: Areas with tables, etc. e.g. areas in schools, cafés, restaurants, dining halls, reading rooms, receptions.</p> <p>C2: Areas with fixed seats, e.g. areas in churches, theatres or cinemas, conference rooms, lecture halls, assembly halls, waiting rooms, railway waiting rooms.</p> <p>C3: Areas without obstacles for moving people, e.g. areas in museums, exhibition rooms, etc. and access areas in public and administration buildings, hotels, hospitals, railway station forecourts.</p> <p>C4: Areas with possible physical activities, e.g. dance halls, gymnastic rooms, stages.</p> <p>C5: Areas susceptible to large crowds, e.g. in buildings for public events like concert halls, sports halls including stands, terraces and access areas and railway platforms.</p>
D	Shopping areas	<p>D1: Areas in general retail shops</p> <p>D2: Areas in department stores</p>
<p>¹⁾ Attention is drawn to 6.3.1.1(2), in particular for C4 and C5. See EN 1990 when dynamic effects need to be considered. For Category E, see Table 6.3</p> <p>NOTE 1 Depending on their anticipated uses, areas likely to be categorised as C2, C3, C4 may be categorised as C5 by decision of the client and/or National annex.</p> <p>NOTE 2 The National annex may provide sub categories to A, B, C1 to C5, D1 and D2</p> <p>NOTE 3 See 6.3.2 for storage or industrial activity</p>		

ANNEXE 3. Imposed loads of concrete building (Eurocode 2)

Table 6.2 - Imposed loads on floors, balconies and stairs in buildings

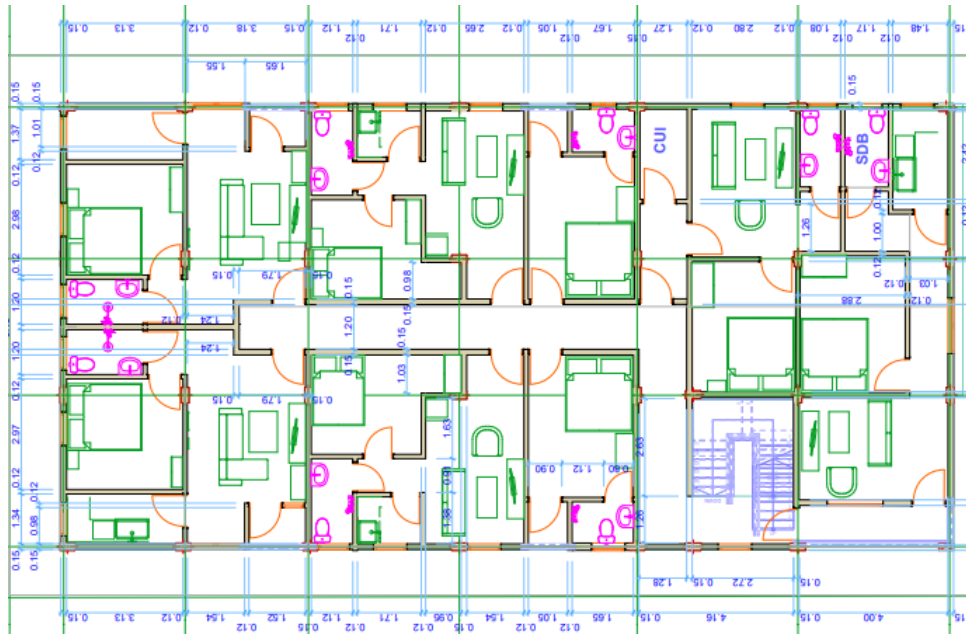
Categories of loaded areas	q_k [kN/m ²]	Q_k [kN]
Category A		
- Floors	1,5 to <u>2,0</u>	<u>2,0</u> to 3,0
- Stairs	<u>2,0</u> to 4,0	<u>2,0</u> to 4,0
- Balconies	<u>2,5</u> to 4,0	<u>2,0</u> to 3,0
Category B	2,0 to <u>3,0</u>	1,5 to <u>4,5</u>
Category C		
- C1	2,0 to <u>3,0</u>	3,0 to <u>4,0</u>
- C2	3,0 to <u>4,0</u>	2,5 to 7,0 (<u>4,0</u>)
- C3	3,0 to <u>5,0</u>	<u>4,0</u> to 7,0
- C4	4,5 to <u>5,0</u>	3,5 to <u>7,0</u>
- C5	<u>5,0</u> to 7,5	3,5 to <u>4,5</u>
category D		
- D1	<u>4,0</u> to 5,0	3,5 to 7,0 (<u>4,0</u>)
- D2	4,0 to <u>5,0</u>	3,5 to <u>7,0</u>

ANNEXE 4. Basic ratios of span/effective depth for reinforced concrete members without axial compression (Eurocode 2)

Structural System	K	Concrete highly stressed $\rho = 1,5\%$	Concrete lightly stressed $\rho = 0,5\%$
Simply supported beam, one- or two-way spanning simply supported slab	1,0	14	20
End span of continuous beam or one-way continuous slab or two-way spanning slab continuous over one long side	1,3	18	26
Interior span of beam or one-way or two-way spanning slab	1,5	20	30
Slab supported on columns without beams (flat slab) (based on longer span)	1,2	17	24
Cantilever	0,4	6	8

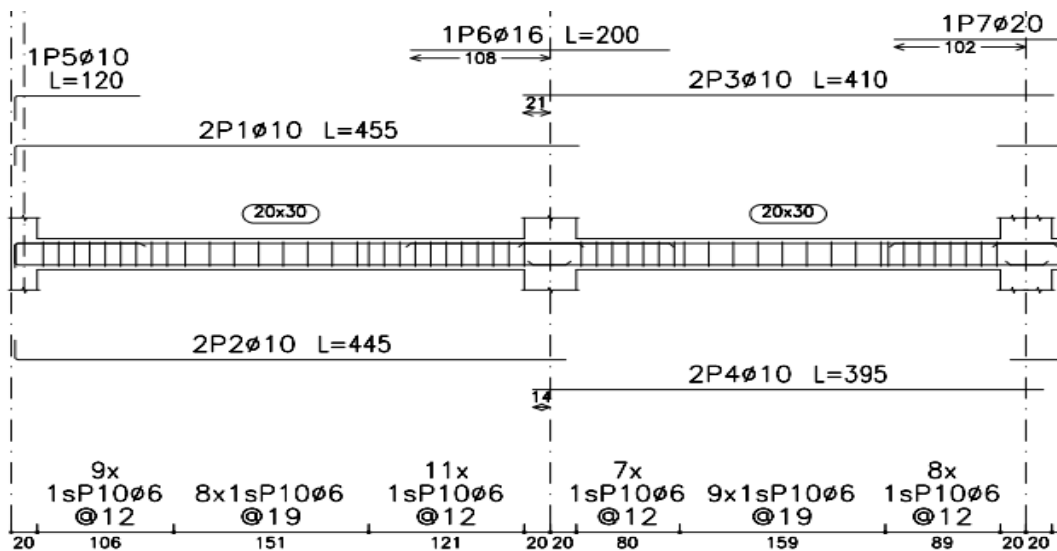
Note 1: The values given have been chosen to be generally conservative and calculation may frequently show that thinner members are possible.
Note 2: For 2-way spanning slabs, the check should be carried out on the basis of the shorter span. For flat slabs the longer span should be taken.
Note 3: The limits given for flat slabs correspond to a less severe limitation than a mid-span deflection of span/250 relative to the columns. Experience has shown this to be satisfactory.

ANNEX 5. Architectural plan of the levels

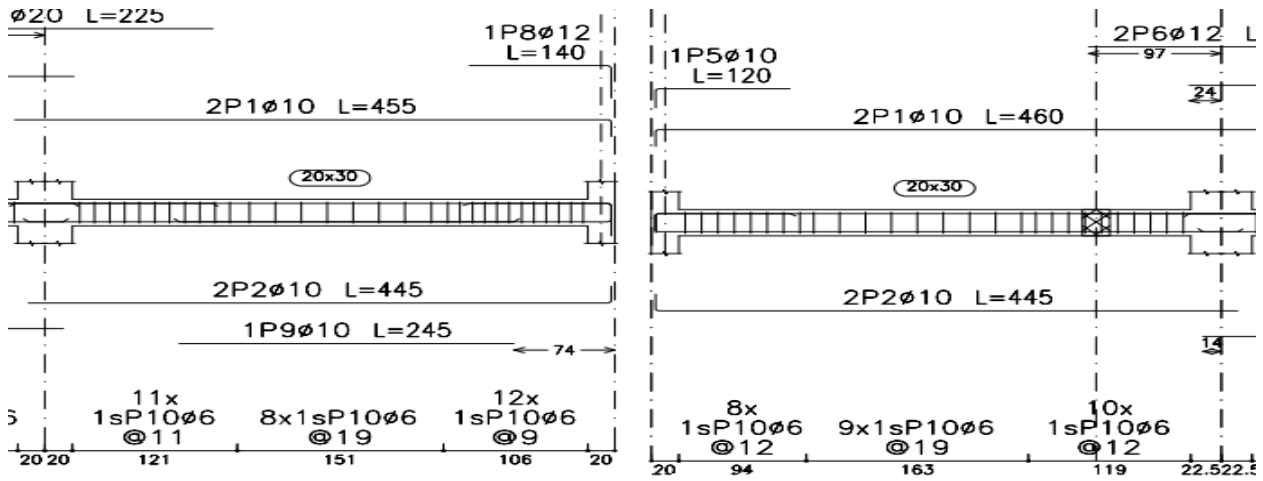


ANNEXE 6. Beams steel reinforcement

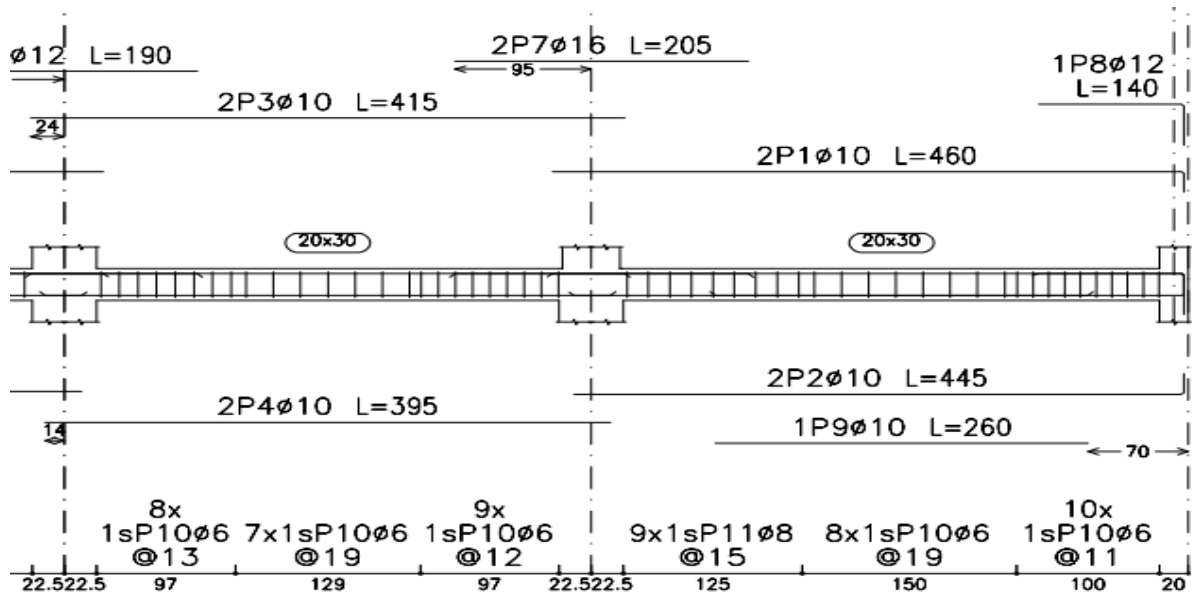
T1 and T2



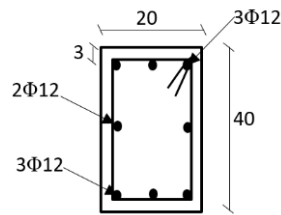
T3 and T4



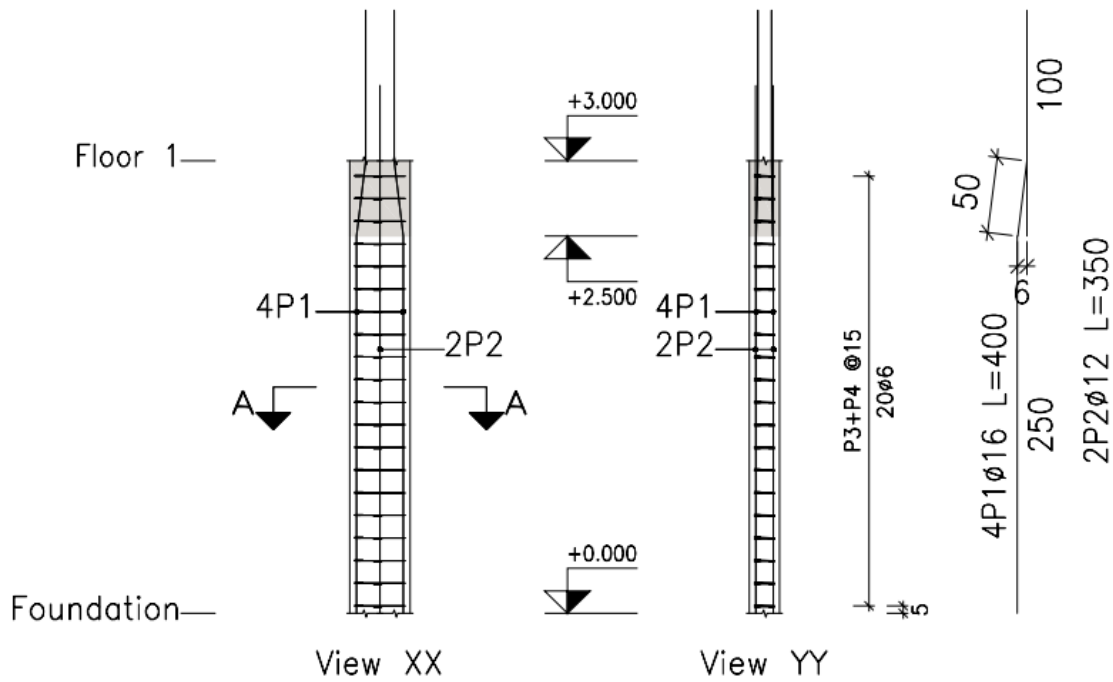
T5 and T6



Beam cross sections



ANNEXE 6. Columns steel reinforcement



Columns cross section

